Advanced Drug Delivery Reviews 177 (2021) 113929

Contents lists available at ScienceDirect

Advanced Drug Delivery Reviews

journal homepage: www.elsevier.com/locate/adr

Topical drug delivery: History, percutaneous absorption, and product development

Michael S. Roberts [a,b,c,*], Hanumanth S. Cheruvu [a], Sean E. Mangion [b,c,d], Azadeh Alinaghi [b,c], Heather A.E. Benson [e], Yousuf Mohammed [a], Amy Holmes [b,c], John van der Hoek [f], Michael Pastore [b,1], Jeffrey E. Grice [a]

[a] Therapeutics Research Centre, The University of Queensland Diamantina Institute, The University of Queensland, Woolloongabba, QLD, Australia
[b] UniSA Clinical and Health Sciences, University of South Australia, Adelaide, SA, Australia
[c] Therapeutics Research Centre, Basil Hetzel Institute for Translational Health Research, The Queen Elizabeth Hospital, Adelaide, SA, Australia
[d] Sydney Medical School, University of Sydney, Sydney, NSW, Australia
[e] Curtin Medical School, Curtin University, Perth, WA, Australia
[f] UniSA STEM, University of South Australia, Adelaide, SA, Australia

ARTICLE INFO

Article history:
Received 25 June 2021
Revised 5 August 2021
Accepted 11 August 2021
Available online 14 August 2021

Keywords:
Topical drug delivery
Skin and its appendages
History
Mechanism
Percutaneous absorption
Product development
QSPR
PBPK
IVPT
Finite dose
Clearance
Bioequivalence
Heterogeneity
Consumer behavior

ABSTRACT

Topical products, widely used to manage skin conditions, have evolved from simple potions to sophisticated delivery systems. Their development has been facilitated by advances in percutaneous absorption and product design based on an increasingly mechanistic understanding of drug-product-skin interactions, associated experiments, and a quality-by-design framework. Topical drug delivery involves drug transport from a product on the skin to a local target site and then clearance by diffusion, metabolism, and the dermal circulation to the rest of the body and deeper tissues. Insights have been provided by Quantitative Structure Permeability Relationships (QSPR), molecular dynamics simulations, and dermal Physiologically Based PharmacoKinetics (PBPK). Currently, generic product equivalents of reference-listed products dominate the topical delivery market. There is an increasing regulatory interest in understanding topical product delivery behavior under *'in use'* conditions and predicting *in vivo* response for population variations in skin barrier function and response using *in silico* and *in vitro* findings.

1. Introduction

The effectiveness and toxicity of topical products are influenced by at least four factors. These are (1) percutaneous absorption of drugs or other chemicals from a product; (2) the application conditions used; (3) the skin physiology in the person using the product; and (4) product perception by the patient and in the consumer marketplace. Each factor can be further broken down into associated interactions between the drug, skin, product, and person that capture a plethora of morphological, physiological, permeation enhancing, sensorial, pharmacological, and adverse effects. These, in turn, ultimately dictate if, how, and when they may apply a topical drug product.

In this paper, we focus on these attributes as they apply to topical products, in which the main site of action is the skin itself. Accordingly, the focus of this paper is very different from our earlier one on transdermal patch delivery into the systemic circulation [1]. In doing so, we recognize that a key challenge in addressing topical delivery is in quantifying and modelling localized skin absorption in humans and efficacy at the putative local site of action. However, considerable advances have been made in understanding opportunities for topical products, developing a mechanistic understanding of percutaneous absorption, creating

* Corresponding author at: Therapeutics Research Centre, Level 5, Translational Research Institute (TRI), 37 Kent Street, Woolloongabba, Queensland 4102, Australia.
E-mail address: m.roberts@uq.edu.au (M.S. Roberts).
[1] Present address: Genoskin, Toulouse, France.

https://doi.org/10.1016/j.addr.2021.113929
0169-409X/

regulatory guidelines for product development, and in translating these findings into products that best suit an individual's needs. The latter may include body site, skin condition, and response. A key consequence is that much of our learning in topical drug delivery is based on *in silico* and *ex vivo* human skin study projections using *in vivo* skin physiology and known pharmacokinetics.

2. Historical overview on topical product development

We begin our review with a brief historical overview of the use of topical products and the development of the range of dosage forms that are used in practice today (Fig. 1). Topical products are amongst the earliest of the "medical" technologies and treatments used by humans, as demonstrated by archaeological evidence that human skin has been used as a canvas for self-expression in the forms of body painting, cosmetics, and tattoos since prehistoric times [2–4]. These practices also protected the skin from the sun and a dry climate. Other skin care products were also used to meet other skin care needs (Fig. 1A). Interestingly, the therapeutic tattoos on the 5300-year-old ice mummy, Ötzi, coincide with many Chinese pressure points [4]. Ointments and potions made of animal, mineral, or plant extracts were in common use in ancient Egyptian and Babylonian medicine by 3000 BCE [5] and there are early examples of prescriptions for the local treatment of skin conditions on a Sumerian clay tablet (from 2100 BCE) [6] and in the Ebers Papyrus (from 1550 BCE) [7] (Fig. 1B). Medicated plasters containing multiple drugs and herbs were also evident in China around 2000 BCE [8]. These topical remedies were anointed, bandaged, rubbed, or applied to the skin for the treatment of a range of skin conditions. The resulting products contained ingredients to manage specific needs, such as moringa, sesame seed, and castor oil as skin protectants; yarrow as an astringent and diaphoretic; clays for cuts and wounds; clay and olive oil for a skin cleansing soap paste; yogurt as a skin peel; milk and honey for skin moisturization and anti-ageing; sea salt for exfoliation; pomegranate and other herbal juices as a skin astringent. In Ancient Greece, olives and olive oil were used for exfoliation and moisturization, with berries and milk being used in face masks, and medicinal plants, honey, tar, pig and goose fat used to treat skin conditions, which Hippocrates (460-370 BC) had recognised may be either local, e.g. acne, or systemic in origin. He also promoted the drying of moist lesions and the use of emollients for dry lesions.

Later topical products used multiple ingredients, with some products, such as Cold Cream by Claudius Galenus (Galen, 129–199 CE) (Fig. 1D) and skin cleansing agents, combining plant extracts such as aloe vera, cucumber or dried flowers with perfumes, thickening agents and coloring agents that are much in use today (Fig. 1C). Indeed, current topical product formulation strategies actively embrace Avicenna's (980–1037 CE) philosophy, outlined in his Canon of Medicine (Fig. 1E) that topical drugs possess two spirits or states: the soft part (i.e. active drug) penetrates the skin whereas the hard part (residual product) does not [9,10]. Avicenna also recognized that topical drug products have several target sites, including local action, in the muscles and joints below the skin and systemically. Further, he advocated the use of systemically acting topical drug products when oral dosing was not possible, with one product being plaster-like with paper as a backing material, i.e. perhaps our first topical patch? As medicinal and scientific knowledge evolved, there was a transition from empirical treatments to more targeted topical treatments. The earliest of these treatments were various topical plaster products described in the 1872 German Pharmacopoeia for topical swellings and infections [1] and, later in the United States Pharmacopoeia, containing belladonna as a local analgesic, mustard as a local irritant, and salicylic acid as a keratolytic agent [1]. Publication of *The Histopathology of the Diseases of the Skin* by Paul Gerson Unna in 1896 is credited with founding the modern approach to dermatology by focusing on the skin as an organ and defining the requirements for topical treatments of skin diseases [11].

Many of the dyes, minerals and herbal extracts present in the topical products used in Ancient times and in the Middle Ages exerted both therapeutic and toxic effects, in some instances not being recognized at the time. Examples include the antimicrobial blue-grey lead sulfide (Kohl) from Egyptian times, the decorative orange to red mercuric chloride (cinnabar), and silver metallic mercury (quicksilver). Rhazes of Persia (865 to 925 CE) proposed the use of mercurial ointments [10], after recording mercury poisoning in animal studies, with Avicenna (Ibn Sina) later recommending it only be used externally. Quicksilver ointments for skin disease were first used by the Arabs and later, along with ointments containing sublimate ($HgCl_2$), calomel (Hg_2Cl_2), and other metallic salts or oxides, in the European Renaissance for syphilis fostered by Paracelsus. Paracelsus (a Swiss physician and alchemist, 1493 – 1541, often seen as the founder of modern toxicology) formulated a mercury ointment (Fig. 1 F) in response to his observations of toxicity from oral mercury treatments [12]. Mercury ointment was widely used to treat syphilis in renaissance Europe and into the 20th century until it was overtaken by penicillin [13]. However, other forms of mercury have continued with phenyl mercuric acetate and phenyl mercuric nitrate salts being used as preservatives in topical products, especially those for the eye, until relatively recently. Further, merbromin (organomercuric disodium salt compound often known as Mercurochrome^{R}) has been used widely as a topical antiseptic until of late when other agents have taken over.

However, it is not just the heavy metals that may be toxic after topical application. There are many reports of adverse systemic effects, including poisoning from belladonna applied as a plaster, liniment, and lotion, headaches after occupational skin exposure to nitroglycerin in explosive factories [14], and hexachlorophene toxicity after topical application to babies [15]. Even today, vigilance is required to prevent systemic steroid suppression and related effects after topical glucocorticosteroid use, especially to an impaired skin barrier, in young children and in prolonged usage [16]. Further to the observation of systemic adverse effects after topical exposure to nitroglycerin, estrone, scopolamine, and nicotine, each drug has now been appropriately formulated, developed, and marketed as transdermal patches [1]. In addition, certain topically applied drugs, e.g. corticosteroids, and xenobiotics may lead to cutaneous adverse effects and some of these may become most evident on prolonged use, including atrophy, striae, rosacea, perioral dermatitis, acne, and purpura. The incidence and severity of these side effects has been related to the chemical nature of the steroid, the vehicle in which it is applied, and the site of application [16]. The principles of cutaneous toxicology in relation to irritation, phototoxicity, allergic contact dermatitis, and skin metabolism were well developed by the mid-1970s [17]. The major development in this field over the last 50 years has been the move away from animal testing to risk assessment by alternative methods, as mandated by regulatory oversight by the European Registration, Evaluation, Authorisation, and Restriction of Chemicals (REACH) and with updated chemical registration requirements applying from 2022 [18]. These methods involve a combination of *in silico* quantitative structure–activity relationships, *in vitro*, cell culture (including reconstituted human skin equivalents), and human volunteer testing [19].

Technological advances over time have paved the way for both an understanding of percutaneous absorption and the development of quality-assured topical products. The beginning of our understanding of the skin barrier morphology began with the imaging of stratum corneum "scales" (squamae) in the *in vitro* magnified glass studies by Antony van Leeuwenhoek in the late

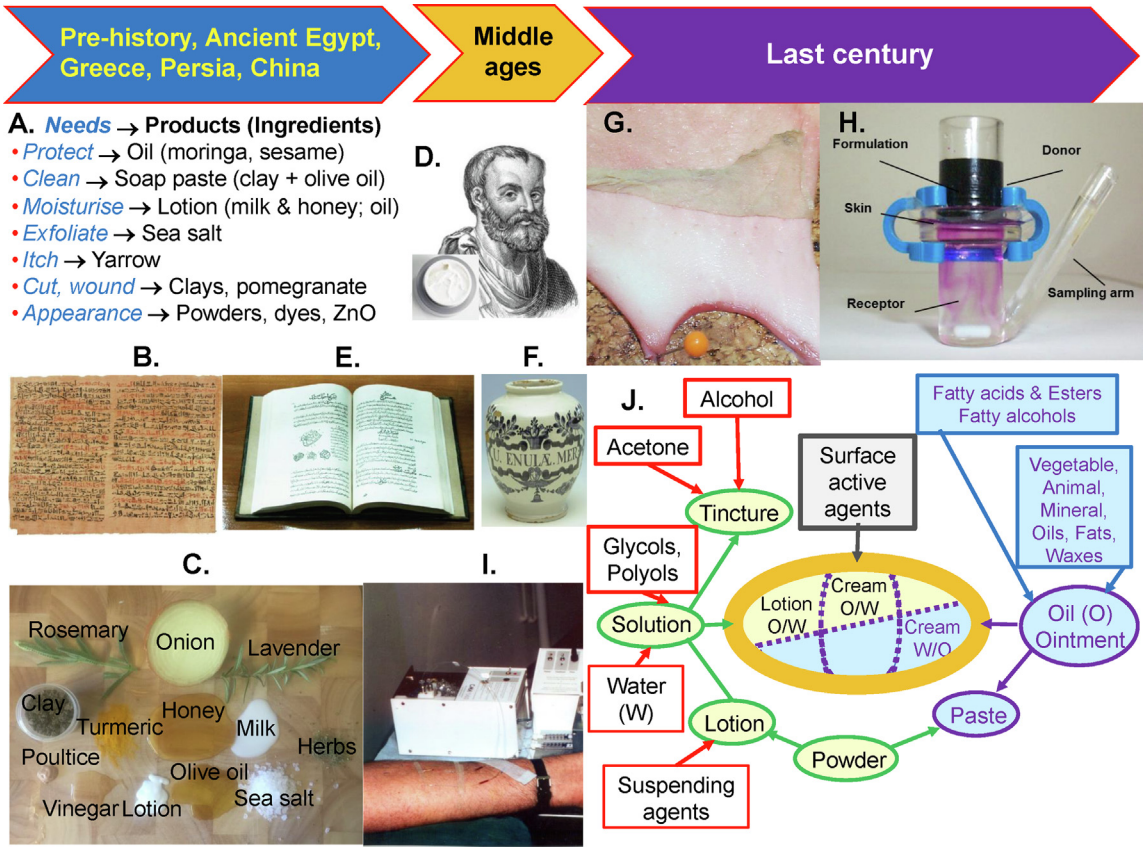

Fig. 1. Some key historical events in the topical product development from earliest times to the last century. A. Topical products used and ingredients to meet skin needs in pre-historic times and in Ancient Egypt, Greece, Persia, and China, with formulations described in B. Papyrus text ~ 1500 BCE (From [10]); C. Pictures of the ancient ingredients and some products in use today and the evolution to more sophisticated products as illustrated in D. by Galen (129 to ~200 CE) and his cold cream (From [10]). The two Middle Ages examples: E. Avicenna's Canon of Medicine (From [10]); F. Mercurial Ointment from ~1400 CE; G. Separation of epidermal membranes for *in vitro* permeation from human skin; H. Franz diffusion cell; I. *In vivo* skin microdialysis of author MR by Chris Anderson, Linköping, 1995; and J. Summary of topical formulations in 1971 [50].

1600s [20,21]. Through the 20th and 21st centuries, an explosion of research has enhanced our understanding of skin morphology, physiology, pharmacology, toxicology, and pharmaceutical science. One key advance in topical drug product development was the quantification of drug permeation through human stratum corneum, epidermis, and dermatomed skin under topical drug product "in use" application conditions. The work of Kligman and Christophers [22], in describing how human epidermal and stratum corneum may be separated from human skin *in vitro,* as illustrated in Fig. 1G, was a major step forward. Tom Franz took the complementary step of applying topical products to excised human skin in upright diffusion cells, as illustrated in Fig. 1H [23]. He found a comparable *in vitro* rate and extent of absorption for each of 12 compounds to that reported *in vivo* by Feldmann and Maibach [24] after mimicking their application protocol. Later, his team reported an excellent correlation between the extent of *in vitro* and *in vivo* absorption (mean ratio 0.96) in 11 data sets from 2 studies where the protocols had been harmonized and a less than 3-fold difference in 85% of 92 records from 30 published reports [25]. The second major advance was *in vivo* skin pharmacokinetic studies, initially based on urinary excretion kinetics for drugs [26–28] and pesticides [29], but later measured in the skin by a range of techniques including skin blisters, imaging of dyes, biopsies [30], dermal perfusion and, most recently, non-invasive multiphoton [31] and Raman imaging of skin *in vivo* [32]. Fox and Hilton first used *in vivo* skin perfusion to study the physiology of sweating [33]. It was then used for skin pharmacology studies [34], using cutaneous microdialysis probes (Fig. 1I), to assess the absorption and bioequivalence of drugs applied from topical dose forms [35], as well as the extent to which non-steroidal and other drugs penetrate into deeper tissues [36,37]. The latest form of this technique, dermal open-flow microperfusion, involves perfusion without a microdialysis membrane and has been used in topical drug dose form bioavailability assessment [38].

A key determinant of a successful topical drug dose is whether the drug will permeate across the skin to a putative therapeutic target site. As pointed out by Scheuplein and Blank, early studies found that skin was relatively permeable to lipid-soluble substances but not to water and electrolytes [30]. Later, *in vivo* studies found systemic drug effects after topical administration of the sex hormones [16], including topically applied follicle stimulating hormone for amenorrhoea in 1938 [39]. Urogenital infections were managed by a topical ointment containing the disinfectant chloroxylenol in the early 1940s [40]. The development and evolution of highly sensitive and specific analytical techniques, such as flame ionization, chromatography, spectrometry, and combinations led to detectable concentrations of various compounds being found in the blood, urine, and feces over the early 20th century. These methods (with developments such as GC-MS/MS and LC-MS/MS in widespread use today), along with pioneering theoretical, *in vitro* skin permeation and *in vivo* studies in the 1960s and 1970s [41], have allowed important determinants of topical bioavailability and skin permeability to be characterized, including drug solubility [42], partition coefficient and thermodynamic activity [43], barriers/mechanisms [44] and quantitative skin permeation - solute structure relationships for a range of mechanistic models [30,45–47].

In the mid to late 19th century, pharmaceutical companies with their roots in community pharmacy fostered a historic transition

from the "hit-and-miss" traditional remedies and skin products made by apothecaries and pharmacies to quality assured products in efficacy, safety, and stability, with associated regulatory oversight [10]. A key next step was the mandating of product safety and banning of false claims through the FDA's 1906 Pure Food and Drug Act, its later 1938 update, which specifically included cosmetics, and related legislation. In the years that followed, various pharmaceutical and cosmetic companies launched branded products and targeted their sales to health professionals and consumers via afluent druggist, department and brand exclusive stores and by brokers. A new generation of active ingredients, excipients and associated topical products emerged for both systemic [1] and topical use. These included antiseptics, local anaesthetics, corticosteroids, antibiotics, antifungals, retinoids, photosensitisers, skin whiteners, tanning agents, sunscreens, emollients and skin care products specific for certain body sites, such as the face. Perhaps, it is significant that one of the best overviews written in the mid 1970s on skin physiology, mechanisms of percutaneous absorption, topical drug formulation studies, products (Fig. 1J), and related methodology had an industrial perspective [50]. Many of the concepts they describe have been incorporated into the "quality-by-design" concept that now drives current topical drug product development and its regulatory oversight. This is discussed later in this review.

A key paper that underpins the academic aspects in this review is the work published by Tak Higuchi in 1960 [43]. In this work, Higuchi points out that the permeability coefficient and maximum flux concept approaches to percutaneous absorption are useful but equivalent in form. As we will see later, Irvin Blank and Bob Scheuplein [30,48,51] applied the first concept, and groups led by Alan Michaels [49] and Gene Cooper [52,53] the second. One of the first collations of a significant human skin permeability dataset was reported by Gordon Flynn in 1990 [54]. His data, replotted in Fig. 2, shows that this dataset's drug aqueous epidermal permeability coefficients are related to both the size and the log *P* of a given drug. Russ Potts and Richard Guy then used this dataset to define their current famous relationship [55], used widely in skin permeability predictions. However, whilst our permeability coefficient data formed part of the Flynn dataset, we have since come to the view that the skin maximum flux may be a better metric than $k_{p,aq}$ [56] in that, firstly, it provides a direct measure of the maximum exposure possible for a given drug and this exposure, in turn, defines both the efficacy and safety of a drug. This exposure is also important in consumer, occupational and environmental toxicology because along with an understanding of the likely systemic effects of a xenobiotic, it defines the additional health risk associated with a topical application. Secondly, topical drug products exist in a range of formulations involving different vehicle components and overall drug solubility in the product. In theory, providing that product is not adversely affecting skin permeability, each product should have the same maximum skin flux. Under ideal conditions, the relative flux for a drug between any topical products should then be related to its fractional solubility in the product as first alluded to by Higuchi [43]. Key confounders in making any comparison are the impact of the product and local environment on skin permeability because, as Higuchi points out, variations in skin hydration can greatly affect the percutaneous absorption of any drug [43].

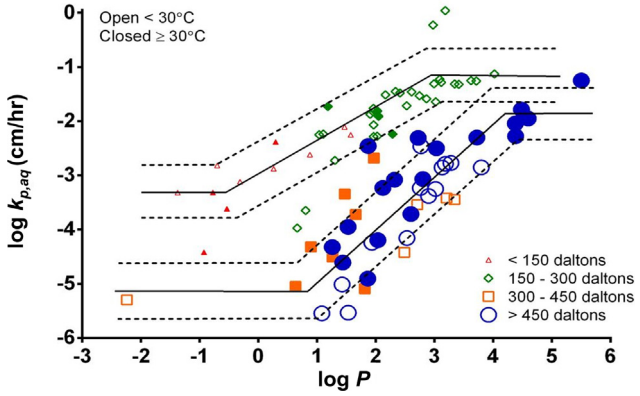

Fig. 2. Physicochemical determinants of aqueous *in vitro* skin permeability coefficients $k_{p,aq}$ include solute lipophilicity (as defined by the logarithm of solute octanol-water partition coefficient, log *P*), solute size (with various symbol sizes representing solute molecular weight in daltons) and study temperature in degrees centigrade). Adapted from [54] and the references referred to in that chapter.

3. Skin target sites and barriers in topical skin delivery

Fig. 3 shows some cross-sectional images of the skin, which define the general target regions of the stratum corneum, viable epidermis, dermis, and hair follicle. Also included in this Figure is an expanded view of the stratum corneum (SC), generally regarded as the main barrier for skin permeation, a furrow which may be a potential skin reservoir site, and an imaging example showing retinyl palmitate being mainly delivered to the outermost stratum disjunctum layer of the SC and the infundibulum of the hair follicle.

3.1. Target site

In general, the first consideration in formulating a topical drug product is whether the drug to be used is sufficiently potent at a local target site of action. As shown in Fig. 4A, there are a range of epidermal, dermal, and appendageal target sites that include the keratinocytes, Langerhans cells, melanocytes, Merkel cells, and blood vessels, as well as deeper tissues such as muscle. A counterbalancing consideration is the potential local and systemic adverse effects for the potential drug. Whilst the skin barrier generally limits local and systemic exposure and usually defines a high therapeutic margin, care must always be taken with any potent drug applied topically. Examples of drugs used to target various local skin sites with topical drug products include topical anesthetics to reduce pain and itch perceived by the skin's nervous system, skin whitening agents targeted at melanocytes, retinoids, corticosteroids modifying keratinocyte and blood vessel behavior, vaccine activation of Langerhans cells and anti-infective agents on the skin surface, in the epidermis and in the appendages (Table 1).

3.2. Skin barrier morphology

Providing protection against the external environment and maintaining internal homeostasis in water content and body temperature is perhaps the main function of the skin. Of particular interest in topical drug delivery is the physical barrier provided by the skin, which mainly resides in the SC. Each of the skin structures, the SC layer, viable epidermis, dermis, and appendages, shown in Figs. 3 and 4A have barrier properties that may impede skin absorption from topical products. However, the most important physical barrier is the non-viable (so-called outermost "dead") SC layer, the viable epidermis and the dermis as well as the appendages. Also included in Fig. 4B is the original electron micrograph of the SC by Brody in which he characterizes the SC as having three zones: basal zone (b, 4–10 cells thick and densely packed keratin fibril), intermediate (I, 8–12 cells, more dense keratin loosely packed in a clearer milieu) and superficial (s, 2–3 cells, with low keratin and intracellular space opacity), which together comprise the stratum disjunctum [57]. All corneocytes have a flat hexagonal shape parallel to the skin surface, are often irregular, interdigitate

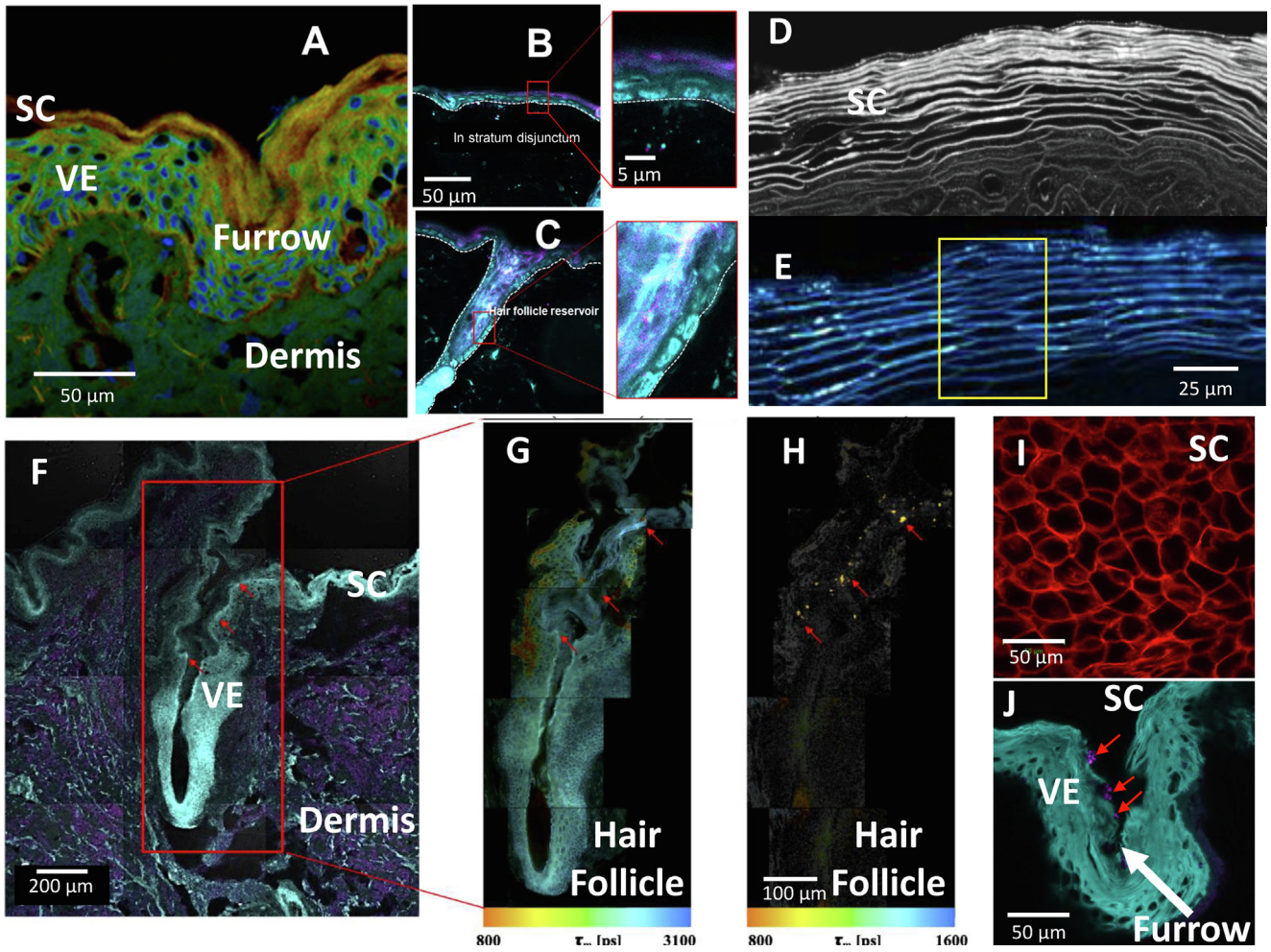

Fig. 3. Cross-sectional MPM FLIM cryosection of human skin showing A. MPM FLIM images of acriflavine stained full-thickness human excised skin showing a range of potential drug target sites (source Amy Holmes, UniSA); B. Stratum corneum and C. Hair follicle within cryosection of excised full-thickness rat skin stained with Nile red (cyan) showing penetration of retinyl palmitate (red, *MW* = 524.9, log *P* = 13.6) from a commercial formulation into the outermost stratum disjunctum layer of the SC and the infundibulum of the hair follicle (source: Sean Mangion, UniSA); D. Cryosection of full-thickness excised human skin stained with Nile red (applied in glycerol) with the SC expanded using KOH (4% w/v) to show each layer of the SC and to determine the number of corneocytes within the SC that would pose a barrier to the ingress of solutes and nanoparticles (source Amy Holmes, UniSA); E. Cryosection of full-thickness excised human skin stained with Nile red (applied in DMSO) with the SC expanded using KOH (4% w/v). Does SC lipid organization inside yellow may facilitate shunting through SC?; F. Cryosection of excised full-thickness human skin showing hair follicle that was dosed with 2% w/v aqueous zinc pyrithione particle suspension stained with ZinPyr-1 (two-photon excitation, cyan region λ_{ex} = 800 nm, λ_{em} = 370–420 nm; single-photon excitation, magenta region λ_{ex} = 488 nm, λ_{em} = 520–560 nm); G, H. FLIM image pseudo-colored to average time-weighted lifetime, τ[picoseconds] (two-photon excitation; λ_{ex} = 740 nm; emission detected using two bandpass filters 405/10 nm for the right and 520/60 nm for the left pane). Arrows mark ZnPT particle deposition (From [414] under open access Creative Common CC BY license.); I. Excised human skin (optical section, 5 µm in the z-range) with SC stained with Nile red demonstrating 'honeycomb' network of intercellular SC lipids, a potential route of permeation for some compounds (source: Amy Holmes, UniSA); I ZinPyr-1 stained (cyan) cryosection of full-thickness excised human skin dosed with 2% w/v aqueous zinc pyrithione particle suspension showing accumulation of particles (pink) within the furrow of the skin potentially acting as a reservoir. (For interpretation of the references to color in this figure legend, the reader is referred to the web version of this article.)

and have a diameter of ~40 µm and a width of up to ~1 µm, with an intercellular lipid region thickness of up to ~0.1 µm. Brody [58] later suggested the intercellular lipid space contained a trilamellar membrane, with an increased width towards the skin surface that, from a minimum of 30 nm, were up to 1, 2, and 3 µm thick in each of the b, i and s layers, respectively. Whilst Brody also suggested that the basal and middle zones combined may correspond to the stratum compactum, as defined by histology [58], others have suggested that the middle zone may be more associated with the histological stratum disjunctum [59].

The SC is a dynamic barrier, which may be modulated by its interactions with topical drug delivery systems that may enable or prevent drug delivery after topical delivery. It is a barrier that is continuously formed and shed over a period of between one week for the forehead, two weeks for back, and three weeks for the back of hand [60] through a highly programmed epidermal cell turnover and death process starting at the stratum basale, nourished and supported by the dermis. Associated with the process is the production of the SC barrier involving packed, flat dead corneocytes with relatively impermeable envelopes meshed in an extracellular lipid matrix with proteolysis of corneodesmosomes. These inter-corneocyte "molecular rivets" take up about 30% of the stratum compactum corneocyte surface, i.e. ~one per µm^2 or 600 to 800 per corneocyte, and only take up ~7% of the stratum disjunctum surface in non-palmoplantar SC, but >50% in the palmoplantar SC [61]. Corneocytes in the lower stratum basale may also be partly held together by tight junctions whereas hook-like rims at the overlapping edges of corneocytes may retard the shedding of corneocytes in the stratum disjunctum [62].

Of particular importance in SC barrier modulation is water as not only is it the main component in most topical drug delivery systems, but its egress from the skin can be modified using mois-

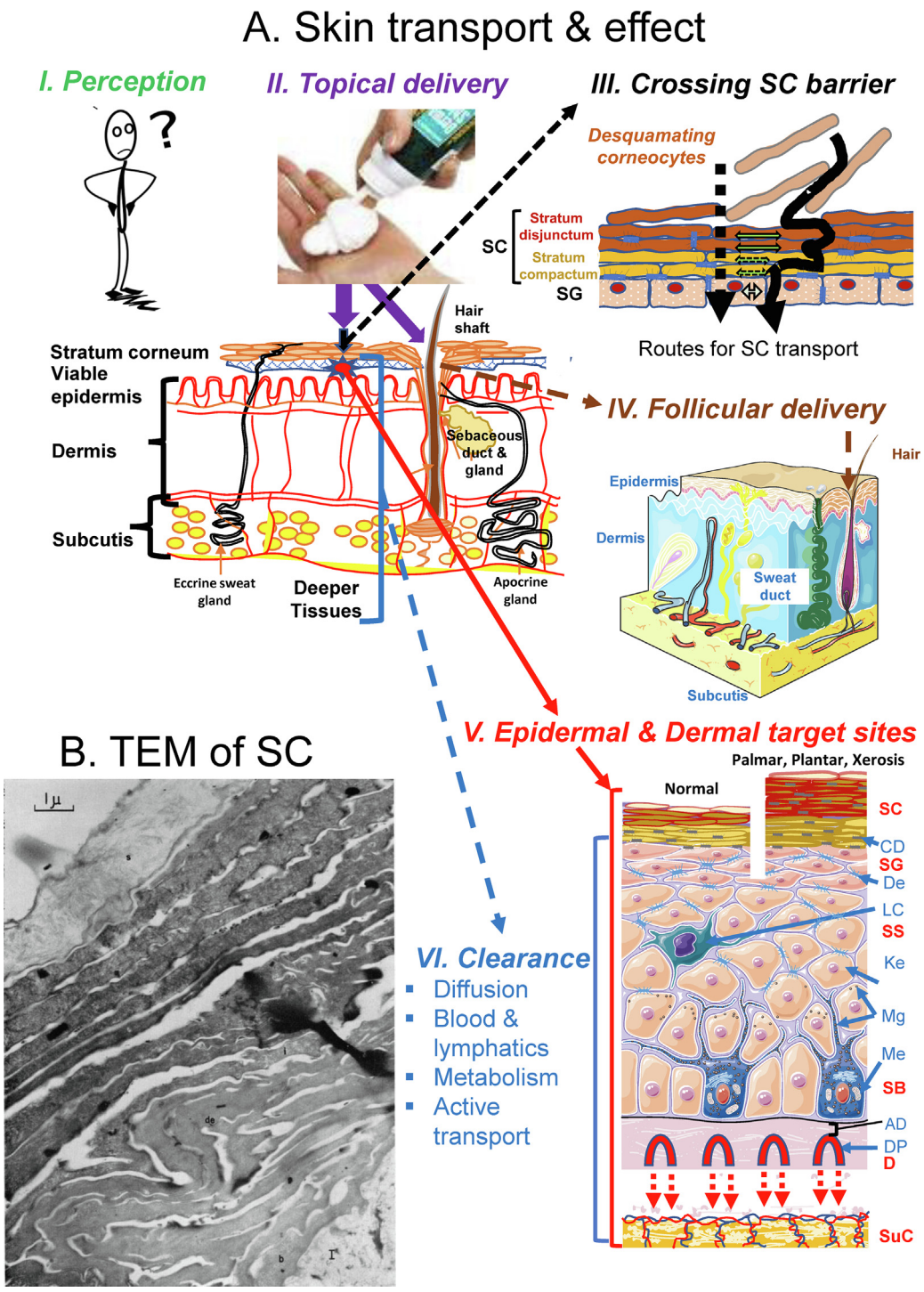

Fig. 4. A. Skin transport and effect after topical application, showing: I. Perception and adherence; II. Applying of a product to the skin; III. Crossing the SC barrier; IV. Follicular delivery; V. Reaching epidermal, dermal, subcutis and deeper target sites and VI. Clearance via various mechanisms. Adapted from [403] with permission of Elsevier. The subpicture from III shows a "brick-and-mortar" barrier model for the SC and the possible intercellular and transcellular pathways (and associated potential intra-corneocyte binding) that may be taken in crossing the SC sub layers (stratum disjunctum and stratum compactum) into the stratum granulosum SG. The subpicture from IV and those from V and VI show depictions of the SC, viable epidermal layers of SG, stratum spinosum SS, stratum basale SB, dermis D, subcutis SuC, sweat ducts, hair follicles, and underlying vasculature and skin target sites: epidermal cells (keratinocytes Ke, Langerhans' cells LC, melanin granules Mg, and melanocytes Me); appendages (sweat ducts and hair follicles); and superficial dermis, including dermal papillae DP and also showing thin and thick SC, corneodesmosomes CD, desmosomes De and the avascular dermis AD (From [402]); B. Transmission electron microscopy TEM of normal human SC, showing 3 sublayers: b, basal; i, intermediate and s, superficial. Uranyl acetate/lead citrate staining X 14,000. Reprinted from [57], with permission of Elsevier.

turizers, occlusion, and its retention in the skin. Of importance here is the use of hygroscopic materials and those that may modify the skin's natural moisturizing factor. It has been long known that water causes the SC to soften, thicken (towards the surface and not laterally), reduce furrow depth and lessen the SC corneocyte undulations seen in Fig. 4A, with the uptake of water to ~4 times the weight of dry SC and, after prolonged hydration, water pools in the intercellular regions [63,64]. Richter *et al.* has used osmotic

Table 1
Examples of local skin sites targeted by therapeutic agents by topical skin delivery.

Skin therapeutic target		Skin disorders	Examples of commonly used drug/chemical class
Skin surface	Stratum corneum	Bacterial, fungal, parasitic and fungal infections	Anti-infectives (malathion) Cosmetics (moisturizer, exfoliant), Insect repellents (DEET) 'Chemical' sunscreens (PABA) 'Physical' sunscreens (ZnO, TiO2)
Viable epidermis	Keratinocytes	Psoriasis Atopic dermatitis Actinic keratosis Skin cancer	Keratolytic (salicylic acid) Corticosteroids (hydrocortisone) Retinoids (tretinoin) 5-fluorouracil
	Langerhans cells		Antibodies (clinical trial phase) Antimitotics (topical corticosteroids) Immunosuppresant (tacrolimus) Immunomodulator (imiquimod) Methotrexate Vaccines (DNA vaccine, inactivated virus – clinical trial phase)
	Melanocytes	Hyperpigmentaion Vitiligo	Whitening agents (melanostatin) Repigmentation agents (psoralen)
Dermis	Nerve endings		Anaesthetics (lidocaine)
Hypodermis and underlying muscle	Cyclooxygenase enzymes	Trauma	NSAIDs (ketoprofen)
Skin appendages	Hair follicles	Acne vulgaris Seborrheic dermatitis Folliculitis Alopecia areata	Antiacne (erythromycin) Anti-dandruff (zinc pyrithione) Anti-infectives (fusidic acid) Hair restorers (minoxidil)
	Eccrine glands		Antiperspirants (aluminium)
	Nail	Onychomycosis	Antifungal (amorolfine)

Abbreviations: CNS, Central nervous system; DEET, N,N-diethyl-m-toluamide; NSAIDs, Nonsteroidal anti-inflammatory drugs; PABA, Para-aminobenzoic acid.

induced changes in SC regional thickness to characterize three hydration zones [65]. Zone 1 has a rapid decline in corneocyte thickness over 1 to 3 layers and corresponds to the steep water gradient at the stratum granulosum - SC interface of from ~65% water to ~40% in the first corneocyte [66]. The middle zone 2 of about 5 to 10 corneocyte layers was relatively unaffected by osmotic effects whereas such effects greatly changed the thickness of zone 1 as well as (to a lesser extent) zone 3. Richter et al attribute the increase in zone 3 to water being easily taken up into this zone [65]. More recent studies have shown that topical formulations mainly alter SC hydration by modulating water content in the stratum disjunctum; there is minimal change in water content within the stratum compactum [67,68].

The other key SC barrier, the insoluble and protective corneocyte envelope, is also affected by SC hydration and its impact on protease activity. This envelope exists in two forms: an irregular shaped, deformable and fragile envelope from the lower SC layers and, in ~80% of the SC corneocytes from the superficial layers, a polygon shaped and resilient envelope [69]. Impairment in SC corneocyte maturation associated with body site-related exposure to the environment and dry skin decreases the proportion of resilient envelopes [69].

It is to be noted that the SC lipids must be crossed to either go through or around the "brick" corneocytes embedded in the mortar of SC intercellular lipids (Fig. 4A). It is also observed that, should the drugs not be able to enter the corneocytes, the pathway for a drug through highly structured SC intercellular lipid lamellae may also involve, in principle, binding to corneodesmosomes and tight junction remnants at the corneocyte edges. However, these are generally only found in the deeper SC layers, interfacing the stratum granulosum [70]. As a consequence, the overall SC lipid transport pathway will be hindered and tortuous. On the other hand, an artificial shunt route is created when a drug can cross into the corneocytes. However, this may also be associated with hindered movement due to diffusional limitations in the corneocytes and may involve drug binding to the keratin, etc. within the corneocytes, as illustrated in Fig. 4A. The description and modeling of these processes, discussed in more detail later in this article, are also impacted by the heterogeneity of the skin, manifested by the undulating and furrow-containing surface, shown in Fig. 3, and by skin turnover and desquamation [71]. The initial tight junction barrier that exists at the SC - viable epidermis interface, evolves into a formidable stratum compactum barrier and then into a looser stratum disjunctum layer with, at the end of the desquamation process, the outer corneocytes shedding off like scales. Also shown in Figs. 3 and 4 are the potential shunt pathways provided by the follicles and sweat ducts. Artefactual skin transport routes and retention sites can also be caused by hydration, solvent, and vehicle effects on the skin, including delipidization and the formation of SC lacunae replacing degrading desmosomes, the formation of water, and lipid pools, denaturing of keratin, and changes in skin polarity [72].

The impact of this skin morphology, which is heterogeneous across body sites and individuals, is to define which and how fast drug candidates can penetrate the skin and, if sufficiently potent, be useful in topical products. As also shown in Fig. 2, in "broad brush" terms, unless some form of skin penetration enhancement technology is employed such as including one or more chemical enhancers in a formulation, only small (molecular weight *MW* <~500 Da), soluble (generally low melting point *MP*) and moderately lipophilic (logarithm of candidate octanol–water partition coefficient log *P* in range 0 to 5) compounds with few hydrogen bonds will readily cross the SC. However, as shown in Fig. 3, a larger and more lipophilic drug like retinyl palmitate (*MW* = 524.9, log *P* = 13.6), present in several topical retinoid products, has more difficulty passing into the more aqueous viable epidermis because of its poor water solubility. As a result, it is mainly found within the upper SC stratum disjunctum layer after 3 hr and is well distributed in the infundibulum of the hair follicle. In contrast, as also shown in Fig. 3, zinc pyrithione (present in many medicated shampoos as microparticles) accumulates in the skin furrows and follicles.

Table 2
Physicochemical properties† of topical drugs in currently marketed dermal products approved by FDA from Orange book [1], data updated from [37] on 25th June 2021.

Drug name	*MW* (Da)	*MP* (°C)	*Log P*	S_{aq} (mg/mL) at 25 °C	H_d	H_a
Acyclovir	225.2	255	−1.56	1.62, 2.50 (37 °C)	3	5
Adapalene	412.5	319–322	8.60	0.000004	1	3
Alclometasone dipropionate	520.2	212–216	3.94	0.14	1	7
Amcinonide	502.6	250–252	2.30	0.0077	1	8
Aminolevulinic acid hydrochloride	167.6	144–151	−2.80	173	3	4
Amlexanox	298.3	300	4.10	0.15	2	6
Ammonium lactate	107.1	91–94	−0.59	866	2	3
Amphotericin B	924.1	170	0.80	0.082	12	18
Avobenzone	310.4	84	4.51	0.0022	0	3
Azelaic acid	188.2	107	1.57	2.40	2	4
Bacitracin zinc	1422.7	250	−2.90	0.025	15	21
Benzoyl peroxide	242.2	103–106	3.46	0.0091	0	4
Benzyl alcohol	108.1	205	1.10	42.90	1	1
Benzyl benzoate	212.2	21, liquid	3.97	0.025	0	2
Betamethasone dipropionate	504.2	178	4.07	0.0046	1	5
Betamethasone valerate	476.6	184	3.60	0.0067	2	7
Bexarotene	348.5	230–231	6.90	0.00015	1	2
Bimatoprost	415.6	63–67	3.20	0.019	4	4
Brimonidine tartrate	442.2	207–208	1.27	0.15	6	9
Butenafine hydrochloride	353.9	208–210	5.67	0.00008	0	1
Calcipotriene	412.6	166–168	4.63	0.014	3	3
Capsaicin	305.4	65	3.04	0.029	2	3
Chlorhexidine gluconate	897.8	Liquid at 25 °C	2.71	0.026	18	16
Ciclopirox	207.3	144	2.30	1.41	1	2
Clindamycin phosphate	504.1	114	0.93	3.12	5	10
Clobetasol propionate	466.2	196	3.50	0.0039	1	6
Clocortolone pivalate	495.0	231–233	4.36	0.0010	1	6
Clotrimazole	344.1	148	0.50	0.00049	0	1
Crisaborole	251.1	129–135	3.24	0.023	1	4
Crotamiton	203.3	Liquid at 25 °C	2.16	0.018	0	1
Dapsone	248.3	175–177	0.97	0.28, 0.38 (37 °C)	2	4
Desonide	416.5	257–260	1.40	0.059	2	6
Desoximetasone	376.2	217	2.35	0.042	2	5
Diclofenac sodium	316.9	284	0.70	0.0048	1	3
Diflorasone diacetate	494.5	221–223	2.10	0.085	1	9
Docosanol	326.6	65–72	9.00	0.000000075	1	1
Doxepin hydrochloride	315.8	187–189	4.29	0.032	1	2
Dyclonine hydrochloride (Dyclopro)	325.9	175–176	4.66	0.049	1	3
Econazole nitrate	443.0	162	4.67	0.0015	1	5
Efinaconazole	348.4	86–89	3.70	0.32	1	6
Eflornithine hydrochloride	218.6	181–184	−2.19	50	4	6
Erythromycin	733.5	191	3.06	0.46	5	14
Fluocinolone acetonide	452.2	266–268	2.48	0.055	2	8
Fluocinonide	494.5	309	3.19	0.0047	1	9
Fluorouracil	130.0	280–282	−0.89	11.10 (22 °C)	2	3
Flurandrenolide	436.5	247–255	2.88	0.0011	2	7
Fluticasone propionate	500.6	261–273	3.38	0.011	1	9
Gentamicin sulfate	516.6	218–237	−3.10	100	8	14
Halcinonide	455.0	276–277	3.30	0.011	1	6
Halobetasol propionate	484.2	213–215	3.73	0.022	1	5
Hexachlorophene	405.8	164–165	7.54	0.14	2	2
Hydrocortisone	362.2	220	1.61	0.32	3	5
Hydrocortisone Butyrate	432.6	210–214	3.21	0.014	2	6
Hydrocortisone Valerate	446.6	217–220	3.62	0.0076	2	6
Hydroquinone	110.1	172.3	0.59	72	2	2
Imiquimod	240.3	292–294	2.70	6.25	1	3
Ingenol mebutate	430.5	153.5	3.12	0.0043	3	6
Ivermectin	875.1	155	5.83	0.0040	3	14
Ketoconazole	530.1	146	4.35	0.00029 (20 °C)	0	6
Lidocaine	234.2	69	2.44	4.10 (30 °C)	1	2
Luliconazole	354.3	149–154	2.59	0.066	0	4
Mafenide acetate	246.3	177	−0.37	5.18	3	6
Mechlorethamine hydrochloride	192.5	108–110	0.91	33.40	1	1
Metronidazole	171.1	158–160	−0.02	11	1	4
Miconazole nitrate	479.1	159–163	3.26	0.026	1	5
Minoxidil	209.3	248	1.24	2.20	3	3
Mitomycin	334.3	360	−0.40	8.43	3	8
Mometasone furoate	521.4	218–220	3.90	0.011	1	6
Mupirocin	500.2	77–78	3.44	0.027	4	9
Naftifine hydrochloride	323.9	172–175	3.59	0.00023	1	1
Neomycin sulfate	712.7	187	−7.80	50	15	23
Nystatin	926.1	160	0.50	0.36	12	18
Octinoxate	290.4	Liquid at 25 °C	5.80	0.00045	0	3
Oxiconazole nitrate	492.1	137	3.80	0.0019	1	6

Table 2 (*continued*)

Drug name	*MW* (Da)	*MP* (°C)	*Log P*	S_{aq} (mg/mL) at 25 °C	H_d	H_a
Oxybenzone	228.2	65.5	3.79	0.0037	1	3
Oxymetazoline hydrochloride	296.2	181–183	4.87	0.0014	3	2
Penciclovir	253.3	275–277	−1.10	7.45	4	5
Permethrin	391.3	34	6.50	cis isomer-0.00020, trans isomer-0.00013	0	3
Pimecrolimus	810.4	135–136	4.40	0.0015	2	11
Podofilox (Condylox)	414.4	228	2.01	0.15	1	8
Polymyxin B sulfate	1301.6	217–220	−0.74	0.074	20	29
Prednicarbate	488.6	114–116	2.92	0.0056	1	8
Prilocaine	220.2	37–38	2.11	0.54	2	2
Retapamulin	517.8	125–127	5.00	0.00039	1	6
Sertaconazole nitrate	500.8	158–160	3.33	0.0064	1	6
Silver sulfadiazine	357.1	285	0.39	7.87	1	6
Spinosad	1287.7	112–123	4.00	0.0024	2	19
Sulconazole nitrate	460.8	130	3.21	0.0013	1	5
Sulfacetamide sodium	236.2	257	−0.96	50	1	5
Tacrolimus	804.0	126	3.30	0.000018	3	12
Tazarotene	351.5	103–105	3.38	0.00075	0	4
Terbinafine hydrochloride	327.9	204–208	3.30	0.00074	1	1
Tetracaine	264.4	41–45	3.51	0.56	1	4
Tretinoin	300.2	180–182	6.30	0.0048	1	2
Triamcinolone acetonide	434.2	293	2.53	0.08	2	7
Trifarotene	459.6	245	6.12	0.00095	2	5

[i]Physicochemical properties are acquired from Pubchem (https://pubchem.ncbi.nlm.nih.gov/), Chemspider (https://www.chemspider.com/), Drugbank (https://www.drugbank.ca/), Pastore *et al.* 2015 [3], chemical book (https://www.chemicalbook.com/) and product information sheet from manufacturers.

3.3. Drug candidates for topical delivery

Not all drugs are suitable for topical delivery. The key requirements for topical drugs are that they can penetrate through or into the skin from a suitable topical product to be delivered to a skin target site where they are sufficiently potent to exert a physiological or pharmacological effect and they and their products meet consumer perceptions and need [73]. Currently, at least 96 drugs are being used in topical delivery that meet these criteria and are applied in a range of dosage forms, including in patch, gel, ointment, and solution (Table 2). In this section, we examine the drug physicochemical properties that define their extent and rate of delivery through the main barrier of the skin, the SC, from a pharmacokinetic and mechanistic perspective.

3.4. Getting the drug to its site of delivery

A key requirement for any drug to be active at a target therapeutic or cosmetic skin site after topical application is it reaches that site in sufficient local site drug concentrations C_{local}. Under ideal "sink" conditions, the steady-state concentration, $C_{ss,local}$, is determined by the skin steady-state flux J_{ss} (i.e. the steady-state amount $Q(t)_{ss}$ permeating per unit area A over a steady-state time period (t_{ss}), the local bioavailability F_{local} (which may be less than 1 due epidermal metabolism and sequestration) and drug clearance from that site per unit area CL_{skin}/A [73,74] (Fig. 4B):

$$C_{ss,local} = \frac{J_{ss}F_{local}A}{CL_{skin}} = \frac{F_{local}Q(t)_{ss}/t_{ss}}{CL_{skin}} \quad (1)$$

In equation (1), J_{ss} may refer to either transport across the SC to deeper underlying viable tissues or, much less commonly, to direct delivery into appendages. Drugs in products applied topically for a local action may also lead to effects elsewhere in the body. Here, in contrast to $C_{ss,local}$ being independent of the area of application A (Eq. (1)), the systemic steady-state blood concentration of a drug $C_{ss,blood}$ is directly related to both J_{ss} and A (as this also determines the total amount absorbed, $Q(t)_{ss}/t_{ss} = J_{ss}.A$), the systemic (dermal first-pass) bioavailability F_{sys} and the drug's systemic clearance CL_{sys}, i.e. $C_{ss,blood} = F_{sys}J_{ss}.A/CL_{sys}$. F_{sys} will only equal F_{local} when there is no further loss of drug due to metabolism, sequestration, carriage to deeper tissues etc before entering the systemic circulation.

A fuller, commonly used expression for the amount of solute permeating across the skin $Q(t)$ applies at all times t after application for a drug from a product vehicle (v) at a constant donor concentration $C_{o,v}$ across an assumed homogenous SC barrier into receptor sink conditions (Crank, 1975 p. 51). Here, $Q(t)$ can be expressed into the form:

$$Q(t) = J_{ss}A\left(t - \frac{h_{sc}^2}{6D_{sc}} - \frac{2h_{sc}^2}{\pi^2 D_{sc}}\sum_{n=1}^{\infty}\frac{(-1)^n}{n^2}exp\left(\frac{-D_{sc}n^2\pi^2 t}{{h_{sc}}^2}\right)\right) \quad (2)$$

where J_{ss} is the steady-state flux and D_{sc} is the diffusion coefficients for a drug diffusing across an SC of thickness h_{sc} and t is time. At very long times, where $t\rightarrow\infty$, $\exp(-\infty) = 0$ and the last term in Eq. (2) drops out to leave a much simpler expression, that describes a straight line after a delay, as shown in Eq. (3):

$$Q(t) = J_{ss}A\left(t - \frac{h_{sc}^2}{6D_{sc}}\right) \quad (3)$$

with a slope of $J_{ss}A$ and an intercept on the x-axis defined by a lag time lag_{sc}:

$$lag_{sc} = \frac{h_{sc}^2}{6D_{sc}} \quad (4)$$

The steady-state flux is also generally expressed in terms of $C_{o,v}$, the SC-vehicle partition coefficient K_{sc} and the SC permeability coefficient for a given vehicle, $k_{p,v}$ as shown in Eq. (5):

$$J_{ss} = K_{sc,v}\frac{D_{sc}}{h_{sc}}C_{o,v} = k_{p,v}C_{o,v} \quad (5)$$

Under thermodynamically stable conditions, the maximum flux of a drug $J_{max,v}$ is defined by its saturation solubility in the vehicle applied. So that for an aqueous solution when $v = aq$, this saturation solubility is S_{aq} and $J_{max,aq}$ is given by:

$$J_{max,aq} = K_{sc,aq}\frac{D_{sc}}{h_{sc}}S_{aq} = k_{p,aq}S_{aq} \quad (6)$$

Obvious larger fluxes may be observed under supersaturation conditions as reported in several studies. The fuller form of Eq. (1) also includes an extra term on the denominator to reflect back-flux when sink conditions do not exist below the target site possibly due to poor solubility in deeper tissues, such as in the dermis, reducing $C_{ss,local}$ [74]. CL_{skin} will also be defined by both diffusion away from the site, associated metabolism/active transport processes (which is often heterogeneous in distribution, e.g. CYP1A1 mainly found in stratum basale whereas CYP1B1 is found elsewhere; both are in the dermis [75]), local blood and lymphatic flow, and potential recirculation from the systemic circulation back into the skin (Fig. 4).

4. Modeling drug permeation through the stratum corneum (SC).

We now consider each of these aspects in more detail and begin with drug permeation across the main barrier for skin permeation, the stratum corneum (SC), and the *in-silico* prediction of drug transport across the SC.

4.1. In silico prediction of permeability

Most of the studies on topical drug delivery have focused on epidermal permeation and, as shown in Table 2, the drugs are quite variable in size (as defined by molecular weight, *MW*, or molecular volume, *MV*), melting point (*MP*), lipophilicity as defined by the logarithm of their octanol–water partition coefficient (log *P*), solvent solubility and the number of hydrogen bond donor (H_d) and acceptor (H_a) bonds they will form. In principle, the maximal skin permeation flux ($J_{max,v}$) for any drug is given by the product of its solubility in the *stratum corneum* (S_{sc}) and diffusivity in the *stratum corneum* (D_{sc}), divided by the pathlength for diffusion in the *stratum corneum* (h_{sc}), where $J_{max,v} = S_{sc,v}\ D_{sc}/\ h_{sc}$ [41] and these can be estimated using these physicochemical properties for the drug and the skin. It was Gene Cooper's group that first showed that the maximum steady-state flux of drugs across the skin was defined by the drug's molecular volume and octanol solubility [52,53]. An important observation made by Kasting in 2013 [53], and not often appreciated by those of us who have used his data from that time, is that, regrettably, his experiments as he described them in 1987 [52] were flawed because both their vehicle (propylene glycol) and receptor phase (1: 1 ethanol: water) enhanced skin permeability.

Using a large dataset derived from solutes delivered from aqueous vehicles, we used a step-wise regression to explore the underlying Quantitative drug Structure skin Permeation Relationships (QSPR) and confirmed that the dominant determinant of a drug's maximum skin flux for aqueous solutions (simply represented here as J_{max}) was the drug's *MW* [56], which had previously been shown to be mainly governed by the free volume for diffusivity of the solutes in the stratum corneum [52]:

$$\log J_{\max} = -3.90 - 0.019\ MW\ (n = 87, R^2 = 0.85) \quad (7)$$

Interestingly, the physicochemical properties of melting point (*MP*), log *P* and estimated solute solubility in octanol (S_{oct}) did not greatly improve the regression (R^2 increased to 0.86 for S_{oct} and to 0.88 for *MP*). These were potentially significant predictors as log S_{sc} should be related to S_{oct} [52] and log S_{sc} to log *P* and *MP* [56] based on log K_m being directly related to log *P* [76] and log S_{aq} related to log *P* and *MP* [77]. However, adding a third covariate of hydrogen bonding acceptor (H_a) with a melting point term (MP^*) did improve the regression to:

$$\log J_{\max} = -4.35 - 0.0154\ MW - 0.293\ MP^* + 0.371\ H_a \quad (n = 87, R^2 = 0.92) \quad (8)$$

Fig. 5A shows that these latter terms have removed the 5 outliers seen in the regression for *MW* only (Eq.7).

Bouwman *et al.* [78] investigated the applicability of 33 QSAR models in regulatory risk assessment on their test dataset and filtered these models that satisfy the five OECD principles for QSAR models: (1) a defined endpoint, 2) an unambiguous algorithm, 3) a defined domain of applicability, 4) appropriate measures of goodness-of-fit, robustness, and predictivity and 5) a mechanistic interpretation, if possible. They found that the Magnusson *et al. MW only* model (Eq. 7) gave better predictions than the other suitable/selected models they considered, such as McKone and Howd [79], Moss and Cronin [80], and SKINPERM [81] models. Further, the Magnusson *et al.* [56] model is widely applicable and had passed external evaluation/validation because the model was developed using solutes with a wide range of physicochemical properties. Milewski & Stinchcomb (2012) [82] analyzed this same Magnusson *et al.* dataset [56] for J_{max} with a more common, but indirect method, based on the highly cited Potts and Guy equation (Equation (2)) [55]. Here, the SC epidermal permeability coefficient from aqueous solutions ($k_{p,aq}$) expressed in cm/hr from the Flynn dataset [54] (Fig. 2) were related to log *P* and *MW* as shown in Eq. 9. Here, $k_{p,aq}$ is estimated from the steady-state epidermal flux for a drug at a given drug concentration in the aqueous solution divided by that concentration or, for a saturated aqueous solution, $k_{p,aq} = J_{max}/\ S_{aq}$. A key assumption made in this work and throughout this review is that transport in the viable epidermis is generally not rate-limiting. However, there are several studies [83,84], including our own [85,86], which show that this is not always the case.

$$\log k_{p,aq} = 0.71 \log P - 0.0061\ MW - 2.7\ (n = 93; R^2 = 0.67) \quad (9)$$

where it also follows that $k_{p,aq}$ equals $K_{sc,aq}\ D_{sc}/\ h_{sc}$, where $K_{sc,aq}$ is the stratum corneum-water partition coefficient, which in a saturated aqueous solution, is given by: $K_{sc,aq} = S_{sc}/S_{aq}$. Many studies have also reported that $K_{sc,aq}$ has a dominant dependence on log *P* [76,83,84,87,88] described most simply by [76,87]:

$$\log K_{sc,aq} = -0.024 + 0.59 \log P \quad \left(n = 45;\ R^2 = 0.84\right) \quad (10)$$

A major step forward was made by Raykar *et al.* [89], who recognized that drugs could partition into both the protein and lipid domains of the SC. This work was then applied in examining the transport of a series of drugs across the SC [90]. The SC partitioning concept was then taken further forward by Nitsche *et al.* [88], who concluded that a two-phase model is preferred to conventional relationships as described in Eq. 10. Eq. 11 shows a recent example of this two-phase model based on the available data [91]:

$$K_{sc,aq} = \phi_{pro}\frac{\rho_{pro}}{\rho_{aq}}K_{pro} + \phi_{lip}\frac{\rho_{lip}}{\rho_{aq}}K_{\mathrm{lip}} + \phi_{aq} = 0.0284\ P^{0.69} + 1.082\ P^{0.31} + 0.782 \quad \left(n = 95;\ R^2 = 0.79\right) \quad (11)$$

where ρ_{pro}, ρ_{lip} and ρ_{aq} represent the bulk density of protein, lipid, and water with values of 1.37, 0.9, and 1 g/cm^3; ϕ_{pro}, ϕ_{lip} and ϕ_{aq} are the average volume fractions of protein (0.187), lipid (0.0316) and water (0.782) phase in fully hydrated SC respectively, with solute partition coefficients for SC from water ($K_{sc,aq}$), SC protein-water (K_{pro}) and SC lipid (K_{lip}) being related to *P*, the octanol–water partition coefficient ($=10^{\log P}$).

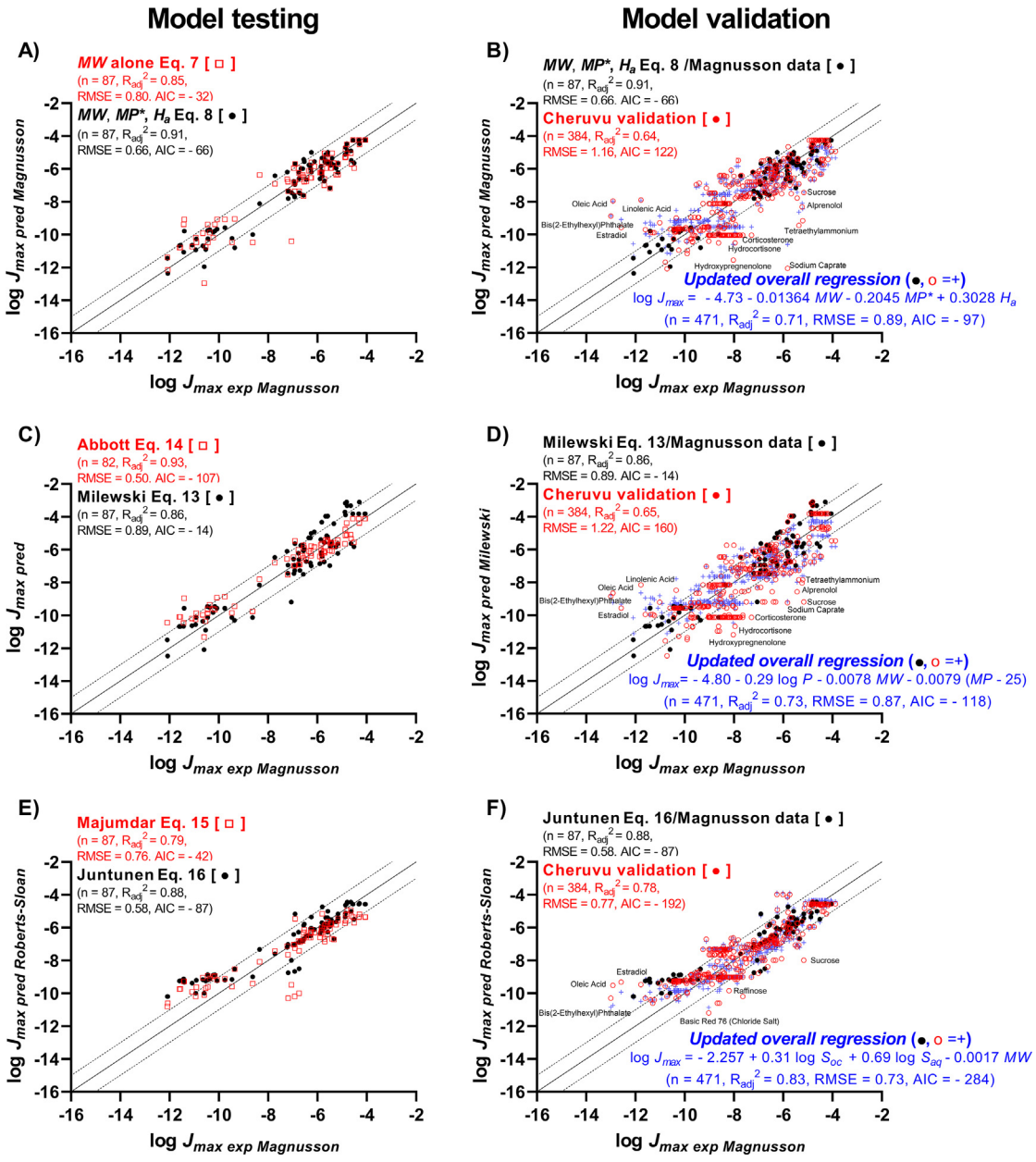

Fig. 5. . Predicted versus observed relationships for solute epidermal J_{max} with various QSPR models using the Magnusson *et al.* training dataset of 87 records in Fig. 5 A, C, and E, and in Figs. B, D, and F, a model external validation using subsequently published aqueous solution data for 384 records from [107]. Also included in Figs B, D and F is a model update using the combined dataset of 471 records. The individual panes are A) Predicted Magnusson *et al.* [56] J_{max} models for *MW* alone and Eq. *MW*, *MP** and H_a versus experimental J_{max} based on *et al.* aqueous training dataset, B) Validated Magnusson *et al.* Eq. *MW*, *MP** and H_a using Cheruvu *et al.* [107] dataset showing the updated overall regression equation, C) Predicted J_{max} of Abbott (Eq. 8) and Milewski (Eq. (6) in [82] adjusted the units of J_{max} to mol/cm^2/h) models versus experimental J_{max} based on Magnusson *et al.* aqueous training dataset, D) Validated Milewski Eq. using Cheruvu *et al.* [107] dataset showing the updated overall regression equation, E) Predicted J_{max} of Roberts-Sloan Eqs. 15 and 16 published in Majumdar *et al.* [100] and Juntunen *et al.* [101] reports respectively versus experimental J_{max} based on Magnusson *et al.* aqueous training dataset, and F) Validated Juntunen Eq. 16 of Roberts-Sloan model using Cheruvu *et al.* [107] dataset, showing updated overall regression equation. The solid black line indicates line of identity while black dashed lines enclose the region of an ideal correlation ± 1 log unit. The blue color plus symbols indicates the predicted values based on the updated overall regression equations using the sum of the Magnusson *et al.* aqueous training and Cheruvu *et al.* validation data sets shown in B, D and F. (For interpretation of the references to color in this figure legend, the reader is referred to the web version of this article.)

A large number of other relationships between $k_{p,aq,}$ and physicochemical properties of solutes have been described, including the solvatochromic [92–94], molecular group contribution [95], and solubility parameter [96]. Kasting has pointed out that the product of $k_{p,aq,}$ and S_{aq}, in turn, also define J_{max} per unit area prediction for hydrated human skin that encompasses the full range of solutes, i.e. from the very polar to the very lipophilic [53]. This relationship, defined earlier by Higuchi [43], was formally tested by Milewski and Stinchcomb [82], who used the general aqueous solubility model for S_{aq} (in mol L^{-1}), where *MP* is in °C [97]:

$$\log S_{aq} = -0.012\,(MP - 25) - 1.031 \log P + 0.424 \qquad \left(n = 580,\ R^2 = 0.97\right) \qquad (12)$$

describing J_{max} (here, in mol cm^{-2} h^{-1}) in terms of $k_{p,aq}$ values in a multiple linear regression of a training (n = 87) and validation

(n = 121) (total 208) dataset, the same dataset used in Eq. 7 [56]. They obtained as a resulting expression for J_{max}:

$$\log J_{max} = \log k_{p,aq} + \log S_{aq} = -4.4 - 0.219 \log P - 0.0086\, MW - 0.0102\,(MP - 25) \quad \left(n = 208,\ R^2 = 0.81\right) \tag{13}$$

A more direct method, described by Steven Abbott [98], also used the Magnusson *et al.* dataset [56] to estimate S_{sc} using 3D Hansen solubility parameters and assume D_{sc} is inversely proportional to drug size (*MW or MV*). This work takes advantage of the prior Hansen dipole (D_d), polar (D_p), and hydrogen bonding (D_h) parameter estimates for skin lipids of 8.0, 6.1, and 5.4 with a radius of 2.45 from the skin permeability for the four solvents DMSO, NMP, DMF and DMAC through human skin [99] and the ideal solubility of a drug in water (X_i), given by the first term in Eq. 12. Abbott also used the Magnusson *et al.* [56] dataset from aqueous vehicles and found by regression [98]:

$$\log J_{max} = -3.00 - 0.0093\,(MP - T_{exp}) + 2.06.e^{-5} MV * HSP_{distance} - 0.071\, MV^{0.748} \quad \left(n = 284,\ R^2 = 0.87\right) \tag{14}$$

where solutes with *MP* above the experimental temperature T_{exp} are solids at (i.e. $MP > T_{exp}$), with this term dropping out to 0 for those solutes which are liquid at T_{exp}, $HSP_{distance}^2 = 4(Dd_1\text{-}Dd_2)^2 + (Dp_1\text{-}Dp_2)^2 + (Dh_1\text{-}Dh_2)^2$ and subscripts 1 & 2 represent the skin and drug, respectively. Abbott's results essentially confirmed the findings of Magnusson *et al.* [56] that *MP* is a significant covariate to J_{max} in addition to *MW* but had a small impact on the overall dominant dependency of J_{max} on *MW*. Fig. 5C shows that, whilst the overall regression is similar for the Milewski and Stinchcomb [82] and Abbott [98] models, the pattern of residuals for individual solutes from the line of identity differ.

Ken Sloan's team developed an alternative QSPR strategy in which they explicitly regressed J_{max} against S_{oct} and S_{aq} of solutes as well as *MW*. Their first (Roberts-Sloan) analysis yielded a QSPR of [100]:

$$\log J_{\max} = -3.008 + 0.732 \log S_{oc} + 0.268 \log S_{aq} - 0.00481\, MW (n = 62, R^2 = 0.93) \tag{15}$$

Their QSPR was then slightly different when tested using an extended database [101]:

$$\log J_{\max} = -2.506 + 0.538 \log S_{oc} + 0.462 \log S_{aq} - 0.00402\, MW (n = 185, R^2 = 0.84) \tag{16}$$

Here, we evaluated these regression equations using the same 87 solute Magnusson et al training data set and obtained the results shown in Fig. 5E. It is apparent that whilst the overall regression appeared to be similar to the earlier ones for Magnusson et al., Milewski and Stinchcomb [82] and Abbott [98] models to the same their extended model had similar regressions to the other models shown in Fig. 5A and C and had removed the group of outliers below the line of identity seen for their initial model (Fig. 5C). Given the similarity of these quite different QSPR regression models, the advantages that one method offers over another are not clear. This question is important given that some authors have suggested that the solubility parameter approach may be preferred over the Potts-Guy approach, for example, in predicting NSAID skin permeability [102].

Gramatica et al. [103] have pointed out that the value of QSPR models in not so much in their ability to describe data (as defined by R^2) but in being able to predict the epidermal permeation for unknown solutes. In their view, whilst internal validation is important, the effective predictive capability of a model is better defined through its generalisability, i.e. external validation. This is traditionally done by splitting an original dataset, as was applied to the Magnusson *et al.* dataset by Milewski and Stinchcomb [82] to arrive at Eq. 13. Blind external validation involves analysis of new samples from an independent dataset, desirably with an adequate statistical power and different investigators to balance optimism from model overfitting with (often) small sample size and to maximize the model's generalisability [104]. Such an approach has been used in Quantitative Structure-Permeability Relationships (QSPR) [105] and has been advocated in Quantitative Structure-Activity Relationships (QSAR) for activity [106]. The subsequent publication of many epidermal permeation studies has allowed us to create a new external database, that we describe in our accompanying paper [107], and that enables us to undertake a blind test external evaluation of previously defined QSPR findings. The accompanying database consists of the maximum fluxes and epidermal permeability for 144 drugs, xenobiotics, and other solutes from aqueous solutions, yielding 471 individual permeability values. Here, we used this data to further develop and validate the relationships discussed above and shown in Fig. 5A, C and E for the Magnusson *et al.* [56] dataset. Here, we apply the new Cheruvu *et al.* 384 dataset values [107] to provide external validation for each model in Fig. 5A, C, and E.

Fig. 5B, D, and F show that the adjusted R^2, RMSE, and AIC with the new dataset [107], that define the predictive accuracy for each model, is lower than had been forecasted by the full Magnusson, Milewski, and Stinchcomb and updated Roberts-Sloan equations using the Magnusson *et al.* training dataset [56]. The updated overall regression equations for the combined dataset (n = 471, based on Magnusson *et al.* [56] aqueous training dataset (n = 87) plus the Cheruvu *et al.* [107] new validation dataset (n = 384)) are shown in Fig. 5B, D and F. Here the corresponding new regression equations based on the best fit models of Magnusson *et al.* [56] (Eq. 8), Milewski & Stinchcomb [82] (Eq. 13) and Roberts-Sloan model from Juntunen *et al.* [101] (Eq. 16) are shown in Eqs. 17, 18 and 19 respectively:

$$\log J_{\max} = -4.73 - 0.01364\ MW - 0.2045\ MP^{*} + 0.3028\ H_a \quad (n = 471,\ R_{adj}^2 = 0.71,\ \text{RMSE} = 0.89,\ \text{AIC} = -97) \tag{17}$$

$$\log J_{\max} = -4.80 - 0.29 \log P - 0.0078\ MW - 0.0079\,(MP - 25) \quad (n = 471,\ R_{adj}^2 = 0.73,\ \text{RMSE} = 0.87,\ \text{AIC} = -118) \tag{18}$$

$$\log J_{max} = -2.26 + 0.31 \log S_{oc} + 0.69 \log S_{aq} - 0.0017\ MW \quad (n = 471,\ R_{adj}^2 = 0.83,\ \text{RMSE} = 0.73,\ \text{AIC} = -284) \tag{19}$$

Importantly, based on regression statistics and outlier distribution the Roberts-Sloan model appears to describe Cheruvu *et al.* new data [107] better than the other models. A key challenge in this area is that when the external validation suggests that the initial model's predictions are not as robust as originally forecasted, as is evident for the QSPR models in Fig. 5B and D, such differences have invariably led to the original model being rejected. A common approach is then to replace it by a new one based on the new data only, but with the same aim [108]. A key consideration then is the potential need for recalibration to adjust for potential data differences in, for instance, study temperatures as well as to understanding temporal (later, new data from same laboratories as in original study), geographical (data from other laboratories) and domain (drug data with very different physicochemical properties to the original database) variability. We have also included in Fig. 5B, D and F updated predictor regression coefficients for each of the models using the entire Cheruvu database (i.e. Magnusson *et al.*

data [56] plus new data). It is evident that the updated regressions don't greatly improve the regression statistics, suggesting that the original equations were appropriate for the physicochemical properties described.

Also identified in Fig. 5B, D and F are the significant outliers. Interestingly, the same outliers are evident for each of the models and include estradiol, oleic acid, and bis(2-ethylhexylphthalate) above the line of identity with certain sugars below the line. Further, the steroid outliers and ionized solutes evident as outliers in Fig. 5B and D don't appear as such in Fig. 5F. Accordingly, it could be argued that an additional parameter should be added to Fig. 5B and D to address this deficiency, recognizing that such models would also need to be externally validated [108]. Other analyses have also included log *P* and *MW*, *MP* [109], H_a and H_d [80,110], $MW^{2/3}$ [111,112], expressions for two pathways [78,81,113], and, as discussed later, non-linear QSPR models [114]. Lian *et al.* [112] have suggested that $k_{p,aq}$ predictions based on Abraham descriptors [76,87,92,93] have collinearity and lack a mechanistic explanation. However, it is only in the Roberts-Sloan model that S_{aq} appears as a parameter. In work using 114 compounds from the Fig. 2 dataset and their prodrugs, Sloan *et al.* related log J_{max} to the logarithm of the drug octanol solubility log S_{oct}, log $S_{aq,}$ and *MW* with an r^2 of 0.887 [115]. This analysis suggests that J_{max} for any potential drug candidate for topical delivery is defined by its solubility in the SC (and, in turn, mainly by its *MP*, $S_{aq,}$ and S_{oct}) and diffusivity in the SC (mainly defined by drug size, i.e., *MW* or *MV*).

Scheuplein and Blank [30] noted some 50 years ago that "*hydrated stratum corneum has an affinity for both water-soluble and lipid-soluble compounds…, its unique, encompassing solubility characteristics cannot adequately be duplicated over the full range of polarity by any lipophilic solvent. For this reason previous attempts to predict permeability constants generally from limited correlations found with olive oil: water or ether: water partition coefficients proved unsuccessful.*" The Roberts-Sloan model, in including both S_{aq} and S_{oct}, meets these criteria. This model also suggests that the best drug candidates for topical delivery are those which are small (*MW* <500 Da), moderately lipid in nature (log *P* from 1 to 4) and have reasonable S_{aq}. However, the regressions found in the Roberts-Sloan model are associated with a considerable scattering of data around the line of identity and it is possible that other drug physicochemical parameters not tested here but which have been shown to affect skin flux, such as hydrogen bonding [76] and melting point (*MP* <200 °C) may also be important determinants of a drug's maximum skin flux.

The scatter plots shown in Cheruvu *et al.* [107] suggest that the further update of the equations described here should also include a log P^2 term, consistent with the maximal parabolic relationship with log *P*, as first shown by Lien and Tong [45,116] and later shown to be the main determinant in J_{max} variation for solutes of similar size [117]. The practical application is that the likely steady-state amount $Q(t)_{ss}$ of a drug penetrating per unit area of skin in time (i.e., the steady-state flux J_{ss} for that drug) is simply the product of the J_{max} and fractional solubility in the product, where fractional solubility is given by the actual concentration of drug in the product divided by its total concentration. Further, the parabolic relationship with log *P* (Eq. 11, [117]) implies that the optimal solubility of a drug in the SC will be for those drugs that best dissolve in SC lipids at optimal log *P*. Then follows that because J_{max} is directly related to S_{sc} [117], an optimal J_{max} will be for those solutes most soluble in SC lipids.

Pecoraro *et al.* has recently presented an excellent overview of the reliability and caveats that need to be applied in using the *in silico* QSPR approach described above [114]. As they point out, there is a danger in regarding drugs such as Scheuplein's set of steroids [118] as outliers when they differ from results from other laboratories [119] but, as large hydrogen bonding drugs, are accommodated by global QSPR analyses of skin permeability datasets containing a more diverse group of chemicals [80]. Further, even if the physicochemical determinants of molecular size and acceptor hydrogen bonds [120], which both contribute to parameters like log *P*, are theoretically decoupled, that does not avoid the intercorrelation present in the "drug-like" database used to interrelate experimental data with these determinants. They also suggest that QSPR analyses should also include robustness and predictivity in assessing regression quality in addition to the goodness of fit measure shown above.

In general, most human skin QSPR studies have assumed that steady-state SC transport can be described by a one dimensional, homogenous diffusion model or approximation thereof when SC transport is much more complex. However, in reality, there are a number of barriers, transport pathways, binding sites, and milieu a drug must cross, weave through obstacles in SC diffusion pathways, and transition into and out of in crossing the SC. Further, as discussed in 3.2, the SC morphology varies with its depth. Pecoraro et al have recently compared the outcomes from non-linear and linear QSPR models describing SC permeability [114]. The non-linear models included artificial neural networks, random forest, and Gaussian regression models. In one example, Sun *et al.* [121] applied a range of non-linear methods to relate human skin permeability coefficients to five molecular descriptors (*MW*, solubility parameter, log *P,* and the number of hydrogen acceptor and donor bonds) using the Flynn database (Fig. 2). The methods included K-nearest-neighbour regression, single-layer networks, the mixture of experts, and Gaussian processes. Of these, Gaussian processes outperformed all other methods including the Potts-Guy relationship [55] in describing the Flynn data [54], with a canonical correlation analysis showing that the variables were not linearly related [121]. Their observation that skin QSPRs are best described by non-linear Gaussian processes is consistent with recent efforts to recognize that there is a statistical variability in SC drug transport mechanisms [122].

That being said, most non-linear QSPR models for skin permeation have applied a "black box' approach and don't recognize, for instance, the possible differing skin partitioning, retention, and permeation behavior between lipid, polar and ionized drugs and the impact of topical formulation on these processes. Further, as noted by Cronin and Schultz, nonlinear QSPR models may be prone to over-fitting and modelling data error [123]. Therefore, as discussed by Pecoraro *et al.* [114], internal cross-validation, now characterized using QLMO2 (leave-many-out) or bootstrap methods, the root mean square errors (RMSE and $RMSE_{CV}$) and external validation are also required. We would further suggest that a Visual Predictive Check (VPC) and its associated outlier analysis, as used earlier in analysing the data in Fig. 5, is another important validation step.

4.2. Physiologically Based – PharmacoKinetic (PBPK) modeling of drug transport through the SC into and through deeper tissues

Essentially, three types of dermal PBPK models are commonly used in modeling SC transport:

(1) *Analytical one dimensional (1D) diffusion* in each skin layer and in the appendages, pioneered by Scheuplein [30,48,51], and developed for a number of scenarios, as summarized by Anissimov & Roberts [74];

(2) *Stirred compartment representation of the skin (and later its layers and appendages) and the body* [28,74,124], evolving into a series of compartments to represent various skin and deeper tissue layers, linked to compartments representing the body and including recirculation to the skin [125,126]. This approach is also used in the modular compartment representation of skin layers, appendages, and the body and its organs, that has been further developed

and incorporated as the modules MechDermA® PBPK and Transdermal Compartmental Absorption & Transit (TCAT™) in Certara's Simcyp [127,128] and Simulations Plus's GastroPlus® [129] widely available population PBPK software.

(3) *More faithful representation of skin morphology and transport processes with 2D and 3D modelling*, supported by relatively complex and computationally intensive, finite element simulations [130–135] and summarised by Wen *et al.* [136].

Each of these model types has pluses and minuses. For instance, diffusion models can simply and accurately describe the space and time dependence of transport processes in the product, in all layers of the skin, and in the appendages. The most commonly used form of this model is a steady-state approximation in which the linear portion of a plot of cumulative amount permeated through the skin from a constant donor solution defines a steady-state flux, and the lag time is determined by back extrapolation of the line to a zero amount. Approximations to define the peak flux, time of peak flux, terminal half-life, and amount absorbed, i.e., paralleling the commonly used pharmacokinetic parameters of C_{max}, t_{max}, $t_{1/2,}$ and *AUC*, have also been defined for the finite dose model [74].

Early PBPK model development. Traditionally, SC permeation had been thought up to the mid-1970s as occurring by diffusion through SC, viable epidermis, and dermis as homogenous barriers. SC transport was postulated to have a polar and lipid pathway, augmented by follicular permeation at early times [30], with successive diffusion across intercellular lipid lamellae and corneocytes in sequence [137]. Michaels *et al.* [49] introduced in 1975 an idealized representation of the SC as a staggered "brick and mortar" structure, with no offset in brick staggering. Here, the corneocytes are the bricks and the mortar was the intercellular lipids, similar to as shown in Fig. 4B. They proposed that, as well as transcellular transport, SC transport could also occur solely via diffusion through the SC intercellular lipid phase, in a process dependent on the effective pathlength through the tortuous lipid pathways around the corneocytes. That, along with the very small area for lipid transport between the cells compared to corneocyte surface area, would require a SC lipid diffusivity about 600 fold more than for bulk diffusion [51]. Albery and Hadgraft [138] appear to be the first to propose permeation of solutes through the SC primarily via the SC intercellular lipid route. Their work is based on a theoretical analysis of their data for the *in vivo* percutaneous absorption of 3 nicotinic acid esters. They suggested that any drug with an intercellular lipid to corneocyte ratio of more than 6 would permeate via the intercellular lipid route. This finding was supported by the experimental *in situ* precipitation electron microscopy butanol data of Nemanic and Elias [139].

In parallel, diffusion-based models began to be derived for topical delivery [140] and transport of drugs through the skin [138,139–143]. Most of these models described the transport of solutes in the SC and viable epidermis (including metabolism) [142] after topical application in the Laplace domain, with short and long time analytical approximations. Bunge has also presented analytical (series) solutions [83,84] while we have solved these models using numerical inversion of the Laplace transforms to characterize changes in the amount of solute transport through excised human epidermal membranes [74]. In all cases, we have recognized that Laplacian and analytical forms of the diffusion models may be intractable when there is a multitude of processes or non-linearities in concentration and time.

Given the complexities associated with the diffusion model, a number of studies have sought to use compartmental models as alternative representations of the diffusion process. Riegelman (1974) [28] was one of the first to apply compartmental modeling to interpret plasma concentrations and urinary excretion of drugs after dermal absorption in terms of competing absorption and elimination processes. Guy *et al.* (1982) [144] then developed a more sophisticated 3-compartment dermal PBPK model and we linked a series of compartments, representing skin and deeper tissue layers, to the body [125,126]. Bunge [145–147] then presented a rational strategy for "converting" diffusion models to stirred compartment models with clearly defined assumptions as well as strategies for choosing the best fit-for-purpose PBPK compartment model. A further modelling advance was the integration of modular "well stirred" dermal layer and appendage compartment "sub" models into physiologically based pharmacokinetic models developed for other inputs into the body. These models, such as Certara's Simcyp MechDermA PBPK model, are growing in popularity because of their ready availability and ease of use, with inclusion of various known or estimated physiochemical and physiological data, QSPR and dose form release equations, enable sensitivity analyses of various parameters being used as necessary. This model is discussed again later in this review.

More recently, a team led by Anissimov has proposed a compartment-in-series approach as a simplified representation of diffusion in each skin layer [148]. We have now used this model for a range of applications such as demonstrating its equivalence to a diffusion model to describe IVPT-*in vivo* relationships for urinary excretion, plasma concentrations, and solvent deposited solutes [86]. An advantage of this compartment approach is that it can enable the concept of modularity and has the capacity of adding further compartments (as shown by Anissimov & Roberts for the liver [149]) to become a finite volume 2D and 3D representation of the SC and other skin layers.

Further considerations in the mechanistic transport by the SC intercellular lipid pathway. When SC transport is assumed to occur into and out of SC lipids with permeation into and out of the corneocytes along the way with the transport through the SC via lipids only (Fig. 4B), the permeability coefficient term in Eq. (5) should be expressed in terms of the effective drug diffusion coefficient in the SC intercellular lipids D_L, the partition coefficient of the drug between the product and the SC intercellular lipids K_L, the intercellular path length h_l and the ratio of the area of lipids on the SC surface to that of the SC, assuming it behaves as a homogenous membrane [103]:

$$k_{p,aq} = \frac{J_{sc,ss}}{C_o} = \frac{K_L D_L}{h_L}\frac{A_L}{A_{sc}} \tag{20}$$

Many authors have re-expressed Eq. 17 in terms of the SC thickness h_{sc} by defining a lipid pathway tortuosity $\tau^* = h_l/h_{sc}$, so that the effective lipid diffusion pathlength is given by $\tau^* h_{sc}$ and the steady-state permeability coefficient $k_{p,aq}$ for a solute permeating through the SC by only the intercellular lipid pathway may be expressed as [111]:

$$k_{p,aq} = \frac{K_L D_L}{\tau^* h_{sc}} \tag{21}$$

A value of $\tau^* h_{sc} \sim 3.6$ cm has been reported for 15 layers of SC with a thickness of 13.1 μm (i.e. $\tau^* \sim 2740$ [150]). It has been suggested that > 82% of τ^* comes from lateral diffusion in the layer of SC lipids (~0.075 μm thick) above and below the longest corneocyte (~40 μm) edges and the rest (<18%) from getting into, through and from the vertical lipid paths (~0.075 μm wide) between the shortest (~0.8 μm) edges of the corneocytes and when SC transport has no resistance [111,150]. Talreja *et al.* estimated a lower geometrical tortuosity of 12.7 ± 2.3 (SD), using alkali expanded stained human SC microscopy and similar thicknesses for corneocytes and lipid lamellae [151]. Frasch and Barbero [103] have estimated that the SC lipid pathway associated with going around ~40 μm corneocytes would be about 37.4 times that for h_{sc}. The experimental values of K_L for lipid-water systems can be related to a drug's octanol–water partition coefficient (P) by $K_L \sim P^{0.7}$ [111] (with the exponent reported to also range from 0.71 to 0.86 [150] and

$D_L \sim 2 \times 10^{-5}.\exp(-0.46.\ r^2)$, where r is the drug radius [111]. Johnson *et al.* have noted that D_L shows an approximate dependence on molecular weight to about 350 Da with a lesser dependence thereafter. Thus, with a D_L of $\sim 10^{-7}$ cm^2 sec^{-1} for a 150 Da drug, the lag time for that drug to reach lateral diffusion equilibrium in a uniform staggered corneocyte and lipid structure (i.e. no offset yields a half corneocyte width $h_c/2$ of 20 μm, i.e. 0.002 cm) is $(h_c/2)^2/(6.D_L)$ [152] ~ 6 sec, about 100 times less than the lag time of 10 to 15 min for the transport of alcohols [30] and phenols [46] of this size across the SC. Kasting and Nitsche [153] also point out that experimentally determined drug lateral diffusivity in lipids [150] underestimates observed SC lag times. Thus, there must be an additional SC barrier to the lateral diffusion of solutes in the SC lipids around corneocytes for solutes being transported solely by this pathway.

Lars Norlen, in personal communication, has highlighted the observed thin linker regions in the SC extracellular lipid space [154], shown in Fig. 6A1 to 4. The SC extracellular lipid space varies in thickness depending on how many repeat lipid bilayers are present in any given cross-section. Each bilayer, illustrated in Fig. 7, is about ~ 11 nm wide and consists of alternating narrow (~4.5 nm) and broad (~6.5 nm) segments [155,156] that appear as parallel electron-dense lines on cryoelectron microscopy imaging. The number of repeats varies between one and ten parallel electron-dense lines [154], giving SC intercellular region thicknesses of 9 nm (illustrated in Fig. 6A3) to 48 nm, with 2 repeats (4 lines, ~22 nm) and 4 repeats (8 lines, ~44 nm) (also illustrated in Fig. 6 A3) being the most common [155]. Fig. 6A1 and A2 also shows examples where these thick lipid regions extend over 41 mm between mid-SC corneocytes whereas the thinnest linker sections have a length of ~ 250 nm [154]. The other structures that can impede drug transport in the SC extracellular lipid space are tight junctions and corneodesmosomes [157,158] mainly seen in the lowermost cell layers of the stratum corneum and in the stratum granulosum – stratum corneum transition zone, where a key role of the tight junctions is to seal the interface between adjacent SG keratinocytes and SC corneocytes (Lars Norlen, personal communication). In general, as illustrated earlier in Fig. 4A, corneodesmosome density thins out with proteolysis in normal skin so that they a high density on the inner intercellular corneocyte surfaces (i.e. in SC compactum), as shown in Figs. 6A5 and A6 but rather sparse on the outer SC surfaces (i.e. SC disjunctum) (Fig. 6A7). These observations are consistent with corneodesmosomes being proteolyzed and lost in the desquamation process to become absent above the fifth corneocyte layer [70]. The space occupied by the corneodesmosome is then replaced by lipid structures that migrate from the sides and are found as mature SC lipid bilayers with 4 repeats (i.e. 4 × ~ 11 nm, ~44 nm) (Norlen, personal communication). These bilayers, as Fartasch et al [159] has observed, may appear within the remnants of a desmosomal plug and desquamation induced widenening of the stratum disjunctum space may be associated with an increased SC extracellular lipid thickness. In one biopsy from the back, her team showed an example of >100 lipid bilayers at one site [159]. However, SC corneodesmosome distribution varies with body site, treatment conditions and disease. As shown in Figs. 6A8 and A9, corneodesmosomes are found on both the inner and outer SC corneocyte surfaces in winter xerotic skin. A similar, more even distribution of corneodesmosomes is also found in the outer SC of palmo-plantar, soap-induced xerotic, ichthyotic and hyperkeratotic skin [160]. Hyperkeratosis may arise from genetic mutations affecting the corneodesmosome proteolysis machinery and, as exemplified by posriasis, may be associated with scaly skin and the survival of corneodesmosomes into the outer SC. On the other hand, humidity, moisturisers (such as glycerol) and skin peels (such as glycolic acid) promote corneodesmosome breakdown and desquamation [160]. Indeed, Mundstock et al noted that applying a range of oil containing topical products to the SC promoted detachment and, in some cases, loss of the stratum disjunctum [161]. Hence, body site, skin condition and topical products can all impact on corneodesmosome degradation and, in turn, on SC thickness. That is not to say that inducing a thicker SC will necessarily mean a less permeable SC. As noted long ago by Scheuplein and Blank [30], water and other solutes can have a 10 times higher permeability through the thick 400 to 600 μm plantar SC compared to the thin 20–30 μm abdominal SC, with up to 150 times difference in SC diffusion coefficient. However, because of the thicker skin, a solute's lag time across plantar skin may be 10 fold that through the abdominal skin. Our current knowledge of how various solutes vary in their permeability across various body sites is discussed later in Section 8.2.

A key conclusion from this work that impacts on PBPK modelling is that drug transport in SC intercellular lipids will vary with location, be it the SC depth or region (on corneocytes edges versus on corneocyte faces) and the impact of environment, topically applied products and skin disease on corneodesmosomes and on SC lipid barrier properties (discussed earlier in this journal by Joke Bouwstra [162]). This modelling will be further complicated by the possible shunting of drugs through lipid pathways associated with a columnar corneocyte arrangement as shown in Fig. 3E and the possible decrease in SC lipid transport as a result of the transverse lipid diffusivity at intersections of lipids being much lower than transverse diffusion along lipid bilayers, as discussed by Nitsche *et al* [134].

Overall, these observations raise questions of whether it is really the tortuous pathway around the corneocytes that is conventionally thought to limit SC intercellular lipid transport, or whether it is the interconnections between the SC lipids at the corneocyte edges that play a key role in rate-limiting transport. Currently, the correlations between *in vivo* skin permeability for benzoic acid and transepidermal water loss (TEWL) with corneocyte surface area [154] have been attributed to an associated reduction in intercellular lipid diffusion pathlength around the corneocytes [163]. This modelling assumed corneocytes were square-shaped so that for a corneocyte with area A_c, the SC intercellular lipid diffusion pathlength required for a drug to cross around the middle of an individual corneocyte l_c is given by $l_c = \frac{\sqrt{A_c}}{2}$, and the total pathlength l^* to go around n cells in crossing the SC, assuming a very small interstitial space and a corneocyte thickness of ~ 1 μm (Fig. 4B) is [163,164]:

$$l^* = n + \frac{(n-1)\gamma_c\sqrt{A_c}}{2} \tag{22}$$

where γ_c is a shape factor and γ_c = 1 for a square shape. In reality, the corneocyte is not square in shape but is better described as interlinking tetrakaidecahedrons [165,166], with their geometric features considered in some depth by Naegel *et al.* [167]. The shortest pathlength for any drug to go between the centers on the two sides of any regular n-sided polygon is defined by the twice the apothem l_a, given by the distance from the center to the right angle of any side, where $l_a = \sqrt{\frac{A_c}{n\tan\left(\frac{\pi}{n}\right)}}$ [168], also yielding $l_a = \frac{\sqrt{A_c}}{2}$ for a square with $n = 4$ and $tan\frac{\pi}{4} = 1$ and for a hexagon, which appears to better describe the shapes of corneocytes found for different body sites in Machado *et al.* [164], with $n = 6$ and $tan\frac{\pi}{6} = \frac{\sqrt{3}}{3}$, $l_a = 2\sqrt{\frac{A_c}{2\sqrt{3}}} = 1.075\sqrt{A_c}$. Thus, providing the same regular n-sided polygon shape is observed for all corneocytes, relationships like that between TEWL and the reciprocal of pathlength for a number of body sites based on the square root of the corneocyte area are to

be expected. The analysis above also shows that the estimated l_a depends on corneocyte geometry, so much so, that l_a for a hexagon is more than twice that for a square with the same corneocyte area and means that the effective intercellular lipid pathway length l^* to SC thickness h_{sc} ratio, discussed in Section 3.4 will also be twice as long. Interestingly, the coefficient of variation in $\sqrt{A_c}$ of 30.7% is very similar to that for TEWL of 22.3%, deduced from the data in Machado *et al.* [164], suggesting that individual variation in corneo-

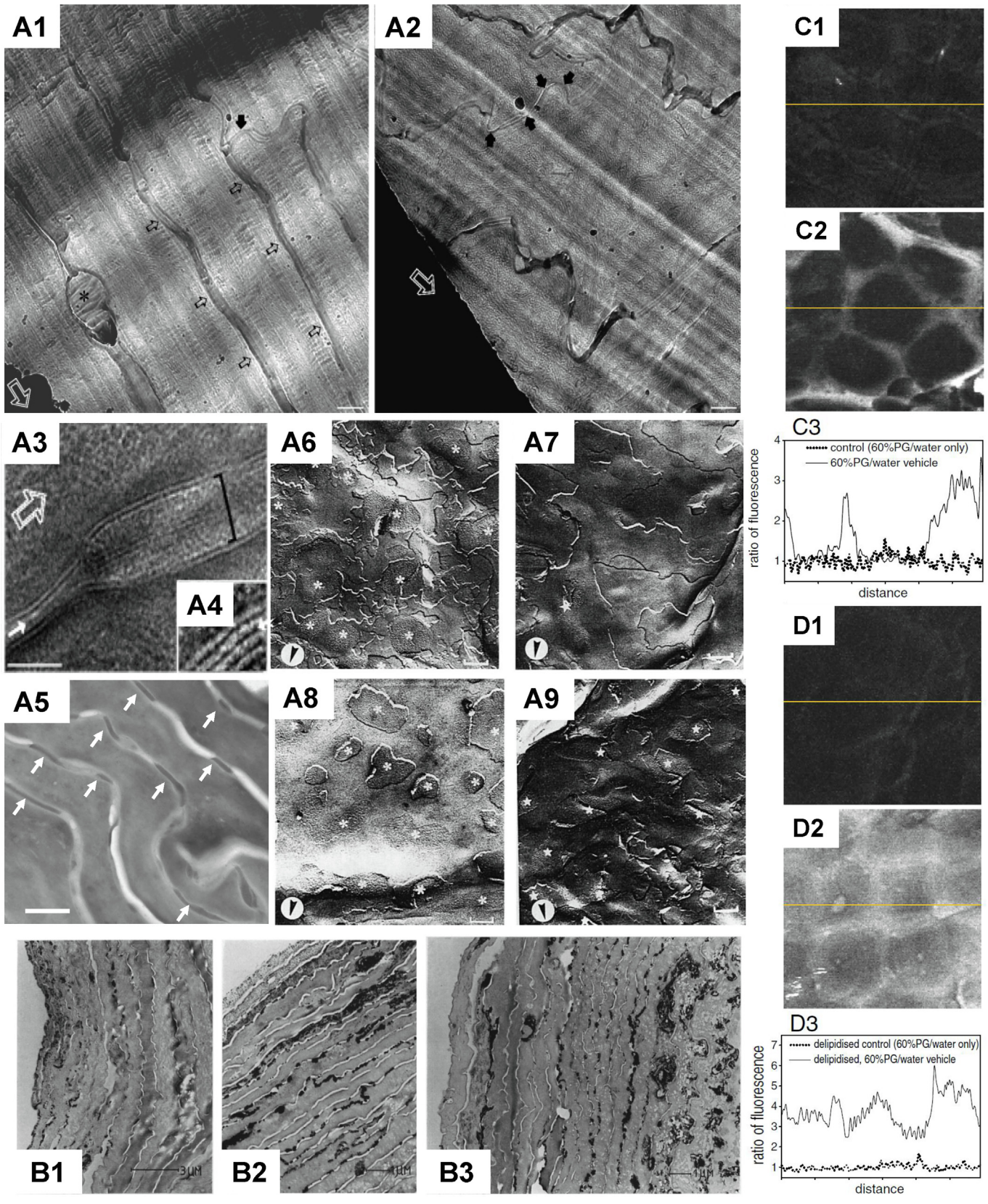

cyte area also determines those individuals' TEWL and likely skin permeation of drugs. Importantly, Machado *et al.* (2010) [164], went on to show a linear relationship between TEWL and the reciprocal of path length for several body sites.

However, following on from the previous discussion on transport pathways through SC lipids, it could also be argued that increasing corneocyte surface area per unit area would also result in an overall reduction in perimeter or corneocyte circumference that defines SC lipid "slit" area per unit area. As the perimeter of a corneocyte of different shapes (e.g. square, circle, and hexagon) is directly related to $\sqrt{A_c}$, the dependency of TEWL and SC drug permeation on corneocyte area can therefore just as easily be explained by corneocyte surface area related alterations in overall intercellular lipid area at the corneocyte edges as can be by corneocyte surface area related changes in SC intercellular lipid pathlength around the cells.

Some of these questions are not straightforward and complex, finite element representation of skin transport in various layers, including SC intercellular lipid transport, has been used by many authors to find answers. The Wittum-Heisig-Naegel-Hansen team has created what is perhaps the best 3D representation of skin transport [165,166]. Alternative models have also been described by Wang *et al.* [132,169], Johnson *et al.* [170], Chen *et al.* [171], Kattou *et al.* [172], and Barbero and Frasch [130]. In their analysis of these models, Barbero and Frasch [130] point out that there is a conundrum in that: "*the most recent models of Wang et al.* [132,169] *and Johnson et al.* [170] *locate the main barrier in the lipid phase, while Naegel-Hansen* [166] *and Chen et al.* [171] *consider the corneocyte phase as the leading barrier*". We suggest that this contradiction arises because of different views of transport in the lipid bilayer. Johnson *et al.* differ from the others in that their model assumes no diffusion through the corneocytes at all. The others consider diffusion in both the lipids and corneocytes. The key difference is whether diffusion in the lipid layers is (or is not) isotropic. Wang *et al.* assume anisotropic diffusion in the lipid layers and diffusion within the corneocytes, whereas Chen *et al.* and Naegel-Hansen assume isotropic diffusion. To fit the experimental data, Wang *et al.* derive parameters describing perpendicular transport across the lipid layers, whereas Chen *et al.* derive parameters for diffusion within the corneocytes. The result of the two approaches is that Wang *et al.* [132,169] predict permeation through the corneocytes whereas Chen *et al.* [171] generally do not. Both models predict the same steady-state values of permeation because both have been fit to essentially the same dataset but, because the two models represent different governing assumptions, they will predict different behaviour in some cases, e.g., the lag time.

Shunting of drugs and xenobiotics across the skin barrier

Drugs may be shunted through the SC by several mechanisms. One, recognized many years ago by Bob Scheuplein, is the transport at early times by hair follicles [173]. This transport has been postulated to be most prominent in the early stages of skin absorption that is evident *in vivo* but, due to skin contraction, may be minimal *in vitro*, as we have shown by modelling the transport of caffeine through open and closed follicles [174]. Discussed later in Section 6 are a number of studies evaluating the hair follicles as a drug transport pathway.

Another is the possible shunting of drugs via a parallel porous pathway, with an estimated pore radius of 15 A^o to 25 A^o [175], which explains under-prediction by the Potts-Guy model of various polar solutes, including sucrose. Drug transport by iontophoresis and low-frequency sonophoresis is associated with similar radii restrictions, leading to a postulate that the polar pathway may be across hydrated intercellular lipid polar head groups [176,177].

Integrating corneocyte permeation, diffusion, and binding into dermal PBPK kinetics.

A further possible shunt pathway is transcellular across corneocytes and interfacing SC intercellular lipids. Most studies to date, including those of Scheuplein [51] and Michaels et al [49] have ignored the potential impact of corneocyte wall permeability. Indeed, Scheuplein [51] explicitly comments in his recent looking back paper: "*Higuchi and Yotsuyanagi included both the cell walls and the intercellular lipid in the cell wall phase (the diffusivity of the cell walls per se seems to have been neglected in recent models; they may yet be shown to be important*". Instead, several studies assume that drugs readily penetrate the corneocytes to make this a viable pathway [49,49,130,130,169]. As we do not have good estimates of the impact of corneocyte permeability (defined by influx and outflux rate constants k_{in} and k_{out}) at this time, we have not addressed this PBPK aspect to any extent here. This task is made all the harder by the realistic and known shunting possible via the appendageal pathways of the follicular and sweat ducts, discussed in a most elegant model comparing SC and shunt transport for polar and lipophilic drugs by Kasting *et al.* [178]. Suffice to say, however, that drug binding to keratin and the associated slow binding desorption kinetics, quantified in a range of studies led by Steffi Hansen [165,165,179] will only be critical to the SC transport for those drugs which have permeated into the corneocytes.

The available imaging data on the extent to which SC corneocyte permeation contributes to overall SC transport is equivocal. The stratum disjunctum and stratum compactum have been long established by histology. Further, as discussed in 3.2, the available evidence is that the stratum disjunctum is affected by changes in hydration status whereas there is little or no change in the stratum

Fig. 6. A. Electron microscopy and other images of the stratum corneum. A1, A2. Cryosection of mid-SC showing extracellular ~ 44 nm thick regions (B, open black arrows) extending over 41 mm (A2, open black arrows), interconnected by greater than 250 nm long, thinner linker regions at corneocyte edges (solid black arrows) and with black asterisks defining an expanded extracellular space in a ~ 50 nm thick section. Scale bar: 200 nm. A3, A4 ~ 9 nm thick linker region containing one line (thin white arrow) associated with an ~ 44 nm thick eight-line region (black square bracket). Scale bar for A3: 50 nm. From [402] with permission of Elsevier. A5. Transmission electron microscopy of normal stratum compactum, with arrows pointing to corneodesmosomes, scale bar 500 nm. Reproduced (CC-BY 4.0) from [161]. A6–A9: Freeze fracture replicas of the intercellular corneocyte surface of normal skin corneodesmosome aggregates (marked with asterix *) have a high density in the inner SC (A4) but are sparse in the outer SC (A5) whereas corneodesmosome aggregates are seen in both the inner SC (A6) and outer SC (A7). In contrast, corneodesmosomes are seen in both the inner SC (A8) and outer SC (A9) in winter xerosis skin. Scale bar: 250 nm. From [160] with permission from Elsevier. [161]. B and C. Images of xenobiotic distribution in SC after topical application. B: Electron microscopy of mercuric sulfide precipitated by ammonium sulfide vapor after application of 5% mercuric chloride (*MW* 271.5; log *P* 0.1): B1. After 1 hr topically - mainly in SC disjunctum lipids, some in corneocytes; B2. After 10 hr topically - more in SC disjunctum corneocytes and deeper, mainly in SC compactum lipids. B3: After 10 hr to the dermal underside of 110 μm dermatomed skin - in SC compactum, mainly in lipids in the intermediate region between SC compactum and SC disjunctum and then in SC disjunctum corneocytes. Reprinted from [180], with permission of Elsevier. C and D: Multiphoton images of β-naphthol (*MW* 144.2; log *P* 2.70) in SC after 4 hr treatment with C1: SC after 60% propylene glycol in water (control); C2: SC after the saturated solution of β-naphthol in 60% propylene glycol in water and D1. Delipidized SC after 60% propylene glycol in water (control); D2. Delipidized SC after the saturated solution of β-naphthol in 60% propylene glycol in water applied to delipidized SC Scale bar shows 20 μm. C3, D3. 2-D plot of intensity (ratio of fluorescence) versus distance across the same position as illustrated by a straight line in the MPM images, from Image J. Reprinted from [404] with permission of Elsevier.

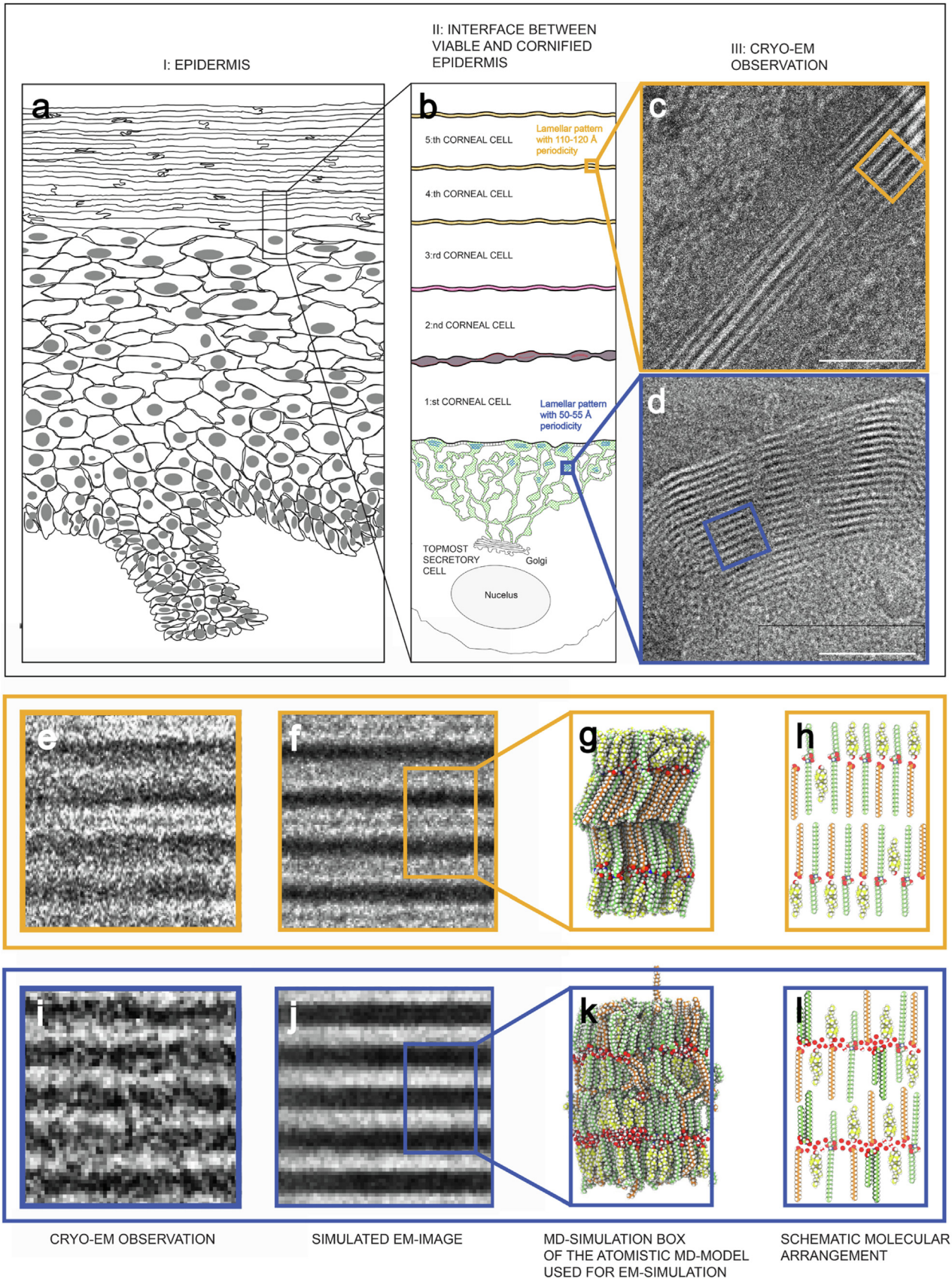
I: EPIDERMIS
II: INTERFACE BETWEEN VIABLE AND CORNIFIED EPIDERMIS
III: CRYO-EM OBSERVATION
a
b
c
d
5:th CORNEAL CELL
Lamellar pattern with 110-120 Å periodicity
4:th CORNEAL CELL
3:rd CORNEAL CELL
2:nd CORNEAL CELL
1:st CORNEAL CELL
Lamellar pattern with 50-55 Å periodicity
TOPMOST SECRETORY CELL
Golgi
Nucelus
e
f
g
h
i
j
k
l
CRYO-EM OBSERVATION
SIMULATED EM-IMAGE
MD-SIMULATION BOX OF THE ATOMISTIC MD-MODEL USED FOR EM-SIMULATION
SCHEMATIC MOLECULAR ARRANGEMENT

compactum. The limited drug and xenobiotic data are also consistent with variations in transport into and through these sublayers. As shown in Fig. 6 B2, mercury distributes mainly into the intercellular lipids in the deeper SC compactum after topical application. However, in the superficial SC disjunctum, mercury also distributes into both the corneocytes and intercellular lipids at short and long times [180] (Fig. 6B1). Further, when mercuric chloride was applied from underneath the SC, there was again a distribution of mercury into both the SC disjunctum corneocytes and intercellular lipids. Harry Bodde's team then went on to obtain reflection contrast microscopy and electron microscopy autoradiographs of 3H-estradiol (*MW* 272.4, log *P* 4.01) and 3H-norethindrone acetate (*MW* 340.5, log *P* 3.66) in human SC after patch application over quite long times. They found again that, in the deeper stratum compactum layer, both estradiol and norethindrone acetate were located mainly in the SC intercellular lipid regions whereas in the superficial SC disjunctum they were found in both corneocytes and intercellular lipids [181]. This finding supports our conclusion that the biphasic steady-state SC distribution seen for clobetasol propionate arises from an enhanced stratum disjunctum corneocyte partitioning as a result of the increased permeabilization of the corneocyte envelope during the desquamation process [182]. In contrast, the somewhat more lipophilic Nile red (*MW* 318.37, log *P* 4.62) appears to only penetrate the SC intercellular regions of the human native epidermis [183], a finding confirmed in Fig. 3I. Our multiphoton imaging studies of the SC distribution of the moderately lipophilic (log *P* 2.70) and small (*MW* 144.2) molecule, β-naphthol [285] for relatively short times suggests that it preferentially diffuses through the SC intercellular lipids with negligible permeation into the corneocytes (Fig. 6C2). However, as shown in Fig. 6D2, high concentrations of β-naphthol are evident in corneocytes after SC-delipidization [285], consistent with corneocyte permeation and high keratin binding, as well as by corneocyte uptake after application of aqueous ethanol and in isopropyl myristate solutions [98]. These findings suggest that the transcorneocyte route, with potential intra-corneocyte binding en route, may be facilitated by the use of appropriate skin penetration enhancers. More recent imaging studies have concluded that whereas lipophilic molecules are mainly located in the SC intercellular lipids, polar dyes are found in both SC lipids and corneocytes [184]. Overall, whilst the available imaging data remains limited, the following trends appear to be emerging. Polar solutes with a limited relative affinity for SC lipids can partition into the SC disjunctum corneocytes and possibly bind to intra-corneocyte keratin and other proteins, whereas lipophilic solutes with a high affinity for SC lipids are likely to remain in the intercellular lipid space. However, the SC intercellular lipid route of SC penetration appears to dominate for both groups of solutes in the SC compactum. This imaging data reiterates that the SC is, at least, a biphasic heterogenous barrier.

Further, the high solute SC D_{sc} [415] and the differing asymmetric profiles for niacinamide (log P −0.37) and testosterone (log P 3.32) [416] observed in SC desorption studies are consistent with the stratum disjunctum being more permeable than the stratum compactum [185]. Accordingly, PBPK models based on a SC transport barrier associated with position related heterogeneity in partition, binding, corneocyte permeability and diffusion [185], including variations in lipid transbilayer diffusivity and corneocyte - intercellular lipid partitioning with SC depth [130], are more likely to better describe SC transport mechanistically than an assumed homogeneous model. However, whether that sophistication is justified given the impact of product design, events beyond the SC, skin heterogeneity, known variability in data and desired outcomes (as discussed later) is yet to be ascertained.

Kasting and Nitsche [153] also point out that SC transport will be affected by transverse swelling of corneocytes and accompanying minimal changes in lateral corneocyte and lipid dimensions. Further, our understanding of ionized drug transport and the impact of slow binding processes within the corneocyte is limited. They concluded by observing that "*appropriate meshing of the polar and lipid pathways through the SC remains an unresolved problem.. (and) the impact of formulation components on SC permeability.. remains a difficult challenge for a priori prediction.*" An important contribution to this challenge is their recent observation that transverse SC lipid bilayer hopping, especially at SC lamellae junctions, is the rate-determining step in the SC transport for most drugs [134].

Given these comments and because there are so many models available, a key question, then, remains: which of the available range of dermal PBPK models will be useful? The answer to this question has been given, in part, by Box [186]: "*All models are wrong, but some are useful*", focusing on his later clarifying question: "*All models are approximations. Assumptions, whether implied or clearly stated, are never exactly true. All models are wrong, but some models are useful. So, the question you need to ask is not "Is the model true?" (it never is) but "Is the model good enough for this particular application?*" [187]. So that raises two points. Firstly, do any of the minutiae of details in complex models matter? And, if so, when and how do they impact a dermal PBPK model being "useful" in meeting a specific need. An associated requirement of simplicity has been strongly advocated by two leaders in dermal PBPK modeling, Gabriel Wittum and Richard Guy, who advocate Einstein's philosophy "*Everything should be made as simple as possible, but no simpler* [188]" and Occam's razor (also called Ockham's razor, the law of parsimony) which has as a problem-solving principle that "*entities should not be multiplied without necessity*", respectively. Brian Barry has gone a step further and commented: *"It is better to be approximately right than absolutely wrong!*"

Box [186] has also advocated that the models should be: (1) an iteration between theory and practice, flexible in seeking out, recognizing, and exploiting errors in the modeling, simple and evocative as possible, able to take particular care to address what is importantly wrong, and aware of the danger of making false tentative assumptions about the real world that we believe to be useful. Further, in our view, any dermal PBPK model used to describe local skin absorption should also be physiologically based and have both validity and identifiability.

Fig. 7. Integration of (a) tissue-scale, (b) cellular-scale (c) cryo-EM observations of mature lamellae in stratum corneum and (d) of primitive lamellae in stratum granulosum and (e) a magnified view of c (marked by the yellow box), with (f) simulated EM-image derived from the molecular dynamics model of stacked bilayers of ceramides in a fully splayed chain conformation shown in g and in (h) the corresponding MD model schematic molecular arrangement. A similar set of images is shown in Figs (i), (j), (k), and (l), where atomic model color codes are: ceramide molecules (green carbon atoms), cholesterol molecules (yellow carbon atoms), FFA molecules (orange carbon atoms), and water molecules (red [oxygen atoms] and white [hydrogen atoms]). EM, electron microscopy; FFA, free fatty acid; MD, molecular dynamics. From [156] with permission of Elsevier, distributed under a Creative Commons CC-BY license. (For interpretation of the references to color in this figure legend, the reader is referred to the web version of this article.)

Scheuplein, in his reflections on our understanding of skin permeation over the last 50 years or more [51], concluded: "*Most current models of skin permeation emphasize intercellular diffusion,. . .. . . are extremely detailed but are inconsistent with existing permeation data and with one another, but virtually all claim a good fit with some permeation data. Some go into extraordinary detail regarding the architecture of the SC and its consequences for permeation. To me, many of these complicated models seem unverifiable. A broad agreement, within 1 or 2 orders of magnitude with collected data from several different investigators is predictable and not compelling. Given the inherent variability in most permeation data and the number of adjustable parameters in many of the new models, such a level of agreement is almost assured. In the quantitative sciences, there is the notion of 'significant figures'. In skin permeation modeling there should be something analogous, like 'unjustified complexity' or 'irrelevant embellishment'. Only a minority of investigators have thoughtfully considered transcellular permeation...*"

4.3. Going to a more molecular level - molecular dynamics simulation

The prediction of the individual diffusivity of solutes through the SC and associated permeability coefficients is generally experimentally measured or estimated using a QSAR approach, as described in 3.3. This is then combined with the continuous and deterministic dermal PBPK approach described in 3.4 to estimate local physiologically based concentrations and effects. However, QSARs are based on training set data, and their applicability to the prediction of the individual diffusivity of solutes through the SC and associated permeability coefficients is very dependent not just on the quality and range of molecules covered by that training set used to generate the QSAR and the extent they can be validated but also on the extent its physicochemical properties are sufficiently consistent with those used in the QSAR.

In contrast, molecular dynamics simulations of drug transport through SC lipids directly focus on the molecular jumps for a given drug, taking into account local forces, molecular geometry, and restrictions between drug and the SC lipids as orientated in the SC diffusion pathway generating probabilistic outcomes of the likely diffusivity in the lipids and when extended to the transport across a large number of lipid bilayers, along with the SC partition coefficient, an individual drug-based estimate of its SC permeability coefficient. Hence, as an analogy, the QSAR approach may be seen as somewhat akin to the macro general relativity approach to physics whereas that of molecular dynamics is more akin to quantum mechanics.

Molecular dynamics simulation of transport through SC lipids, on the other hand, is based on validated biomolecular force fields governing atomic interactions between drugs and lipids and being molecular-based can directly simulate changes in drug diffusion caused by changes in temperature, chemical penetration enhancers, hydration, and skin disorders [189]. A key goal in molecular dynamics or Monte Carlo simulations is to estimate the difference in free energy between two relevant thermodynamic end states [156]. One approach is to apply force fields derived from a set of potential functions to describe the covalent interactions between atoms, non-covalent interactions, and electrostatic forces between (partially) charged atoms within a defined environment [190]. Molecular dynamics simulations of ceramide bilayers, the most abundant SC lipid, were first reported in 2006 [191] and followed by studies using realistic SC lipid bilayer configurations made with cholesterol, fatty acids, and ceramides in 2009 [192] with the impact of water reported in the next year [193] and analyzed by cryo-EM and molecular dynamics simulation [194]. Others have shown that the interaction of sebum with these SC intercellular lipids can modify predicted SC permeability [195]. Gupta *et al.* [196] used an SC lipidic matrix to study the permeation of water, and eleven small molecules (oxygen, ethanol, acetic acid, urea, butanol, benzene, dimethyl sulfoxide (DMSO), toluene, phenol, styrene, and ethylbenzene) through a skin lipid bilayer using a constrained molecular dynamics simulations technique at 310 K. Their permeability coefficients showed qualitative agreement with experimental data, with their free energy profiles suggesting that the main barrier for the permeation of polar solutes, such as water, ethanol, DMSO, acetic acid and urea, was the lipid core whereas, for hydrophobic solutes, the polar head-group region was their main barrier to transport.

Molecular dynamics simulations have been used to suggest that the SC penetration enhancer dimethyl sulfoxide may cause SC lipid fluidization [197] as well as leading to pore formation [198,199]. Pore formation is a surrogate describing solvent extraction of SC lipids as molecular dynamics simulations do not allow for such loss [189]. Others have used molecular dynamics simulations to show SC lipid - skin physical enhancer effects, such as electroporation in the presence of external electric fields [200], chemical interactions for oleic acid [201], menthol [202,203], ethanol [204], and other chemical penetration enhancers [205], the latter for in-silico screening. Mechanistically, molecular dynamics simulations suggest that azone and oleic acid disrupt skin lipid packing, which may result in SC lipid phase separation [189]. Whilst the impact of water on the transport of drugs through the SC lipids has been modeled using molecular dynamics simulations by associating water with the SC lipid polar head groups, showing increases in the permeability for codeine, ethanol, nicotine, testosterone [189], consistent with experimental expectations, water also permeates through the corneocyte wall and accumulates in high amounts in the corneocytes [206], doubling the thickness of the SC [207] with likely additional impacts on SC fluidity.

An interesting molecular dynamics simulations outcome, shown using both constrained and unconstrained coarse-grained modeling is that 1–6 nm gold nanoparticles disrupt the lipid packing and enter the interior lipid bilayers rapidly [208] and, in doing so, can facilitate the penetration of horseradish peroxidase (HRP) protein [209], noting that both molecular dynamics simulations and experimentation had shown HRP does not penetrate by itself. In later work, Gupta and Rai [210] used molecular dynamics simulations to forecast that nanoparticles with a 2:1 homogeneous ratio for hydrophobic to hydrophilic regions had promise in the transdermal delivery of proteins. At the same time, they showed that gold nanoparticles complexed with interferon-alpha (INF) could facilitate INF delivery [211]. Most recently, they have studied the active translocation and permeation of ferulic acid encapsulated into Gelucire 50/13 nanoparticles using molecular dynamics simulations [212]. Another pithy example is the use of molecular dynamics simulations in the multiscale modeling of transdermal drug delivery of fentanyl [213], where the microscopic diffusion coefficient of fentanyl was first calculated as a function of position in the bilayer, then homogenized to an effective macroscopic diffusion coefficient using an SC brick and mortar microstructure model followed by finite element method simulations of its release profile. The outcome was a somewhat estimated smaller peak fentanyl flux than observed experimentally. This work was followed by multiscale molecular dynamics modelling of fentanyl, caffeine, and naphthol through the SC lipid layer [214]. Most recently, Bozdaganyan *et al.* [215] used coarse-grained molecular dynamics simulations of a fully hydrated SC model membrane to explain the effects of ethanol and linoleic acid on lidocaine permeability using changes in both SC structural properties and in free energy changes associated with lidocaine "jumps" through the lipid bilayers in the SC intercellular lipid pathway.

The current state-of-the-art in estimating the SC permeability of drugs through the SC intercellular lipid pathway by a molecular dynamics simulations approach is summarized in Figs. 7 and 8.

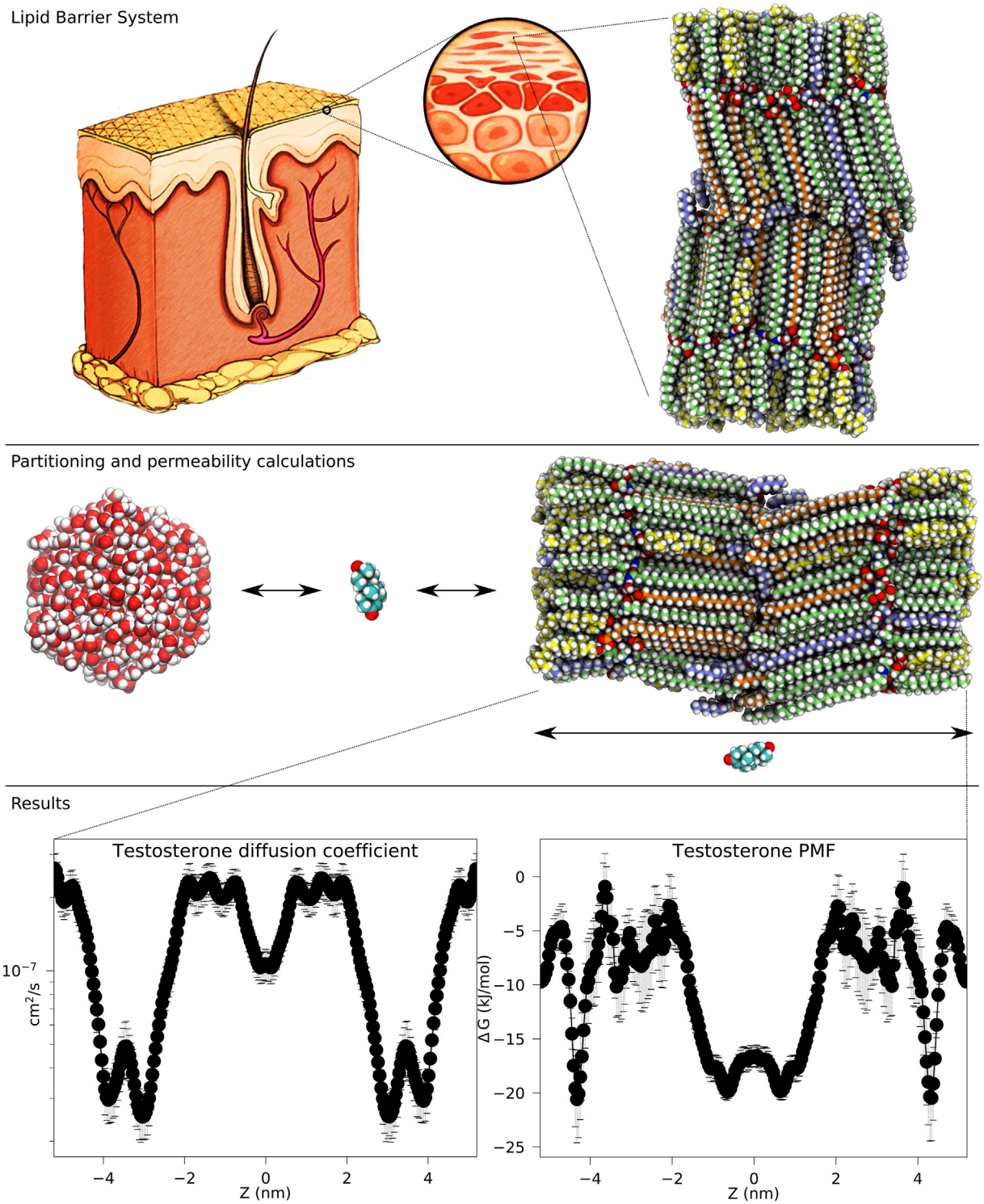

Fig. 8. Calculating the permeability through the skin barrier using molecular dynamics simulation. The top panel shows the location of the lipid barrier and an atomistic representation, based on cryo-EM images. The middle panel illustrates the calculation of the free energy difference of a permeant in a solvent or formulation (testosterone in water in this example) compared to being in the skin barrier system, as well the interactions of the permeant with its surroundings as it moves through the barrier system. The bottom panel shows the calculated local diffusion coefficient and the potential of mean force (PMF), i.e. the relative free energy compared to water, throughout the barrier system. The PMF profile is aligned with the lipid barrier system in the middle panel. The local diffusion coefficient and the PMF can be used to calculate the permeability coefficient across the lipid barrier structure. All parts were supplied by Magnus Lundborg and Christian Wennberg of ERCO Pharma and, other than the top left schematic drawn by Milad Ghanbari for ERCO Pharma, were drawn by them.

Fig. 7 shows recent work by Lars Norlen and colleagues interrelating cryo-EM SC lipid morphology observations with molecular dynamics simulations of SC lipid transport whereas Fig. 8 is a snapshot showing how this work is translated into the practical estimation of SC permeability by his spin-off company, ercopharma.com. Their general approach can be described as follows for a single component system [216] (Fig. 8): (1) Calculate the permeant solvation free energy in the desired solvent or formulation; (2) Calculate the mean force potential and local diffusion coefficient across SC lipids and (3) Estimate a drug's permeability coefficient for trans-

port through ~ 80 stacked lipid bilayers. In a more complex formulation, involving chemical penetration enhancers, a similar approach would be applied but, in the first step, applied to all components in the formulation and across the lipid barrier system, taking into account the extent each excipient partitioned into and equilibrated with the lipid barrier system. The estimation of mean force, local diffusion coefficient, and permeability coefficient for any permeant across 80 layers of lipids would then follow.

At present, the main focus in their molecular dynamics simulations is the simplest representation to provide robust and verifiable estimates of SC permeability. Consequently, these simulations are limited to axial homogeneous transport in the SC lipid barrier using only one bilayer repetition to simplify the modeling process and the requirement for computing time. However, it is recognized that, in reality, there is large heterogeneity in the actual SC lipids composition and hydration across the SC, especially between the stratum disjunctum and compactum, that will modify the predicted outcomes. Effectively addressing this issue across a broad range of SC heterogeneity requires, however, defined SC lipid and water composition at different depths along with distinct cryo-EM images able to deduce differences in lipid packing and enable a good atomistic representation of the SC lipids. Further, the transport emphasis is on axial diffusion along with SC lipids although it is recognized that radial diffusion may also play a role in transport, especially in facilitating the transport of drugs into corneocytes. Future work addressing the variation in SC lipid composition for different body sites, other states, and diseases requires high-quality cryo-EM images that characterize the skin from these situations, desirably accompanied by an accurate SC extracellular lipid composition. The likely effect of such changes on skin permeability may be initially tested by modifying the SC lipid compositions and evaluating the resulting effects.

Magnus Lundborg (*personal communication*) has advised that their regression coefficient, derived from the comparison of molecular dynamics predictions versus experimentally determined permeability coefficients, is R^2 ~0.79, i.e., at the upper end of what is usually achieved by QSPR estimations (Section 3.3). The strength in a molecular dynamics simulation approach is not so much in determining permeability coefficients for simple solutions, as these are relatively easily obtained by experiment or by QSPR but to gain a better detailed mechanistic understanding of the SC extracellular lipid permeation process, its barriers, and the effect of chemical enhancers [189].

A challenge in going forward for those in the dermal PBPK field will be to integrate the concepts of QSPR, PBPK and the molecular dynamics simulation approach, in much the same way as general relativity and quantum mechanics have been brought together as relativistic quantum mechanics (RQM) using relativistic quantum field and other theories. In principle, this may be best achieved by further developing the molecular dynamics simulations and predictions of individual drug transport through SC intercellular lipids and combining it with dermal PBPK and with QSARs to describe SC-product partitioning, drug transport elsewhere in the skin, and in the deeper underlying tissues.

5. Topical formulations

5.1. Topical product market

Topical products now have a global market valued at US$92.4 billion in 2020 (amid the COVID-19 crisis), which is expected to reach US $129.9 billion by 2027 [217]. As shown in Fig. 9A, the generic product market share has been increasing with time so that, now, the bulk (about 74% of all approved topical products) are generic equivalent forms of a reference listed drug (RLD). Fig. 9B shows the relative market share of various formulations that make up today's topical drug products approved by the FDA and on the market. It is readily apparent that creams, ointments, lotions, sprays, and solutions dominate the market for both topical reference listed and topical generic drug products. The various liquid, semi-solid, and solid topical delivery products comprise combinations of water, water-miscible, surfactants, oils, skin penetration enhancing, colloidal, propellant, solid, and polymer ingredients in solutions or in dispersions. Products can range from comprising liquid ingredients with low viscosity (solution, lotion, suspension), to more than 50% liquid ingredients with a moderate viscosity (gel, cream) to products with <50% liquid ingredients (often solids, waxes, hydrocarbons, and polyethylene glycols), to those that are very viscous (ointments and patches) and, lastly, to being a solid (patch) dose form.

Fig. 9C shows the icons that symbolize each of these products and the key "change agents" that have brought about their development as a transition from the products shown in Fig. 1 to those approved and on the market today. The main consideration in the development of each of these topical dosage forms has been the patient need, as perhaps exemplified by the dictums that: (1) raw wounds should be kept clean and moist and may involve cleaning with water, moisturizing, and protecting [218]; (2) dry skin and its associated conditions of atopic dermatitis, ichthyosis, irritant contact dermatitis, psoriasis, and eczema craquelé require emolliency where the ideal formulation contains combinations of non-physiological and physiological lipids, humectants and compounds with antipruritic, soothing and supporting epidermal differentiation properties [219] and (3) specific skin needs, such as relieving inflammation, hair loss, acne, sun protection, infections, whitening, immune stimulation, pain relief, etc. (Table 1), will require the appropriate delivery and targeting of drugs applied in a suitable topical dose form (Fig. 4). For instance, an aerosol may provide an immediate and short duration of action without touching the injury site whereas a patch may provide a prolonged and controlled release ensuring adherence. Certain products may also not be the most suitable for application to lacerated or hairy skin areas, to mucous membranes, or around the eyes.

The second consideration in choosing a topical dosage form is the drug's physicochemical properties (Table 2). It is evident from Table 2 that the drugs now approved range from very water-soluble, polar drugs with a low log *P*, to drugs soluble in water and oil with moderate log *P* to water-insoluble and oil-soluble drugs with high log *P*. Here, the key adage in their dosage form design is "like dissolves like" and so it may be anticipated that the water-soluble drugs may be formulated in aqueous topical delivery systems, such as solution, lotions, and creams whereas the water-insoluble drugs may be dissolved in oily products or solubilized in surfactant systems.

A key challenge in meeting the above two needs is the provision of accessible, affordable, effective, and safe topical products. This additional consumer need is exemplified by generic topical dermatologic medication prices increasing 10 fold more than inflation for the period 2005 and 2016 [220]. In general, regulatory approvals of generic topical products have lagged the market requirements as clinical equivalence studies (clinical trials) have been the gold standard. Such studies usually involve high subject numbers, time, and costs to provide the sufficiently sensitive clinical end point assessment needed to address variations in skin condition, body site, product use, and placebo response as well as environmental, genetic, ethnicity, and other biological differences. As discussed later in 5.6, specific topical bioequivalence methodology is now being invoked for those products which fail both the first step in the "strawman" decision tree of ingredient, ingredient concentrations, and product microstructure sameness, have a narrow therapeutic margin or safety issue, and cannot be analyzed by a surrogate clinical method. Examples of the latter method are the

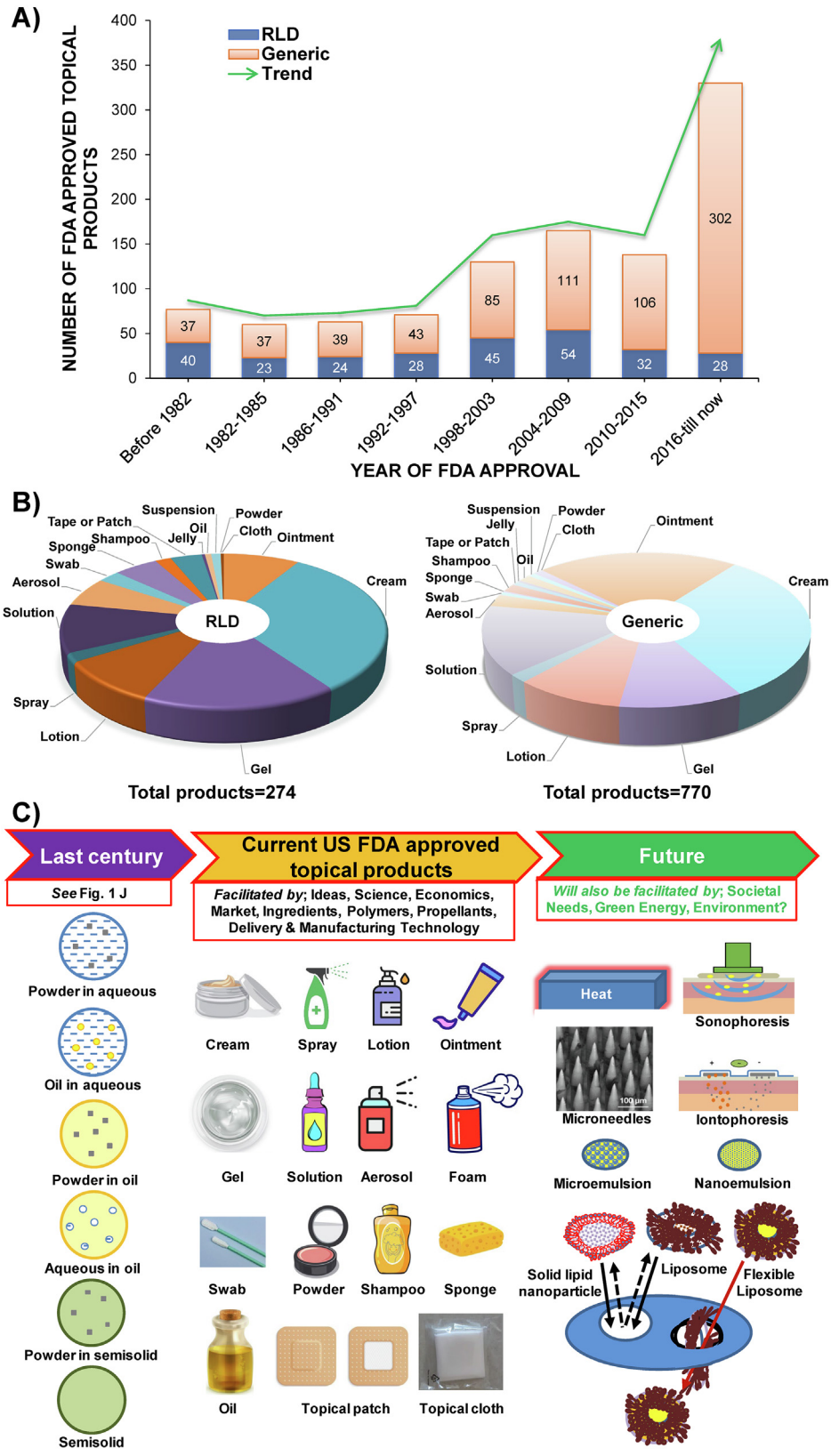

Fig. 9. A. Evolution of FDA-approved reference listed drug (RLD) and generic topical products on the market from before 1982 to June 2021; B. The current range of products approved: Source: FDA Orange book [405]: C. Evolution of topical drug products from that described in 1971 (Fig. 1) to today and beyond. Also shown here are the facilitators for those products now developed and, in future products, both products which have been of great academic interest as well as those who have not yet had the potential realized. Shown on the bottom right is an illustration of the deformity test for flexible liposomes (elastic vesicles), in which liposomes can be extruded under pressure through a membrane pore that is somewhat smaller in diameter than the liposome over a short time period. Elastic vesicles and micro-/nano-emulsions should pass through the pore with high recoveries and with a return to their original size whereas non-flexible liposomes and solid lipid nanosomes are unlikely to [218,224]. (For interpretation of the references to color in this figure legend, the reader is referred to the web version of this article.)

vasoconstrictor test used for corticosteroid product bioequivalence and drug plasma/tissue concentrations when these are quantifiable after topical application [221].

Also, shown in Fig. 9C are potential products of the future. These include products that have been in development and in trials for a considerable time but, generally due to technology or cost issues, have not quite yet realized their potential. In our view, the continuing growth of large biologicals which cannot be given orally creates an opportunity that may well be met through the ability of low-frequency sonophoresis, microneedles, electroporation and iontophoresis, and related techniques to increase SC permeability for large drugs, vaccines, and protein delivery as also discussed in detail elsewhere [222].

Two other groups of products, one based on nanotechnology principles and the other on nano-and micro-emulsions, have been discussed in recent reviews we have written [223,224]. We will not elaborate to any extent on the nanotechnology concepts here, other than to say that we believe flexible liposomes, such as transfersomes, ethosomes, niosomes, secosomes, and related vesicular systems offer great potential in enabling drug delivery to the deeper layers of the skin after topical application.

5.2. Product use

The delivery of a solute through the skin is dependent on several factors which can be solute/formulation-related, skin-related, and dosing-related [225]. Dosing-related factors include the dose administered, the duration/frequency of the application, the surface area in contact with the topical formulation, the thermodynamic activity of the drug in the formulation (most easily defined by the fractional solubility of the drug in the product), and the extent vehicle-skin interactions promote skin permeation [41]. Enhanced skin permeation may be further facilitated in finite dose products containing volatile solvents by the processes of supersaturation on the initial evaporation of the solvent and the later concentration of topical ingredients, such as propylene glycol, that may further enhance permeation [226]. Another consideration is how thickly or thinly a topical product is applied as this thickness, along with the product viscosity and fractional composition of volatile components defines the nature of the residue after topical application. We have previously reported that increasing the viscosity of a product decreases the skin permeation of a thickly applied product, whereas such an effect is not seen for thin *in-use* products. Indeed, our observation was that the thicker residue from a highly viscous product may leave a more occlusive residue and through hydration enhance skin permeation [227].

5.3. Product evaluation

In general, dosing effects for topical products are based on the outcomes of *in vitro* skin permeation studies, which may be performed under conditions of finite or infinite dosing. Infinite doses require the application of doses greater than 10 mg/cm^2 or 100 μL/cm^2 [228]. In these cases, the effective donor concentration remains constant and steady-state absorption can be achieved after a lag time that varies according to the penetrant and the experimental conditions. On the other hand, finite dosing, using doses of 1–5 mg/cm^2 or 10 μL/cm^2 [228] is often recommended to mimic conditions occurring in the *in vivo* situation. With finite dosing, steady-state absorption may be achieved only for a short time, or not at all, as the more limited amounts of penetrant present in the donor material may become depleted over time.

Differences in the effects of formulation evaporation and occlusion may also be seen between finite and infinite dosing. The loss of volatile penetrants or excipients with evaporation during infinite dosing can lead to changes in penetrant concentration and a deviation from a steady-state absorption pattern typically seen with this form of dosing [229]. Covering or occlusion of the diffusion cells can limit evaporation.

5.4. Product behavior under in-use conditions

Evaporation from the surface of thinly applied donor materials in finite dosing experiments can also have significant effects on skin absorption. An example of this is found in work [226] where minoxidil was applied to excised human skin as a 2% solution in three different mixtures of ethanol, propylene glycol, and water in ratios of 60:20:20, 80:20:0, and 0:80:20 (formulations 1, 2, and 3). At 32–35 °C, evaporation of ethanol, followed by water, is rapid, whereas evaporation of propylene glycol is much slower, and the authors hypothesized that by about 2 h, the material remaining on the skin consisted of minoxidil dissolved in propylene glycol. Furthermore, based on the initial proportions of solvents in the three formulations, the concentration of minoxidil in formulations 1 and 2 was anticipated to have risen from 2% to 10%, while in formulation 3, the increase would be more modest, from 2% to 2.5%. The four-fold ratio of minoxidil concentrations in formulations 1 and 2 over that in formulation 3 was expected to be reflected in instantaneous minoxidil flux, which in turn would be reflected in the amounts of minoxidil recovered from the receptor fluid, skin, and appendages (hair follicles). The experimental results confirmed this prediction. A similar mechanism may explain the findings of Tata *et al.* [230], who showed minoxidil deposition from binary ethanol: propylene glycol solutions applied to excised mouse skin and the skin of *in vivo* mice increased with increasing ethanol content. In addition, enhancement of skin and hair follicle deposition by ethanol has also been explained as a "pull effect" [231], in which highly soluble solutes are carried along with ethanol into lipid-rich skin compartments, including follicles.

Modelling drug permeation after product application to excised human skin membranes after IVPT measurements is not straightforward as there may be changes in the product behavior as a result of water and other volatile solvent evaporation as well as percutaneous absorption occurring over a short time. One of the simplest PBPK models is that for minimal evaporation of product. We have derived Laplace solutions for various IVPT finite dose scenarios including situations where the viable epidermis, dermis, and sampling rate are rate-limiting. In the specific case of SC limited permeation, $\widehat{Q}(s)$, the Laplace equivalent of $Q(t)$ (Eq. (2)) can be described in terms of the dose applied, a dimensionless number parameter V_{dN} (given by $V_{dN} = \frac{V_d}{K_{sc,v} V_{sc}}$, where V_d is the amount of product applied, $K_{sc,v}$ is the stratum corneum - vehicle partition coefficient and V_{sc} is the volume fo stratum corneum), a diffusion time t_d ($=h_{sc}^2/D_{sc}$) and s, the Laplace operator for time t [232]:

$$\widehat{Q}(s) = \frac{dose}{s} \frac{1}{\cosh\sqrt{st_d} + V_{dN}\sqrt{st_d}\sinh\sqrt{st_d}} \tag{23}$$

Eq. (23) has two asymptotic solutions. When the product volume (reflected in V_{dN}) becomes very large, the *cosh* term drops out and the analytical solution to the remaining equation is Eq. (2). On the other hand, when the product volume is very small, the V_{dN} term drops out and we are left with a simple equation describing effectively a vehicle deposited active on the SC surface. The corresponding IVPT profile for a product applied to an area A is characterized by a peak permeation flux of ~ $1.850\ dose/(At_d)$ with a peak time of ~ $t_d/6$ [232,233]. Lehman [234] used this model to simulate and interpret the IVPTs for several topical products. There are now many studies seeking to understand finite dose behavior under various conditions applying appropriate modelling that addresses evaporation, phase changes, supersaturation, skin penetration enhancement, and so on.

5.5. Skin permeation enhancement

In addition to ethanol, numerous natural and synthetic substances can act as penetration or permeation enhancers (PEs), including DMSO, azones, alcohols and glycols, fatty acids such as oleic acid, surfactants, and terpenes. Numerous mechanisms have been proposed for their activity [235]. In order to be useful as a PE, a substance must reduce the skin barrier resistance reversibly [235] and it should not cause unacceptable levels of skin irritancy or damage. For example, anionic surfactants can act as PEs but have also been reported to damage human skin [236]. Propylene glycol (PG), is a commonly used excipient in topical formulations that has permeation enhancing properties. One of the proposed mechanisms involves the partitioning of PG into the skin, where it alters the properties of the SC to enhance the solubility of other permeants and promote their partitioning into it [235]. In the minoxidil studies discussed above [226], it was hypothesized that the increase in minoxidil flux that occurred after about 12 h with all formulations was due to the incorporation of PG in the stratum corneum that promoted the absorption of minoxidil into the skin.

In a series of reports over recent years, Abd *et al.* [237-234] investigated the effects of various formulation manipulations on the delivery of permeants into and through human skin. The overall goal of this work was to cast light on the mechanisms of enhancement and to investigate whether skin compartments could be differentially targeted using tailored formulations. Nanoemulsions containing either the monoterpenoid eucalyptol (1,8-cineole, EU) or oleic acid (OA) as the oil phase were used to deliver the hydrophilic molecule caffeine (log *P*, −0.07) [238] or minoxidil (log *P*, 1.24) [238] to excised human skin. The mechanism of permeation enhancement of both molecules due to both EU and OA was found to be largely driven by increased diffusivity, rather than increased partitioning into the stratum corneum, indicating that these formulations are likely to cause increased fluidization and disruption of the stratum corneum lipids. Results of delivery and retention of the drugs in various skin compartments indicated that these could be differentially targeted by appropriate formulation manipulation. The EU and OA formulations caused similar retention of caffeine in the stratum corneum and deeper skin layers, whereas, for minoxidil, it was greater with the EU formulation. The effect of the PEs on the follicular route was clearly differentiated, with greater caffeine and minoxidil permeation via the follicular route and retention in the follicles with OA, compared to EU. In other studies with vesicular formulations [239] in which caffeine was encapsulated in liposomes along with EU or OA and in transfersomes and niosomes without PEs, caffeine retention in hair follicles was significantly enhanced in the liposomes with OA and in the transfersomes. Caffeine retention in the stratum corneum and permeation into the receptor was greatest in the transfersomes and niosomes, followed by the liposomes containing PEs. These promising results suggest that further formulation refinement is likely to result in more accurate skin targeting. This work is part of a major growth area where tailored nanocarriers are being developed for enhanced dermal targeting [240–242].

Finally, it is emphasized that skin penetration enhancement may be facilitated by the stratum disjunctum being less coherent than the deeper stratum compactum due to the SC desquamation process. For instance, as described in Fig. 4 A and in Section 4.2, the SC rivets, the corneodesmosomes are widely distributed in the stratum compactum but, due to proteolysis are largely absent from the stratum disjunctum where, when found, are mainly found in the ‘‘slits’ at the corneocyte edges – leading to sloughing off (‘basket – weave appearance”) in histology processing unless the skin is properly fixed and mounted before cutting (Nancy Monterio-Riviere, personal communication to M. Roberts). Mundstock *et al.* [161] give several examples of microemulsions swelling intercellular spaces and disrupting the stratum disjunctum with in order of severity in action: water in oil > oil in water > gel.

5.6. Topical bioequivalence

A key requirement for topical generic products, in moving away from assessments by clinical bioequivalence, is to show that they have equivalent performance to the Reference Listed Drug (RLD) product [243]. However, a difficulty in the regulatory assessment of topical products is that they are often applied, as discussed in Section 8.2, to different body sites [244]. A range of alternatives to the clinical equivalence of topical products developed over the last two decades is effective in evaluating the rate and extent of topical drug delivery [245]. Hence, assessment tools based on *in vitro* permeation testing using different types of diffusion cells with excised human skin membranes and *in vitro* product release have to be able to be extrapolated to these sites to be useful as regulatory tools [244,246]. *In vivo* tools such as dermatopharmacokinetics and dermal microdialysis/open flow dermal microperfusion studies in conjunction with available *in vivo* clinical trial data have been used to develop *in vitro in vivo* correlations and reduce the need for future clinical trials.

Increasingly, *in vitro* to IVPT and *in vitro* to *in vivo* extrapolations (IVIVE) are being made *in silico* using a combination of topical dose form behaviour on application to the skin surface with PBPK modelling of drug permeation into the skin to local and/or systemic target sites and clearance organs. In principle, it may be possible to predict dose form behaviour based on its formulation, manufacturing and packaging characteristics. However, in this early stage of IVIVE development, a first step is to predict IVPT performance from a combination of its ingredients and formulation variables, its critical quality attributes and its potential failure modes as shown in Fig. 10A. The following step, discussed later in Section 8.2, is the scale up from *in vitro* to *in vivo*.

An approved topical semisolid product containing an RLD has been designed and shown to deliver a consistent, defined rate of the RLD to the site of action in the skin or underlying tissues for the localized treatment of dermatological, musculoskeletal, and other conditions. Therein lies the greatest challenge in establishing bioequivalence or sameness between a RLD containing reference product and a generic product. It is extremely difficult to assess local bioavailability at the site of action *in vivo*. Several sampling and imaging techniques are under development; however, none is ready to be used for regulatory approval purposes. An *in vitro* approach, however, can be of significant advantage. With this aim, more recently, regulatory authorities including the U.S FDA have been encouraging an *in vitro* approach through product-specific guidances. These guidances were published in 2016 [247] and in 2019 [248,249]. They recommend product regulation through a combination of characterizations and *in vitro* tests. Before these guidances, preceding recommendations did not allow *in vitro* evaluations, e.g. the 2014 lidocaine guidance [250]. Within a short span, the characterization-based approach contributes to 6–8% of generic product applications [251]. The first generic developed through this approach was launched in 2019 [248]. This approach has the potential to disrupt the generic as well as new drug product market, leading to the availability of affordable and high-quality medications for everyone. The regulators and industry hence rely on a Quality by Design (QbD) approach, rather than quality by testing that retrospectively assesses quality. Recent work has highlighted what a Quality Target Product Profile (QTPP) for a topical product should ideally include [252].

The quality of a pharmaceutical product can be classified on three levels, designated as Q1, Q2 and Q3. Here, Q1 specifies that any new product has the same components as the RLD product; Q2 has the same components in the same concentration as the

RLD product; Q3 has the same components in the same concentration with the same arrangement of matter (microstructure) as the RLD product. In the case of semi-solid topical drug products, well-defined critical quality attributes (CQAs) are required to effectively characterize these products and their influence on bioequivalence and bioavailability. The CQA most likely to influence performance is the physical/chemical properties of the formulation components, including solubility, particle size, pH, rheological properties, globule size, presence of polymorphic states, type of emulsion, and oil to water phase ratio. The manufacturing variables can influence the CQA of the formulation, in particular the globule size and coalescence, phase separation, rheology, product uniformity, precipi-

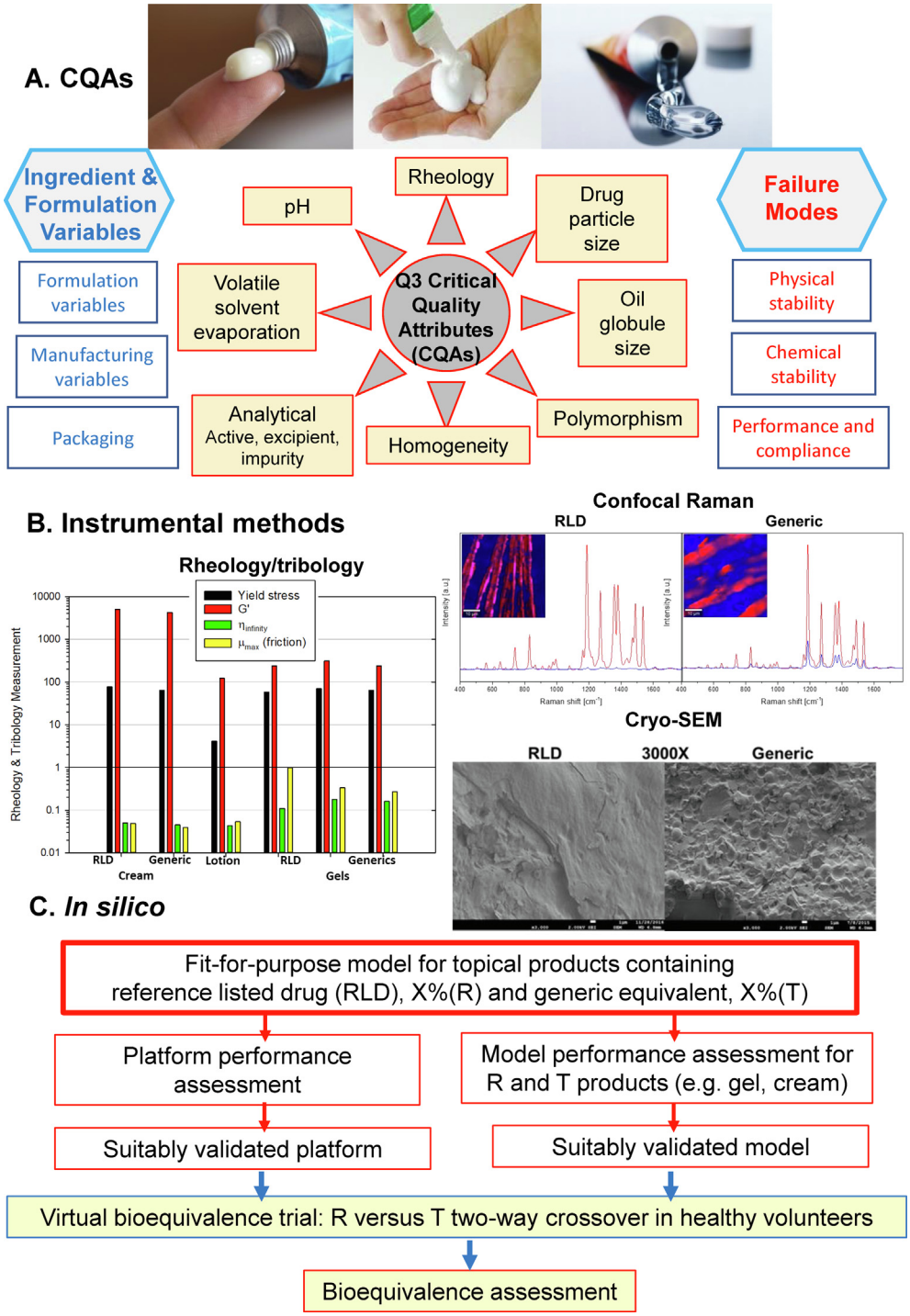

Fig. 10. *In vitro* and *in silico* bioequivalence testing of topical drug products. A. Quality by design and testing: ingredient and formulation variables, potential critical quality attributes (i.e. Q3), as defined by an articulated battery of *in vitro* physicochemical tests and the failure modes they may cause. B. Three instrumental test methods for assessing product microstructure - with results on comparing a RLD containing topical drug product and one or more generic equivalent topical dose forms: rheology/tribology, confocal Raman spectroscopy and cryo-Scanning Electron Microscopy (cryo- SEM). Adapted from [361]. C. Overview of *in silico* model validation methodology for topical product bioequivalence assessment. Adapted from Tsakalozou *et al.* [128], applying their fit-for-purpose dermal PBPK models for a dermatological reference listed drug product (RLD), *X%* (reference, R) and the generic equivalent drug product, *X%* (test, T).

tation, recrystallization, and stability of actives. Hence, righty, the emphasis of the *in vitro* bioequivalence approach is primarily on Q3 attributes and CQAs. As carefully mitigating failure modes in these products are often underpinned on matching Q3 attributes and *in vitro* performance/penetration testing (IVPT). Fig. 10A shows some examples of the battery of physicochemical tests that may be done as part of the *in vitro* testing for product critical quality attributes (i.e. Q3), together with Ingredient and Formulation Variables and potential Failure Modes. Also shown are some examples of results carried out on a RLD and generic products with confocal Raman, cryo-scanning electron microscopy and rheology/tribology tests.

Earlier in this section, we introduced the concept of assessing bioequivalence using an *in silico* apporach. These *in silico* methods are often supported by strong *in vitro* data and can provide timely results, bringing down costs and the need for expansive *in vivo*/*in vitro* studies. These can be limited and a large proportion of the required criteria can be met *in silico*. In a recent publication, FDA scientists presented two alternative approaches for a virtual bioequivalence assessment, one based on a platform performance (where they used the "bottom-up" based Simcyp's MechDermA PBPK model, discussed further in Section 8.2) and the other based on model performance (Fig. 10B) [128]. Quite disparate platform-predicted and observed plasma diclofenac concentrations were reported. The authors concluded that the diclofenac partition coefficient from the vehicle (topical gel, 1%) to the SC and the diclofenac partition coefficient from the SC to the viable epidermis were impactful parameters and they went on to manually optimize parameters to derive a simulation with a good visual prediction check (VPC). However, contrary to our observation that diclofenac is shunted to deeper tissues by the blood because of its high plasma protein binding [253], a modification that has now been made in the Simcyp MechDermA PBPK platform, this work assumed that "longitudinal solute diffusion within and between the different skin layers is modeled after Fick's Law." Importantly, though, they did include within their initial modeling recirculation of solutes from the systemic circulation back into the skin, a phenomenon we have reported to occur with drugs poorly cleared from the systemic circulation [126] but not with those which have a high systemic clearance [254].

6. Confounding effects of deeper layers

6.1. Clearance and binding

Determinants of local bioavailability and clearance from a skin site that can modify $C_{ss,local}$ (Eq. (1)) include irreversible binding at the skin surface and in the skin en route to the skin site, limited diffusion through the viable epidermis and other tissues, local metabolism, convective flow (blood, lymphatic and interstitial), and deeper tissue diffusion. Metabolic enzymes are primarily located in the viable epidermis (especially the stratum basale), the dermis (within the skin appendages), and in the stratum corneum (extracellular spaces) [255]. Those processes acting on the drug before it reaches the putative skin site affect the local bioavailability F_{local} whereas those acting in the skin after leaving the site contribute to the skin clearance CL_{skin} (Eq. (1)). Both contribute to the systemic bioavailability F_{sys}, also called the skin first-pass effect. F_{sys} has been determined for several topically applied drugs that are today incorporated into topical and transdermal products, including testosterone (about 40% in viable excised mouse skin [256] and 50% in an organotypic human skin model [257]), and nitroglycerin (availability of 75% in healthy volunteers with loss attributed to a combination of retention in the skin, cutaneous metabolism and tissue binding [258]). More recently, an analysis of human cutaneous microdialysis data demonstrated that while poorly plasma protein-bound drugs such as nicotine are primarily transported to deeper tissues by tissue diffusion, the transport of highly plasma protein-bound drugs such as diclofenac is further facilitated by convective blood, lymphatic and interstitial flow in the dermis [253].

Local vasoconstriction produced by phenylephrine (selective α_1-adrenergic receptor agonist) increases local drug tissue concentrations of topically applied lidocaine, salicylic acid, and tritiated water in a concentration-dependent manner [259]. Similar effects have been reported for antipyrine and diclofenac [260]. Vasodilators on the other hand have been found to enhance plasma levels, indicative of enhanced clearance, of ibuprofen combined with tolazoline (α-adrenergic receptor antagonist) [261]. Tissue protein and plasma protein binding are important for these effects with drugs that have a high plasma protein binding demonstrating enhanced local penetration [253]. Ultimately, the cutaneous microcirculation is maintained under local, neural and humoral control in either a nutritive or non-nutritive (anastomotic) flow state [262]. Modulation of the balance of these opposing effects will be important for the design of topical agents designed for deep tissue penetration or systemic delivery.

According to Eq. (1), clearance is just as important as SC flux in determining local drug concentrations after topical application. In our early work in this field, we attempted to quantify dermal clearance in both anesthetized and sacrificed animals and relate that clearance to dermal and deeper tissue blood flow. Blood flow - defined clearance dominates overall drug dermal clearance and is related to drug size but not lipophilicity [126]. Later analysis of human dermal data suggests that drug transport in the dermis is mostly by blood/lymphatic flow to the systemic circulation and deeper tissues, rather than molecular diffusion [263]. Most recently, Maciel Tabosa *et al.* [264] estimated dermal clearances for 19 transdermal drugs as the product of a terminal elimination rate constant on the removal of a patch after transdermal delivery arose from dermal clearance and the steady-state distribution volume of distribution of a drug in the skin taking into account its blood-dermis partition coefficient, using literature values [265]. They then did a quantitative structure - property relationship (QSPR) for clearance, in which their cross-validation involved splitting their data into training and test sets with appropriate analyses. They found that the main determinants of dermal drug clearance were drug molecular size, log *P* and topological polar surface area (*TPSA*, A^{o2}):

$$\log [CL_{skin}/Area\ (cm/h)] = -0.937 - 0.008\ MW + 0.391 \log P + 0.011\ TPSA (n = 19, R^2 = 0.67) \quad (24)$$

Noting that *TPSA* is "*related to the polarity, hydrogen-bonding potential and water solubility of organic molecules*" [264], the relationship shown in Eq. 24 correlates with our earlier findings for SC permeation in Section 4.1, where the main determinants for drug SC J_{max} were *MW*, log *P*, and water solubility.

6.2. Drug metabolism in the skin

The skin is often used as a route for drug delivery that bypasses first-pass metabolism occurring in the liver, therefore, the potential for the skin itself to act as a drug-metabolizing organ is an important question that deserves consideration. It has been known for some time that the skin expresses xenobiotic-metabolizing enzymes involved in both phase 1 functionalization (e.g. oxidation, reduction, hydrolysis) and phase 2 conjugation reactions (e.g. glucuronidation, sulfation, acetylation) [417,418]. Xenobiotic metabolizing enzymes can be involved in drug de-activation leading to reduced therapeutic effect, drug activation in the case of pro-

drugs, the formation of reactive metabolites with potential for toxicity, or the detoxification of drugs before reaching the systemic circulation in the case of soft drugs.

While the highest rate of metabolism occurs in the liver, the skin is the largest metabolizing organ by size and therefore despite having lower activity on a tissue-weight basis, the surface area of exposure presents the opportunity for significant metabolism to occur [266,267]. Further, metabolizing enzyme isoforms, such as N-acetyl transferase-1 (NAT1) are dominant in the skin whereas NAT2 is mainly in the liver [268,269].

Anatomical differences from donor sites in metabolism may exist. For instance, whilst cortisol is actively metabolised by the skin, two of its metabolites are found in foreskin but not in abdominal skin [270]. Indeed, testsoterone transdermal delivery systems have been developed for non-scrotal skin sites because scrotal skin has high 5-$\propto$ reductase activity and an elevated dihydrotestosterone to testosterone ratio not seen in the abdomen, chest, arms or legs [271]. Anatomical site variation may in part be explained by the different relative amounts of skin appendages present. Sebaceous glands, eccrine sweat glands [272], and hair follicles [273] have been shown to have high metabolic activity, followed by differentiated keratinocytes and basal cells [274,275]. While the dermis does have metabolic activity, the residence time of drugs here is reduced due to microcirculation, and therefore it is considered less important for overall metabolism. Ultimately, variability in excised human skin studies may be due to a range of factors, including race, age, gender, hormonal status, diseases such as psoriasis and acne [276-276], transport conditions, anatomical site, and even differences in microflora living on the skin surface [279,280].

6.3. Active transporters in the skin

Transporters belonging to either the ATP-binding cassette (ABC) superfamily or solute carrier (SLC) superfamily may be expressed at both mRNA and protein levels in the skin of humans and animals [281–283]. The general problem of inter-individual variability should be taken into account for interpretation in these studies as the number of skin samples studied is typically small. There is a similar constitutive expression of ABC and SLC transporters in human skin and human skin models [281]. Multi-drug and extrusion protein (MATE1, SLC47A1) in one study was found to be the highest expressed in human skin of 11 transporters studied [283]. Of note, multidrug resistance proteins ABCB1 (P-glycoprotein) and ABCG2 (breast cancer resistance protein) have also been reported as localized to the basal layer of the epidermis and the epithelial compartment of sebaceous and sweat glands [284]. They have also been reported as highly expressed at the hair follicles [285].

The skin also contains different families of cell channels that are involved in maintaining water, ion, and nutrient balance. Aquaporins are involved in the movement of water, while aquaglyceroporins permit the movement of glycerol and small solutes. [286]. These are expressed at the basal layer of the epidermis (AQ3) [287], sweat gland (AQP5) [288] and stratum granulosum (AQP5) [286].

7. Appendageal delivery

7.1. The pilosebaceous unit

It is estimated that humans have around 5 million hair follicles [289] with density ranging from about 0.1% for the forearm [290] up to approximately 14% for the forehead and nasal skin, (290 follicles per cm^2 [291] and 1220 follicles per cm^2 respectively [292]). The importance of follicle density to drug delivery is underscored by experiments that show that the forehead has a higher drug absorption rate [293] and, at the other extreme, appendage-free scarred skin has a decreased absorption rate. The dimensions of the follicle also differ, with the calf region having the largest orifice size [290,294]. Lastly, active follicles are the most receptive to delivery. These have sebum flow and hair growth (anagen phase [291]) in comparison to inactive follicles that have no hair growth or sebum production and tend to be covered with a mixture of dry sebum, desquamated corneocytes, and cell debris [291]. In the upper forearms, about 74% of the follicles have been reported as open [291].

7.2. Transfollicular delivery

Much of the history associated with transfollicular delivery has been associated with adverse effects. As Shelley and Melton point out studies reporting local wheals after topical application of histamine go back to 1917 and that work has been repeated in various ways since [413]. Shelley and Melton's own work in 1949 is interesting in that they systemically examined the effect of the vehicle on the extent of urticaria after the application of various concentrations of histamine without and with occlusion. Their observation of a more pronounced histamine urticaria with (1) increasing histamine concentration in the vehicle, (2) using histamine as its free base rather than as salt form and (3) using vehicles that dissolved histamine and facilitated intimate contact with follicles, such as water [413] is consistent with modern topical product design principles. The histology of the hair follicle (with the hair removed) is illustrated in Fig. 3E to F. As illustrated in Fig. 4, the hair follicle consists, firstly, of the infundibulum which is an open space where the hair emerges and is surrounded by epithelia. Deeper down, the hair follicle becomes near the epithelia at the isthmus, where the sebaceous gland opens to release sebum that lubricates the hair and the skin. Further down is the bulge and its complement of stem cells that can generate all epithelia, including keratinocytes, sebocytes, and hair. At the base are the hair bulb and dermal papillae. So, after application to the skin, a product may enter the infundibulum, where its absorption can follow one of two routes. Small molecule drugs may penetrate the epithelium into the viable epidermis or dermis in a process known as transfollicular penetration [295], while large molecules and particles are believed to become entrapped forming a drug reservoir [296] in a process known as intrafollicular delivery. The barrier properties of the follicle are different from the barrier properties provided by the stratum corneum of interfollicular skin, which aids in transfollicular transport. In the upper portion of the follicle, the infundibulum, the stratum corneum is still intact and relatively impermeable, however, the barrier function is weakened in the lower region [297]. For these regions, the follicle has been shown to have barrier-forming tight junctions in the outermost layer of the external root sheath from the infundibulum to the suprabulbar region which likely acts to compensate for the weak and/or absent stratum corneum barrier [298]. Lastly, a rich blood supply of the follicle will also support trans-follicular absorption and uptake into the circulation, driving sustained drug flux.

7.3. Intrafollicular delivery

Whilst the reservoir of the interfollicular stratum corneum is located in the uppermost cell layers, known as the stratum disjunctum (5 μm thick) [299], which can quickly deplete via desquamation, washing, and textile contact [296], the reservoir of the hair follicle extends much deeper (the practical portion for delivery is the funnel-shaped infundibulum which occurs in the top 500 μm) and can only be depleted by penetration across the follicle epithelium or by leaving the follicle with sebum flow and active

hair growth [300]. Small crystals [301] and colloidal particles like liposomes [302,303] have been shown to effectively target the follicle. There has been increased interest in this delivery method with the idea of manipulating the drug (size, lipophilicity, charge, solubility) or formulation (particle, vesicle storage dosage, sebum miscible excipients) to improve targeting ability.

A rich supply of lipids irrigates the follicle infundibulum and therefore it has been shown that lipids resembling the composition of sebum can promote follicular penetration [304]. There is further evidence that higher lipophilicity vehicles [305] as well as hydrophobic drugs or lipid nanoparticles [306,307] improve targeting. In one study, lipid-coated silica nanoparticles penetrated further into the follicles than bare nanoparticles, which display more skin surface adhesion [308]. An alternative view is that polar vehicles like ethanol improve targeting, potentially through the solvent effect or by dissolving and drying out the sebum allowing easier access for drug particles [309].

A number of studies have now studied the relative penetration of small (*MW* <500 Da) polar and lipid drugs via the follicular pathway with the human skin sandwich technique offering unique insights [310-310]. Other studies have used COMSOL and other modelling techniques to define follicular transport for drugs with differing physicochemical properties [130,172,178,313] and shown that polar have shorter follicular lag times than more hydrophobic drugs. The follicular route is especially important for drugs with an *MW* larger than 500 Da and particles-based drugs with high melting points, as these drugs often display limited if any, penetration through the stratum corneum [300,314]. Particles provide several advantages as drug carriers for follicular targeting, including a high surface-area-to-volume ratio, potential for deep follicular penetration, and the potential for sustained release, with enhanced uptake, an extended duration of action, and the possible limiting of adverse effects (e.g. corticosteroid therapy). Studies using size characterized fluorescent polystyrene microspheres in suspension have shown that there is a trend of microspheres penetrating skin appendages proportional to size [315,316]. A size effect has been shown for microparticles, with those having a diameter of 3–10 μm selectively penetrating the follicular duct, those larger than 10 μm remaining on the skin surface and those <3 μm showing equal follicle and surface distribution [315].

Lipid nanoparticles, polymeric nanoparticles, and metallic nanoparticles, [317] are of particular interest as they make it possible to deliver higher concentrations of drugs to target structures, improve the solubility of strongly hydrophobic drugs and increase physical and chemical stability. Nanoparticles have already been used to prolong the residence time of sunscreen agents in the stratum corneum [318], and in polyhexanide emulsion systems to achieve longer-lasting antisepsis of human skin [319]. They are reported to accumulate in hair follicles in a time and size-dependent manner [318]. Smaller particles were found to accumulate more in one study comparing 20 nm particles to 200 nm particles [318]. Toll has suggested that the deepest penetration occurs for particles of 750 nm, which was further enhanced by removing the plug in closed follicles by skin stripping and the application of massage [314]. This concurs with work by Lademann suggesting an optimal size of 643 nm for polylactic-co-glycolic acid (PLGA) particles, and 646 nm for silica particles. In this study, smaller (300 nm) and larger particles (920 nm, 1000 nm) had lower penetration profiles, and while silica particles penetrated further than the size-matched PLGA particles, size was the strongest factor in determining penetration depth [320,321]. Since a three-minute massage was used to apply these particles, a mechanical influence on the penetration process involving the movement of hairs was suggested [322].

Massage application has an important effect in driving delivery, with detection up 10 days post-dosing under *in vivo* conditions [323]. Lademann's group has shown that massaging can drive nanoparticles to different depths inside the hair follicles, dependent on nanoparticle size – those of ~100 nm to the infundibulum of the hair follicles, a depth of up to ~500 μm; 230 to 920 nm to the sebaceous gland at ~800 μm and 300 to 643 nm to the bulge region at >900 μm by a "geared" pump mechanism [317]. Assessment of morphology of the hair shaft has shown that the optimal size for delivery corresponds to the thickness of cuticula cells that line the shaft. Meanwhile, stochastic theoretical modeling demonstrates how particles of this size range can interact with the zigzag microrelief provided by the follicular epithelium and hair shaft cuticles upon massage, creating a ratchet-like pumping action [324]. Under *in vivo* conditions, this pump mechanism also occurs through the continuous movement of the body [322]. Further investigation is needed to understand how the viscosity of the formulation and factors such as hair shaft adhesion, surface charge, incubation, and massage times may effect these processes [317]. Current drug delivery strategies are now seeking to apply these findings to the controlled release, using pH, temperature, chemical, light, etc., of drugs in managing acne and sebaceous gland conditions [317].

There has been concern about the use of nanoparticles in topical products and potential for toxicity (e.g. zinc oxide sunscreens), however, no transfollicular penetration of nanoparticles into the viable epidermis has ever been reported under *in vivo* conditions [31,325]. *In vitro,* some studies have reported skin penetration of nanoparticles, but only after disruption of the skin barrier [326]. There is an indication that particles larger than 100 nm are unable to penetrate or permeate intercellularly via the stratum corneum or transfollicularly if performed *in vivo* on intact skin [295]. An emerging research area is triggering the gradual and controlled release of encapsulated drugs for therapeutic purposes (e.g. treating inflammation). Here, intrafollicular delivery using particle nanocarriers is used as a targeting method, and then transfollicular can follow upon stimulated release endogenously (e.g. through the change in temperature [327] or pH [328]) or exogenously (e.g. infrared radiation [329]).

Lademann's group investigated the effect of nanoparticles size on follicular penetration [320,330], including the influence of massage on the follicular penetration depth of the particulate form (average diameter 320 nm) and the non-particulate form of the fluorescent dye fluorescein *in vitro* using porcine skin as a surrogate for human skin. Following a 3 min massage of the two formulations and a 1-hour topical application, skin biopsies were taken and obtained histological sections were analyzed using fluorescence microscopy. While both particulate and non-particulate formulations penetrated down to about 300 μm without massage, the application of massage resulted in a penetration depth of just over 400 μm for the non-particulate formulation and well over 1500 μm for the particulate formulation [323]. They suggested that the zigzag structure and thickness of the cuticula (~530 nm in human vellus and terminal hairs; ~320 nm in porcine ear bristles) could influence the penetration of nanoparticles. As described earlier, the movement of the hair in massaging acts as a geared pump pushing the particles into the hair follicle infundibulum [322,324]. Mathes *et al.* [298] investigated the follicular uptake of clobetasol-containing particles (nanospheres, nanocapsules, and lipid-core nanocapsules) labeled with the fluorescent marker Rhodamine B *ex vivo* in porcine ear skin. The particles were applied as a topical formulation in an aqueous dispersion or in the hydrogel, and a standardized 3-minute massage was applied. After a one-hour incubation, a differential stripping method [331] (tape stripping combined with cyanoacrylate skin surface biopsy) was used to distinguish follicular and stratum corneum transport. When clobetasol, was formulated and applied as an ethanolic solution or hydrogel, the amount recovered in the hair follicle was negligible

with and without application of massage. In contrast, uptake into hair follicles was observed for the three types of nanoparticles, with a higher update when applied with massage compared to no massage. The highest uptake was obtained for the nanocapsules when formulated as an aqueous dispersion formulation (% recovery of Rhodamine B-labelled polymer: 3.06% for nanocapsules in an aqueous dispersion with massage vs. 1.61% with no massage). These results contrast with our recently published study in which the influence of massage on the penetration of topically applied ZnO nanoparticles (coated and uncoated) was investigated in human volunteers. Using state-of-the-art non-invasive techniques of multiphoton tomography with fluorescence lifetime imaging microscopy to visualize and quantify these nanoparticles, we found massage facilitated ZnO nanoparticles penetration into the skin furrows and infundibulum of human volunteers but not into the skin itself [332].

7.4. Sweat glands

The body has approximately 2–4 million sweat glands [333,334], which produce a hypotonic solution important for temperature regulation. Eccrine and apocrine glands are the two types of sweat glands that exist [335], differing in anatomical structure and location. Eccrine glands have ducts that connect directly to the skin surface, forming a pore opening at the distal end, while apocrine glands are about 10 times larger [336] and have ducts that link in with the hair follicle and pilosebaceous unit. While the eccrine gland can be found body-wide, making up 90% of all sweat glands, apocrine glands are mainly found at the axillae, mons pubis, external auditory meatus, areole, and circumanal area [337].

Little is known about the direct role of sweat glands in drug delivery. The density of eccrine glands ranges from 700 per cm^2 on the palms and soles of the feet to approximately 64 per cm^2 on the back [333] and therefore depending on site they may form a significant passage route. The sweat ducts themselves may be a target for delivery in the case of aluminum-based antiperspirants designed to block and prevent sweat secretion (51). Massage for 10 min has been shown to enhance antiperspirant efficacy by 25% suggesting improved delivery [338,339], meanwhile, the addition of surfactant or lipid solvent did not affect efficacy [340,341]. The sweat ducts may also be of interest for assessing exposure for other compounds. We have visualized elevated zinc levels within the sweat glands following the application of zinc pyrithione using X-ray fluorescence microscopy [342]. Zinc pyrithione is a coordination complex of zinc and therefore whether the elevated zinc is due to intact zinc complex or dissociated zinc ions is not known. It is also important to consider the role that sweat glands have when functionally active, capable of producing up to 3 L of sweat per hour [343]. This can have the effect of diluting topical agents applied to the surface such as sunscreens and insect repellents. Sweating in humid climates can also have significant impact and presents a challenge on topical products for wounds.

Since eccrine glands form pores on the skin surface these are more likely to act as shunt routes compared to apocrine glands, provided they are unobstructed by keratinous debris, which may be the case in diseases such as atopic dermatitis or psoriasis. The diameter of the ductal portion has been estimated at between 20 and 60 μm [344,345] and can extend for up to approximately 1000 μm, therefore providing a channel for drugs either in solution or as fine particles. Further work is needed to elucidate specific pathways here. Drugs could either form a reservoir in the sweat gland and duct or could pass into deeper tissues layers by crossing the tubular epithelia [346], which is composed of a double layer of luminal and basal ductal cells. The luminal cells have dense tonofilaments that strengthen the tube wall, especially where it forms a pore with the skin surface in the stratum corneum, a particular region known as the acrosyringium. The relative barrier that the tubular epithelia provide as compared to the stratum corneum is not currently known. Delivery to these structures likely depends on drug and formulation factors such as size, charge, viscosity, and lipophilicity. Improved targeting would be particularly useful in conditions such as hyperhidrosis and also for non-sweat gland-related conditions as a way of enhancing general epidermal and dermal penetration.

8. Heterogeneity on skin transport, retention, and response

Heterogeneity in skin transport applies to both variations in the drug skin transport pathway as well as between skin from different anatomical skin sites, gender, and age, all of which can be associated with variations in local skin absorption [130,347]. Heterogeneity can also be induced by the product-skin-environment effect that can modulate the product evaporation, skin permeation, and reservoir effect. A number of studies have also explored how heterogeneity in the skin barrier at a given site may affect drug transport, as discussed earlier in 4.2.

8.1. Skin reservoir

The nature of the skin reservoir is at this stage still ill-defined but is most likely to involve all parts of the skin sequestering various types of solutes and particles as we discussed in a recent review [348,349]. The skin reservoir effect can result from the low diffusivity of drugs through the stratum corneum (i.e. long lag times) or from the depot of drugs in the stratum corneum. This was first described by Vickers who showed that the vasoconstriction associated with topical corticosteroid use could be reactivated for up to two weeks after the first topical application by repeatedly occluding the application site [350]. The skin reservoir effect for steroids is most evident when these are released from the stratum corneum on its hydration by occlusion and other mechanisms [351].

The four main determinants of the stratum corneum reservoir effect are the diffusivity of the drug in the stratum corneum, a high stratum corneum uptake/binding, clearance via the epidermis [56], and epidermal turnover (i.e. stratum corneum desquamation) [71]. Highly lipophilic drugs are likely to be retained in the SC because of their affinity for SC lipids and poor solubility into the viable epidermis. High molecular weight (>350 Da) drugs will also be retained in the SC because they diffuse through the SC slowly with long lag times. Corticosteroids, being large, lipophilic, and widely used, are therefore the best-documented group of drugs having an SC reservoir effect [348]. The retention of these and other drugs will also be dependent on the rate of epidermal turnover [71], which in normal skin is 28 to 40 days but it may be much less when the skin turnover is rapid, such as in psoriasis, where the skin turnover rate may only be 3–4 days. Potential retention sites for drugs in the SC include the skin lipids, corneodesmosomes, and related structures and binding to keratin within corneocytes, especially in the more permeable stratum disjunctum layer (4.2, Fig. 6B) for drugs with a high affinity for and a slow rate of dissociation from keratin [165,165,179]. This is also the SC layer most likely to become hydrated after application of topical products [67,68], facilitating the release of corticosteroid and other drugs from this potential reservoir [348]. However, drug in the stratum disjunctum will be the first to be lost in the continual formation and desquamation of SC.

The viable epidermis can both facilitate reservoir formation and also be potential reservoirs. For instance, the viable epidermis may be a significant barrier to the skin permeation of large and/or lipo-

philic solutes [83,84], facilitating SC retention. Further, lipophilic β-blockers bind to both SC lipids and viable epidermal cells (keratinocytes) [352]. PBPK modelling of viable epidermal transport has suggested that drug retention is greatest for more lipophilic solutes and related to the relative volumes of cytoplasm 87.9%, lipid 0.1%, and extracellular fluid (which will contain about half the protein content seen in plasma) 12.0% [134].

The dermis is also a potential barrier and reservoir for topically applied drugs. It is estimated that the distance from the avascular region of the dermis between the dermal papillae and the dermal-epidermal junction is ~40 μm [353]. Thereafter, it would be expected that drugs would be rapidly cleared into the systemic circulation and deeper tissues by the dermal circulation. As both dermatomed and full-thickness skin are avascular, a potential dermal reservoir effect will be more pronounced in these tissues. We have reported that diclofenac, econazole, retinoic acid and desoximetasone are also highly bound in the dermis [263,354] and a number of other studies, including our own, have quantified the binding of a wide range of other drugs in the dermis [355,356]. In general, as the dermal diffusion coefficients of drugs in their unbound form are similar to in water [265], dermal binding largely determines the dermal reservoir effect both through the extent of binding but also in, *in vitro* studies, by the thickness of the dermis being used. In the latter case, binding will slow down dermal diffusion (effective diffusion coefficient = fraction unbound X unbound diffusion coefficient) and desorption from the dermal reservoir.

There has been some considerable recent interest in the reservoir effect associated with drug crystallization of fluocinolone acetonide, acetylsalicylic acid, hexachlorophene, sodium fusidate, ibuprofen, diclofenac acid, and hydrocortisone. Here, various solvents carry a drug into the SC and it crystallizes in the SC intercellular lipids after being left behind and exceeding its SC intercellular lipid solubility on the rapid evaporation and further SC permeation of the solvents that carried it into the SC [357].

As discussed in Section 7.3 and shown in Fig. 3C, F, G, and H, various nanoparticles can get trapped in the infundibulum of the hair follicle and serve as a reservoir. Nanoparticles can also be trapped in skin furrows as we have shown for zinc oxide nanoparticles [358] and shown in Fig. 3I. Other high protein binding topically applied compounds may also be retained in the skin as a result of binding to corneodesmosome remnants and accessible keratin in the SC disjunctum as well as to SC lipids as discussed earlier in Section 3.

Furrows can also be a reservoir or facilitating reservoir formation, especially for drugs retained from a product and for particles, in that the topical product may be seen to remain in the furrow after washing [31,358]. In addition, furrows can influence the micro transport of drugs in lateral and transverse directions affecting the distribution of product on the skin surface especially after rubbing, massage, and flexing particularly when there are loose squamae. A greater lateral spread will mean less is available directly below the site of application. Lateral spreading is a time-dependent process [359-357] and is particularly relevant for compounds that are designed to target the skin surface. This includes sunscreens such as zinc oxide, [361], anti-fungal agents [362], and insect repellents. Further, lateral spread of drugs across the skin surface is important in their delivery to appendages, such as the hair follicles (which can then act as a reservoir or shunt route for deeper delivery in the transverse direction).

8.2. In silico and IVPT scale-up for in vivo prediction

A key challenge is providing topical products to consumers that meet their individual skin needs, which can vary greatly between individuals. Heterogeneity in skin permeability of different body sites is also important as various topical products are applied all over the body to meet different indications. As shown in Fig. 11, the skin absorption for a large number of drugs has been shown to vary greatly with the site of application. In general, the order of skin permeability ranking is genital > forehead, scalp, back > hand, abdomen, chest, plantar > thigh, lower leg, and palm. Scrotal skin is the site with the fastest rate of topical absorption, due to a combination of its thin stratum corneum and high blood supply, which is followed by the forehead, scalp, and neck [363]. While the thickest stratum corneum is located on the soles of the feet, this is not the site with the lowest rate of absorption, rather it is the forearm, suggesting other factors, as well as physical thickness, contribute to absorption. [293,364,364]. Indeed, differences in lipid content have been reported from the skin on the abdomen, leg, face, and sole [365], with variations in neutral lipids as opposed to sphingolipids, suggested to be the main contributor to the variation in barrier function at the different sites. Infant skin is more permeable as a result of increased hydration and an altered acid mantle [366], while aged skin is drier and less permeable particularly for hydrophilic substances [367]. Concerning ethnicity, there are conflicting and sparse reports on differences in absorption, however, the skin of color has been reported to have more stratum corneum cell layers and higher lipid content than Caucasian skin [368], which is important for the development of physiologically based models.

The software Certara's Simcyp MechDermA PBPK model, described in Fig. 12A and widely used by the pharmaceutical industry and FDA, provides dermal PBPK based assessments for topical products which take body site into account. As shown in Fig. 12A, it allows various drug and product attributes to be integrated into the skin absorption process and allows for population variations in age, gender, weight, height, and disease state, as well as location variations, capturing SC thickness, number of SC layers, hair follicle density, hydration state, and many other parameters.

Highlighted in Fig. 12A (in red) is diseased skin, which may show significant changes in structure and function that can either increase or decrease the absorption of topical compounds [369]. In psoriasis for instance there is an increased stratum corneum thickness and altered lipid composition. In other conditions such as atopic dermatitis, permeation may be increased two-fold [370] due to barrier compromise. In acne, the follicles, which are key sites of drug action, are hyperkeratotic and plugged and there is increased steroid metabolism [277]. Inflammation is a common element to most skin disorders, involving an increase in the release of local vasoactive factors that will enhance microcirculation. In some conditions such as melanoma, an increase in MRP1 transporters has been reported [371].

However, defining the impact of these changes *in vivo* for a given product is not straightforward and generally involves the strawman decision tree described in 5.1, recognizing that monitoring local drug concentrations in SC or dermis is challenging. One possible way forward is to apply either *in silico* or *IVPT* data in predicting normal skin permeation of a drug from a given product *in vivo* and then adjusting those predictions for the site and other differences in permeation *in silico*. As discussed earlier in Section 2, the published literature suggests that extent of absorption between *in vitro* (*IVPT* data) and *in vivo* studies is highly correlated when study protocols are harmonised, but less so otherwise [25]. Fig. 12 B shows an example of *in vitro - in vivo* relationship (IVIVR) for nitroglycerin patches being developed by a combined *in silico*, IVPT, and compartment-in-series PBPK modelling approach [85]. This approach is analogous to that recommended by the FDA for extended-release (ER) product *in vitro - in vivo* correlations (IVIVC) [372]. It is evident that the IVPT data combined with the known disposition data for the Nitro-Dur II product predicted its plasma concentration–time course *in vivo*. However, external validation

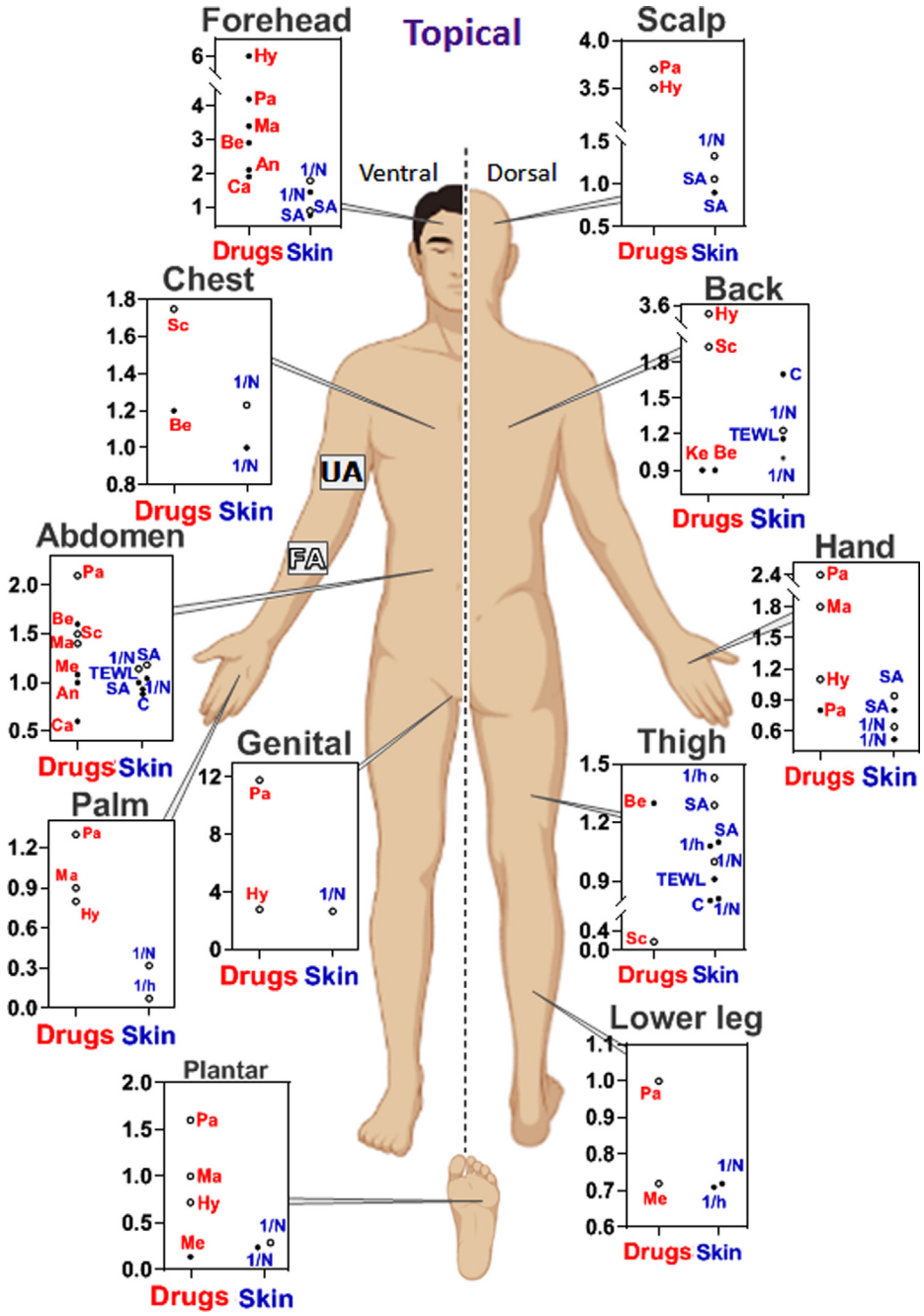

Fig. 11. Effect of body site on the skin absorption of various drugs after topical application and the skin physiological parameters. Black filled circles are the estimated absorption of topical drugs and skin physiological parameters, normalized to values for the upper arm (UA) and black open circles are the estimated absorption of topical drugs and skin physiological parameters, normalized to values for the forearm (FA). Data used here were obtained from the literature for topical drugs: An-Aspirin [406], Be-Benzoic acid [407], Ca-Caffeine [408], Hy-Hydrocortisone [409], Ke-ketoprofen [410 60], Ma-Malathion [363], Me-Methyl Salicylate [406], Pa-Parathion [363]; Skin parameters: C-conductance, TEWL-transepidermal water loss, 1/h-inverse of SC thickness, 1/N-inverse of the number of SC layers. The SC thickness values were derived from the work of Polak *et al.* [411], except for the palm*, which was reported by Bohling *et al.* [412]. The SC values for the number of SC layers, TEWL, and conductance (SC hydration) came from a study by Ya-Xian *et al.* [404].

with other brands of nitroglycerin products failed, indicating that generalizability is not straightforward [85]. There are a number of potential sources for these differences, including product design-related variations in drug release profiles and differences in IVPT and *in vivo* skin permeability. The latter arises because skin used *in vitro* and *in vivo* studies are from different individuals, the individual pharmacokinetics may vary from that of the population, different application methods in the two populations, and environmental/procedural differences when studies are carried out at different sites. As Liu *et al.* [85,86] point out, the SC model parameters used to derive the IVIVR demonstrated in Fig. 12B can be adjusted to account for variations in body site and skin condition, as defined by skin morphology, biochemistry, and function, in predicting *in vivo* pharmacokinetics. The broader challenge is in predicting individual consumer outcomes for topically applied products based on that individual's skin site, condition, and method of application, as well as taking into account environmental and other effects.

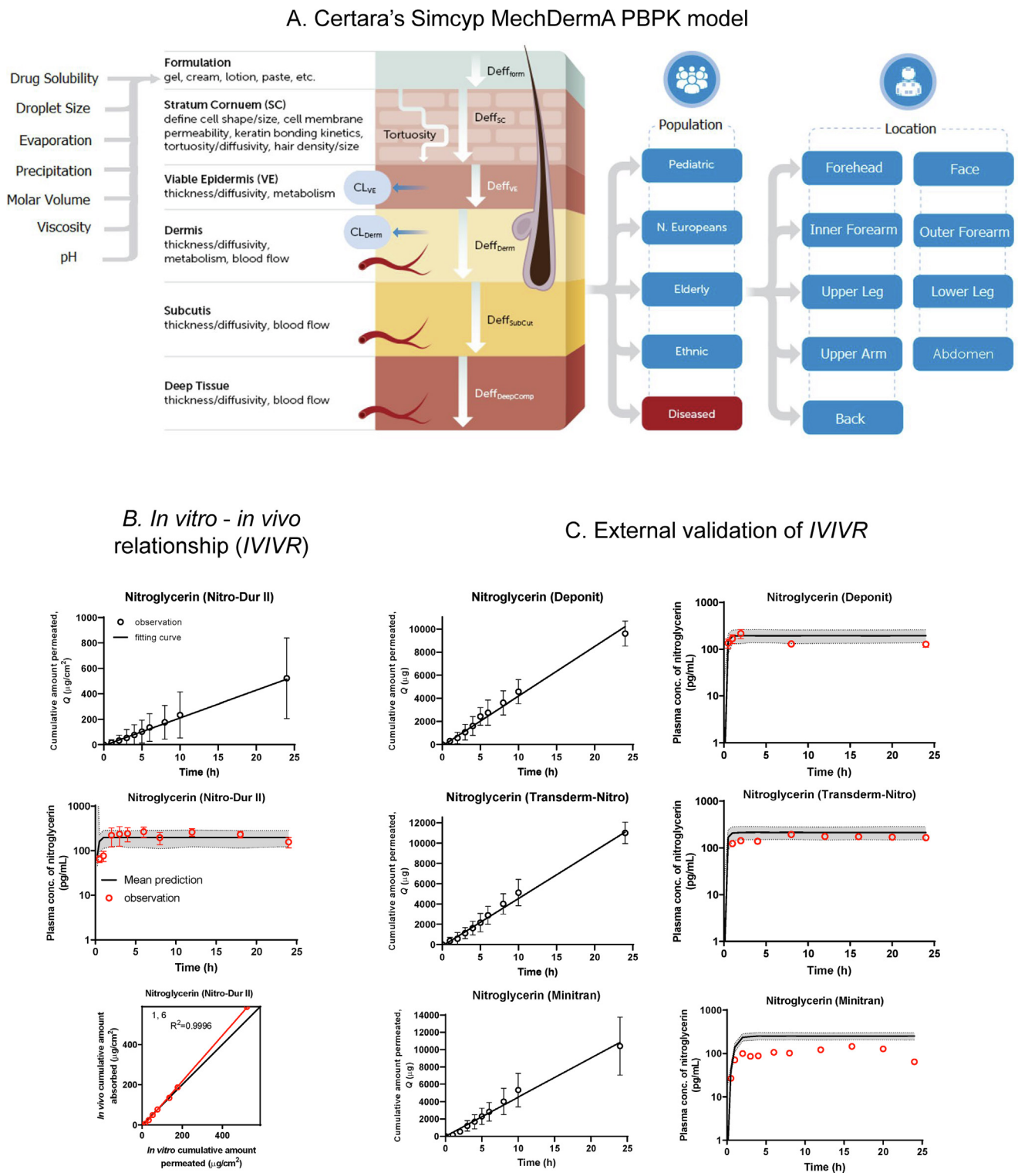

Fig. 12. *In silico*, *In Vitro* skin Permeation Test (IVPT) and *in vivo* relationships. A. Snapshot of Certara's Simcyp MechDermA PBPK model software (courtesy Sebastian Polak, Certara). B. Nitroglycerin dermal *in vitro – in vivo* relationship (IVIVR) for Nitro-Dur II, based on an SC compartment – in - series drug transport model of SC IVPT data combined with intravenous pharmacokinetics, and C. External validation of IVIVR with other nitroglycerin products. From [85] with permission of Elsevier.

8.3. Meeting consumer perceptions and need

Effective topical product performance is defined not only by whether an individual consumer's observations about a product working without adverse effects but also on their perception of the product. We now consider each of these two aspects here.

8.3.1. Efficacy and safety of topical products

As we have recently reviewed the safety of topical products from both the *cutaneous margin of safety*, in which inter-subject variability and toxicities, such as irritancy, photosensitization, and corrosivity, together with the *systemic margin of safety* such as topically applied corticosteroid suppression of the adrenal gland

in the hypothalamic–pituitaryadrenal axis [373], we are not considering this aspect in this review. We are also not addressing to any extent the corollary measure of *cutaneous efficacy* also addressed in the same chapter. The cutaneous margin of toxicity and safety are both related to their putative concentration obtained at the local site of action (Eq. (1)). The approach of using a putative concentration at the local site of action has been widely used in percutaneous absorption of antivirals, where this concentration has been referred to as the free drug concentration at the local target site (C^*), equivalent to $f_u.C_{ss,local}$ where f_u is the fraction unbound and the target site is assumed to be the epidermal basal cell layer [373,374].

In principle, both the efficacy and toxicity of a given drug are defined as the product of the potency of a drug multiplied by its local site of action concentration. Thus, the key determinants of both the safety and toxicity of a drug at its site of action are its potency, rate of delivery through the skin, and clearance from the site, noting that toxicity can also arise at other sites. Thus, as is well known, impaired clearance, as occurs when local anesthetics are administered with vasoconstrictors, results in a more prolonged effect. Further, application of a topical dosage form to impaired skin or at a higher fractional solubility in a given dose will also have a heightened response.

8.3.2. Consumer perception of topical products

Consumer perception may be influenced by the nature of excipients present in a product, how the product looks, smells, and feels, whether the product is stable and how the product is packaged and labeled. Also important is whether the product may alleviate concurrent skin conditions associated with the primary cause of the skin disorder [373]. For example, consider an underlying fungal skin infection being treated with an antifungal product. The skin at this site may also be chapped and irritated due to the infection. From a consumer perspective, moisturizing and soothing, as may be provided by an emollient, may be just as important as bringing the fungal infection under control [375].

The large placebo response associated with topical product application emphasizes the role played by a consumer's perception of product performance. As one example, 20–30% of the response for a number of topical anti-infectives used to treat acne vulgaris arose from a placebo response. In that study, the age-related placebo response difference was greater than the age-related therapeutic response with the placebo effect being lower for a more severe condition [376]. However, this response may be an underestimate as Chiou [377] has reported placebo responses in acne vulgaris ranging from 9 to 89% for two studies, with means of 55 and 58%. It is now well recognized that the modern consumer (including the patient) cares at least as much about the experience of applying a topical product as they do about the alleviation of disease. The consumer perceptions are well understood by the cosmetic industry. As a consequence, consumer testing panels are used to assess product sensorial feel and "the experience" of the consumer [378].

The "bitter pill psychology" [379-380] also plays a role in topical product perception. Here, textural, and perceptive qualities of semisolid products applied on the skin such as a strange smell may be indicative of a product stability issue [382] or when perceived to be inferior because it may, for instance, be gritty may impact on whether the product is perceived to work. A key challenge for the generic equivalent products, now widely used in the USA (Fig. 9A) and elsewhere [383], is a general opinion held by many professionals [384] and consumers [385] that generics are less effective than the RLD products.

Consequently, there is now a strong push to identify methods predictive of *in vivo* performance [243]. A key component in that approach is to characterize the impact of variations in excipient nature and concentrations [382], especially when those excipients, such as emollients, are adjuncts to topical therapy [386] and also constitute the texture, feel, and perception of the product by the patient. Product failure may occur due to poor patient compliance caused by poor aesthetics (sensory attributes) of the product. Sensorial evaluation is described as behavioral science and as a scientific method to elicit, measure, analyze and interpret responses to products/materials through the sense of sight, odor, touch, taste, and hearing [387]. Overall, these topical products may exert either positive (placebo) and/or negative (nocebo, literally "harmful") perceptions independent of whether any active ingredient is present or not. Their role in reinforcing our perceptions of good and bad is well recognized by industry who now color tablets to enhance or reinforce a therapeutic effect-blue for sedation, red and orange for stimulants, yellows to depict positivity for antidepressants, green for anxiety, and white for pain, with brighter colors and embossed brand names used to heighten effects [388]. Importantly, cultural differences also affect responses, so that, for instance, blue is used to "inspire" the Italian soccer team and yellow equates to the better antimalarial drugs in Africa. In addition, verbal comments and prior experiences partly determine the itch response to an applied antihistamine cream [389]. It is not just response but adherence that can be impacted by placebo and nocebo effects. An often-cited example is that some children do not complete their course of medicines because it is unpalatable [379]. Sensorial and perceptive attributes are also important in building and retaining brand loyalty.

A typical cosmetic product sensory evaluation panel assesses the product for its perceptibility, consistency, smoothness, spreadability, smoothness after drying/penetration (film formation, residue), assessment of product thickness/viscosity by perception, greasiness, and time to absorption to name a few [390]. Whilst properties of a topical formulation affect consumer perception, the properties of the skin to which it is applied and the finger with which it is applied are also important [391]. Accordingly, evaluations are highly subjective [392] and need an adequately powered study [393]. The alternative is to move to an instrumental assessment of product characteristics such as their low shear viscosity [394–396]. Indeed, product consistency and uniformity are now routinely assessed and are often a regulatory requirement [397]. A product consistent at very low shear (typically lower than the shear experienced during simple spreading or vigorous massaging) may or may not be consistent upon rubbing and massaging [398].

9. Conclusion

In this review paper, we have sought to characterize the drug delivery of topical products from the perspectives of their development over time, their need, the likelihood that a drug candidate may cross the skin, and how it gets to its target site. In doing so, we have reviewed the various QSAR methodologies for determining skin permeability, the various models defining the dermal PBPK of drugs, explored the contribution to understanding skin permeability by molecular dynamics simulations, and considered the range of topical products on the market and how they have been formulated. We have also considered other factors that may affect local product delivery such as dermal blood flow, dermal metabolism, appendageal delivery, and heterogeneity in skin absorption. Lastly, we recognized that the efficacious use of topical products not only depends on their safety and efficacy but also on consumer perceptions of those products and that topical product regulation has moved from a predominantly clinical trial assessment to quality by design and performance assessment.

Our conclusion is that, whilst we have learned much about local skin drug delivery in recent years, we still have not fully under-

stood what aspects of skin transport have been accurately captured by the models we are using, and what aspects have not. The first two questions raised in this review are: (1) What are the relative contributions played by the stratum disjunctum and stratum compactum in the skin permeation of drugs from topically applied drug products? and (2) To what extent is SC drug transport intercellular and/or transcellular? Our current perspective for the first question is somewhere in the middle of one view that "*the innermost two-thirds of the stratum corneum formed the principal barrier to free diffusion in agreement with the histologic concept of a stratum corneum consisting of a proximal, compact stratum compactum and a distal, porous stratum disjunctum*" and the alternative view that "*the entire stratum corneum forms a barrier and that is composed of a compact, multilayered tissue*" as put by Brody [58], recognizing also that, in his interpretation of the SC transmission electron microscope image in Fig. 4A, the "*basal and middle zones seem to correspond to what histologists have termed stratum compactum*". This raises the further question as to whether, in future PBPK modelling, we should further subdivide the stratum disjunctum into Brody's outer zone along with an inner zone that has significant barrier properties. Such a model is consistent with our earlier speculation that drugs may partition into the stratum disjunctum to be bound to keratin and other structures more so than in the stratum compactum, explaining a non-linear steady-state concentration – SC depth relationship [182] that may enhance the SC concentration gradient [185] and our use of a three compartment-in-series PBPK model of the SC in describing the percutaneous absorption of SC transport for topical and transdermal products [85,86]. Irrespective, it is evident that Brody's view in 1989 "*Contradictory to the view(s) of (many), (these) studies suggest that the intercellular space represents an important element in the entire stratum corneum*" holds firm today. However, perhaps the "compactness" of the SC intercellular lipids in the stratum compactum, facilitated by corneodesomosomes and other structures in the deeper SC layers and along with anisotropic diffusion [134], hinders SC intercellular lipid diffusion more than in the upper SC layers, resulting in longer SC lag times than one may deduce from a combination of observed SC diffusion coefficients and a tortuous intercellular pathway [150] alone. This response to the first question, our analysis of the data to date in Section 4.2, and our own modelling [185] suggests that drugs will permeate into the stratum disjunctum corneocytes and may bind to keratin, especially in the outermost layer. However, it is less clear that this permeation occurs in the stratum compactum, where the current evidence favors SC transport here mainly via the SC intercellular lipid pathways.

A third question raised in this work is: Which QSPR model best describes percutaneous absorption of drugs from topically applied products? Our review of our own and other models using external validation using newly published data has shown them wanting and that the best model describing J_{max} was the Roberts-Sloan model (Section 4.1). The inclusion of drug solubility in both oil and water, along with drug size, in this model [115] also meets the bifunctional drug solubility characteristics of the SC observed by Scheuplein and Blank [30]. The later finding that dermal clearance is related to these same parameters [264] (Section 6.1) is an interesting parallel. The follow-on question that follows is can we better predict QSPR of SC drug permeability by understanding the interactions between drugs and the SC intercellular lipid pathway? The answer to this question offers unique opportunities in predicting potential new drugs for topical product application, along with associated skin penetration enhancers [399,400]. Molecular dynamics modelling offers exciting possibilities here, especially in further understanding the impact of physical, chemical, and other SC permeation enhancers on SC lipid diffusivity and, thence, on SC permeation. A fourth question is what is the impact of a topical drug product on the skin after application? In particular, how much drug, what form it is in, and how it is applied all affect percutaneous absorption with massage able to affect the percutaneous absorption of drugs into the SC [401] and nanoparticles into the appendages (see Section 7.3).

However, the use of any QSPR, PBPK, and/or molecular dynamics simulation drug delivery model is only useful if it, firstly, can predict IVPT performance but, secondly and most importantly, *in vivo* topical dermal performance. These, in turn, are defined by the model limitations as defined by assumptions used and starting points. Further, for the model to be useful in scaling up to *in vivo* situations, we need to record both the model's uncertainty and scope noting that both very simple models and very complex models will have limited useability. Lastly, whilst models used to describe topical drug delivery may be "wrong" in terms of precisely mimicking what happens in the skin, they can and have been shown to be useful. Much of the focus in topical drug delivery system development has been on describing SC transport. However, what happens in the product [419] and beyond the SC [420], as discussed in Sections 5 to 8, also matters and, as Ken Walters pointed out some 20 years ago, the key challenge of "*. . .quantifying solute (drug) concentrations in the lower layers of the epidermis in vivo in dynamic studies*" [421] remains. He went on to suggest that In vitro human skin permeation was the only realistic option [422] but noted that technology and "*. . .transdermal therapeutic systems have advanced our understanding of the structure of the skin and the mechanisms of transport through the barrier membrane*" [423]. Topical drug product development has also been nurtured by the additional economic and social needs of access, alternatives to animal testing and cost. Here, government, industry and academia have recently come together to meet these needs with a combined Quality by Design [252], human IVPT and PBPK (Sections 5.3, 5.6, 8.2) regulatory approach and there is much to learn! So, we must also recognize that an additional challenge in the further development of topical drug products will be unraveling the 'unknown unknowns'!

Declaration of Competing Interest

The authors declare that they have no known competing financial interests or personal relationships that could have appeared to influence the work reported in this paper.

Acknowledgments

We dedicate this review to Ken Walters, an inspirational leader and mate, who gave so much to our discipline. This review is an update of presentations MSR made at the invitation by **Claus-Michael Lehr** at the 4th Galenus Workshop "Drug Delivery To The Human Skin – State-Of-The-Art And Future Perspective" 17 April 2018; "Drug Delivery to Human Skin" Saarland University and Helmholtz Institute for Pharmaceutical Research Saarland (HIPS); Saarbrücken, Germany; 25th – 27th of February, 2015; Organizers: Dr. Maike Windbergs, Prof. Dr. Claus-Michael Lehr; and Extension of the J_{max} Concept at 10th International Conference and Workshop on BIOLOGICAL BARRIERS 16-21 February 2014; Helmholtz-Institute for Pharmaceutical Research Saarland and Saarland University www.uni-saarland.de/biobarriers2014.

In writing this review, MSR acknowledges the Australian NHMRC (#1107356, APP1049906), Australian ARC (DP120104792), US FDA (U01FD006700, 1U01FD006496-01, U01FD006522, 1U01FD005226-01, 1U01FD005232-01) for the support of his work in this area. SEM acknowledges the support provided by an Australian Government Research Training Program (RTP) Scholarship. We thank Richard Guy and Annette Bunge for their constructive comments on the section entitled "Physiologically based – pharmacokinetic modeling of drug transport" as well

as Lars Norlen for discussions and providing an updated Fig. 1 from their recent JID paper and Magnus Lundborg for his figure showing how SC molecular dynamics is translated into practical use and reviewing the manuscript.

Declaration of Interest

This work was undertaken at the Translational Research Institute, Woolloongabba, QLD, and at the Basil Hetzel Institute for Translational Health Research, Woodville, Australia. The Translational Research Institute is supported by a grant from the Australian Government. The authors have no other relevant affiliations or financial involvement with any organization or entity with a financial interest in or financial conflict with the subject matter or materials discussed in the manuscript apart from those disclosed. The views expressed here do not reflect official policies of the Department of Health and Human Services; nor does any mention of trade names, commercial practices, or organization imply endorsement by the United States Government.

References

[1] M.N. Pastore, Y.N. Kalia, M. Horstmann, M.S. Roberts, Transdermal patches: history, development and pharmacology, Brit. J. Pharmacol. 172 (2015) 2179–2209.
[2] N.G. Jablonski, Skin A Natural History, University of California Press, Berkeley, 2013.
[3] C.S. Henshilwood, F. d'Errico, K.L. van Niekerk, Y. Coquinot, Z. Jacobs, S.E. Lauritzen, M. Menu, R. Garcia-Moreno, A 100,000-year-old ochre-processing workshop at Blombos Cave, South Africa, Science 334 (2011) 219–222.
[4] D. Piombino-Mascali, L. Krutak, Therapeutic Tattoos and Ancient Mummies: The Case of the Iceman, in: Purposeful Pain, Springer, 2020, pp. 119-136. https://link.springer.com/chapter/10.1007/978-3-030-32181-9_6.
[5] M.J. Geller, Ancient Babylonian Medicine, 1 ed., Wiley-Blackwell, Malden, 2010.
[6] S. Selwyn, The topical treatment of skin infection, in: H.I. Maibach, R. Aly (Eds.), Skin microbiology, relevance to clinical infection, Springer-Verlag, New York, 1981, pp. 317–328.
[7] B. Ebbell, The Papyrus Ebers: the greatest Egyptian medical document, Levin & Munksgaard, Copenhagen, 1937.
[8] Y.W. Chien, Development of transdermal drug delivery systems, Drug Dev. Ind. Pharm. 13 (1987) 589–651.
[9] H.R. Moghimi, A. Shafizade, M. Kamlinejad, Drug delivery systems in Iranian traditional pharmacy (in Persian), Traditional Medicine and Materia Medica Research Center, SBMU, Tehran, Iran, 2011.
[10] G.L. Flynn, M.S. Roberts, M.D. Donovan, Physical and Biophysical Foundations of Pharmacy Practice: Issues in Drug Delivery, Michigan Pub. in partnership with the University of Michigan College of Pharmacy, 2015. https://babel.hathitrust.org/cgi/pt?id=mdp.39015095766716&view=1up&seq=407&skin=2021.
[11] L. Pelner, Paul Gerson Unna, NY State J. Med. 12 (1971) 2895–2896.
[12] J.F. Borzelleca, Paracelsus: herald of modern toxicology, Toxicol. Sci. 53 (2000) 2–4.
[13] J. Firth, Syphilis - its early history and treatment until penicillin, and the debate on its origins, JMVH 20 (2012) 49–58.
[14] G.E. Ebright, The effects of nitroglycerin on those engaged in its manufacture, JAMA 62 (1914) 201–202.
[15] G. Martin-Bouyer, R. Lebreton, M. Toga, P.D. Stolley, J. Lockhart, Outbreak of accidental hexachlorophene poisoning in France, Lancet 1 (1982) 91–95.
[16] U.R. Hengge, T. Ruzicka, R.A. Schwartz, M.J. Cork, Adverse effects of topical glucocorticosteroids, J. Am. Acad. Dermatol. 54 (2006) 1–15.
[17] H.I. Maibach, Cutaneous pharmacology and toxicology, Annu. Rev. Pharmacol. Toxicol. 16 (1976) 401–411.
[18] Upcoming changes to REACH information requirements. ECHA/NR/21/19. , in, 2021. https://echa.europa.eu/-/upcoming-changes-to-reach-information-requirements. Accessed 2 August 2021.
[19] M.A. Ngo, H.I. Maibach, Dermatotoxicology: historical perspective and advances, Toxicol. Appl. Pharmacol. 243 (2010) 225–238.
[20] A. van Leeuwenhoek, Letter of 1683-09-16 (AB 75) to Anthonie Heinsius. https://lensonleeuwenhoek.net/content/wrote-letter-1683-09-16-ab-75-anthonie-heinsius. Accessed 25 June 2021.
[21] A. van Leeuwenhoek, Letter XLIII of 1717-09-17 (AB 342) to Members of the Royal Society. https://lensonleeuwenhoek.net/content/skin-and-fat-skin-human-hand-and-nose. Accessed 25 June 2021.
[22] A.M. Kligman, E. Christophers, Preparation of isolated sheets of human stratum corneum, Arch. Dermatol. 88 (1963) 702–705.
[23] T.J. Franz, Percutaneous absorption. On the relevance of in vitro data, J, Invest. Dermatol. 64 (1975) 190–195.
[24] R.J. Feldmann, H.I. Maibach, Absorption of some organic compounds through the skin in man, J. Invest. Dermatol. 54 (1970) 399–404.
[25] P. Lehman, S. Raney, T. Franz, Percutaneous absorption in man: *in vitro-in vivo* correlation, Skin Pharmacol. Physiol. 24 (4) (2011) 224–230.
[26] D.E. Wurster, S.F. Kramer, Investigation of some factors influencing percutaneous absorption, J. Pharm. Sci. 50 (1961) 288–293.
[27] R.J. Feldmann, H.I. Maibach, Percutaneous penetration of steroids in man, J Invest Dermatol. 52 (1969) 89–94.
[28] S. Riegelman, Pharmacokinetics, pharmacokinetic factors affecting epidermal penetration and percutaneous absorption, Clin. Pharmacol. Therapeut. 16 (1974) 873–883.
[29] R.J. Feldmann, H.I. Maibach, Percutaneous penetration of some pesticides and herbicides in man, Toxicol. Appl. Pharmacol. 28 (1974) 126–132.
[30] R.J. Scheuplein, I.H. Blank, Permeability of the skin, Physiol. Rev. 51 (1971) 702–747.
[31] Y.H. Mohammed, A. Holmes, I.N. Haridass, W.Y. Sanchez, H. Studier, J.E. Grice, H.A.E. Benson, M.S. Roberts, Support for the safe use of zinc oxide nanoparticle sunscreens: lack of skin penetration or cellular toxicity after repeated application in volunteers, J. Invest. Dermatol. 139 (2019) 308–315.
[32] C. Herkenne, I. Alberti, A. Naik, Y.N. Kalia, F.-X. Mathy, V. Préat, R.H. Guy, In vivo methods for the assessment of topical drug bioavailability, Pharm. Res. 25 (2008) 87–103.
[33] R. Fox, S. Hilton, Bradykinin formation in human skin as a factor in heat vasodilatation, J. Physiol. 142 (1958) 219–232.
[34] M. Greaves, J. Sondergaard, Continuous skin perfusion in vivo as a method for study of pharmacological agents in human skin, Acta dermato-venereologica 51 (1971) 50–54.
[35] R. Holmgaard, J.B. Nielsen, E. Benfeldt, Microdialysis sampling for investigations of bioavailability and bioequivalence of topically administered drugs: current state and future perspectives, Skin Pharmacol. Physiol. 23 (2010) 225–243.
[36] M. Müller, H. Mascher, C. Kikuta, S. Schäfer, M. Brunner, G. Dorner, H.G. Eichler, Diclofenac concentrations in defined tissue layers after topical administration, Clin. Pharmacol. Ther. 62 (1997) 293–299.
[37] S.E. Cross, C. Anderson, M.S. Roberts, Topical penetration of commercial salicylate esters and salts using human isolated skin and clinical microdialysis studies, Br. J. Clin. Pharmacol. 46 (1998) 29–35.
[38] M. Bodenlenz, K.I. Tiffner, R. Raml, T. Augustin, C. Dragatin, T. Birngruber, D. Schimek, G. Schwagerle, T.R. Pieber, S.G. Raney, Open flow microperfusion as a dermal pharmacokinetic approach to evaluate topical bioequivalence, Clin. Pharmacokinet. 56 (2017) 91–98.
[39] B. Zondek, Cutaneous application of follicular hormone, The Lancet 231 (1938) 1107–1110.
[40] B. Zondek, The excretion of halogenized phenols and their use in the treatment of urogenital infections: percutaneous chemotherapy, J. Urol. 48 (1942) 747–758.
[41] M.S. Roberts, Solute-vehicle-skin interactions in percutaneous absorption: the principles and the people, Skin Pharmacol. Physiol. 26 (2013) 356–370.
[42] S. Rothman, The principles of percutaneous absorption, J. Laborat. Clin. Med. 28 (1943) 1305–1321.
[43] T. Higuchi, Physical chemical analysis of percutaneous absorption process from creams and ointments, J. Soc. Cosmet. Chem 11 (1960) 85–97.
[44] I.H. Blank, Penetration of low-molecular-weight alcohols into skin. I. Effect of concentration of alcohol and type of vehicle, J. Invest. Dermatol. 43 (1964) 415–420.
[45] E.J. Lien, G.L. Tong, Physicochemical properties and percutaneous absorption of drugs, J. Soc. Cosmet. Chem, Citeseer (1973).
[46] M.S. Roberts, R.A. Anderson, J. Swarbrick, D.E. Moore, Permeability of human epidermis to phenolic compounds, J. Pharm. Pharmacol. 29 (1977) 677–683.
[47] M.S. Roberts, R.A. Anderson, J. Swarbrick, D.E. Moore, The percutaneous absorption of phenolic compounds: the mechanism of diffusion across the stratum corneum, J. Pharm. Pharmacol. 30 (1978) 486–490.
[48] R.J. Scheuplein, Mechanism of percutaneous adsorption: I. Routes of penetration and the influence of solubility, J. Invest. Dermatol. 45 (1965) 334–346.
[49] A. Michaels, S. Chandrasekaran, J. Shaw, Drug permeation through human skin: theory and in vitro experimental measurement, AIChE J. 21 (1975) 985–996.
[50] M. Katz, B.J. Poulsen, Absorption of drugs through the skin, in: B.B. Brodie, J.R. Gillette, H.S. Ackerman (Eds.), Concepts in Biochemical Pharmacology, Springer, Berlin, Heidelberg, 1971, pp. 103–174.
[51] R. Scheuplein, A personal view of skin permeation (1960-2013), Skin Pharmacol. Physiol. 26 (2013) 199–212, https://www.karger.com/Article/FullText/351954.
[52] G.B. Kasting, R.L. Smith, E.B. Cooper, Effect of lipid solubility and molecular size on percutaneous absorption, in: B. Shroot, H. Schaefer (Eds.), Skin Pharmacokinetics, Karger, Basel, 1987, pp. 138–153.
[53] G.B. Kasting, Lipid solubility and molecular weight: whose idea was that, Skin Pharmacol Physiol 26 (2013) 295–301.
[54] G.L. Flynn, Physicochemical determinants of skin absorption, in: T.R. Gerrity, C.J. Henry (Eds.), Principles of Route-to-Route Extrapolation for Risk Assessment, Elsevier Science, New York, 1990, pp. 93–127.
[55] R.O. Potts, R.H. Guy, Predicting skin permeability, Pharm Res 9 (1992) 663–669.

[56] B.M. Magnusson, Y.G. Anissimov, S.E. Cross, M.S. Roberts, Molecular size as the main determinant of solute maximum flux across the skin, J. Invest. Dermatol. 122 (2004) 993–999.
[57] I. Brody, The ultrastructure of the horny layer in normal and psoriatic epidermis as revealed by electron microscopy, J. Invest. Dermatol. 39 (1962) 519–528.
[58] I. Brody, A light and electron microscopy study of normal human stratum corneum with particular reference to the intercellular space, Upsala J. Med. Sci. 94 (1989) 29–45.
[59] M. Ito, F. Sakamoto, K. Hashimoto, Comparative studies of scanning electron microscopy and transmission electron microscopy, Bioengineering of the Skin, CRC Press, 2006, pp. 57–76, https://www.taylorfrancis.com/chapters/edit/10.3109/9781420005516-7/comparative-studies-scanning-electron-microscopy-transmission-electron-microscopy-masaaki-ito-fumiko-sakamoto-ken-hashimoto.
[60] H. Baker, A.M. Kligman, Technique for estimating turnover time of human stratum corneum, Arch. Dermatol. 95 (1967) 408–411.
[61] R. Voegeli, A.V. Rawlings, Desquamation: it is almost all about proteases, in: M. Lodén, H.I. Maibach (Eds.), Treatment of dry skin syndrome, Springer, Berlin, Heidelberg, 2012, pp. 149–178.
[62] R. Wepf, T. Richter, S.S. Biel, H. Schlu, Multimodal imaging of skin structures: imagining imaging of the skin, in: K.-.-P. Wilhelm, P. Elsner, E. Berardesca, H. I. Maibach (Eds.), Bioengineering of the Skin, CRC Press, Boca Raton, 2006, pp. 77–96.
[63] M.S. Roberts, M. Walker, Water. The most natural penetration enhancer, in: K. Walters, J. Hadgraft (Eds.) Pharmaceutical Skin Penetration Enhancement, Marcel Dekker New York 1993, pp. 1-30.
[64] M.S. Roberts, J. Bouwstra, F. Pirot, F. Falson, Skin hydration-a key determinant in topical absorption, in: K. Walters, M.S. Roberts (Eds.), Dermatologic, cosmeceutic, and cosmetic development: therapeutic and novel approaches, Informa, New York, 2008, pp. 118–128.
[65] T. Richter, C. Peuckert, M. Sattler, K. Koenig, I. Riemann, U. Hintze, K.-P. Wittern, R. Wiesendanger, R. Wepf, Dead but highly dynamic–the stratum corneum is divided into three hydration zones, Skin Pharmacol. Physiol. 17 (2004) 246–257.
[66] R.R. Warner, M.C. Myers, D.A. Taylor, Electron probe analysis of human skin: determination of the water concentration profile, J. Invest. Dermatol. 90 (1988) 218–224.
[67] J. Bouwstra, N. Nahmoed, H. Groenink, M. Ponec, Human skin equivalents are an excellent tool to study the effect of moisturizers on the water distribution in the stratum corneum, Int. J. Cosmet. Sci. 34 (2012) 560–566.
[68] M.F. Galliano, A. Tfayli, R.H. Dauskardt, B. Payre, C. Carrasco, S. Bessou-Touya, A. Baillet-Guffroy, H. Duplan, Comprehensive characterization of the structure and properties of human stratum corneum relating to barrier function and skin hydration: modulation by a moisturizer formulation, Exp. Dermatol. 30 (2021) 1352–1357.
[69] C.R. Harding, S. Long, J. Richardson, J. Rogers, Z. Zhang, A. Bush, A.V. Rawlings, The cornified cell envelope: an important marker of stratum corneum maturation in healthy and dry skin, Int. J. Cosmet. Sci. 25 (2003) 157–167.
[70] S. Chapman, A. Walsh, Desmosomes, corneosomes and desquamation. An ultrastructural study of adult pig epidermis, Arch. Dermatol. Res. 282 (1990) 304–310.
[71] M.B. Reddy, R.H. Guy, A.L. Bunge, Does epidermal turnover reduce percutaneous penetration?, Pharm Res. 17 (2000) 1414–1419.
[72] G.K. Menon, S.H. Lee, M.S. Roberts, Ultrastructural effects of some solvents and vehicles on the stratum corneum and other skin components: evidence for an extended mosaic-partitioning model of the skin barrier, Drugs Pharmaceut. Sci. 91 (1998) 727–751.
[73] H.S. Cheruvu, X. Liu, J.E. Grice, M.S. Roberts, Modeling percutaneous absorption for successful drug discovery and development, Expert. Opin. Drug. Discov. 15 (2020) 1181–1198.
[74] Y.G. Anissimov, M.S. Roberts, Mathematical models for topical and transdermal drug products, in: V. Shah, H.I. Maibach, J. Jenner (Eds.), Topical Drug Bioavailability, Bioequivalence, and Penetration, Springer, New York, 2014, pp. 249–298.
[75] S.K. Katiyar, H. Mukhtar, M.S. Matsui, Ultraviolet-B exposure of human skin induces cytochromes P450 1A1 and 1B1, J. Invest. Dermatol. 114 (2000) 328–333.
[76] W.J. Pugh, M.S. Roberts, J. Hadgraft, Epidermal permeability—Penetrant structure relationships: 3. The effect of hydrogen bonding interactions and molecular size on diffusion across the stratum corneum, Int. J. Pharm. 138 (1996) 149–165.
[77] S.H. Yalkowsky, S.C. Valvani, Solubility and Partitioning .1. Solubility of Non-Electrolytes in Water, J. Pharmaceut. Sci. 69 (1980) 912–922, https://doi.org/10.1002/jps.2600690814.
[78] T. Bouwman, M. Cronin, J. Bessems, J. Van de Sandt, Improving the applicability of (Q) SARs for percutaneous penetration in regulatory risk assessment, Hum. Exp. Toxicol. 27 (2008) 269–276.
[79] T.E. McKone, R.A. Howd, Estimating dermal uptake of nonionic organic chemicals from water and soil: I. Unified fugacity-based models for risk assessments, Risk Anal. 12 (1992) 543–557.
[80] G.P. Moss, M.T. Cronin, Quantitative structure–permeability relationships for percutaneous absorption: re-analysis of steroid data, Int. J. Pharm. 238 (2002) 105–109.
[81] W. ten Berge, A simple dermal absorption model: derivation and application, Chemosphere 75 (2009) 1440–1445.
[82] M. Milewski, A.L. Stinchcomb, Estimation of maximum transdermal flux of nonionized xenobiotics from basic physicochemical determinants, Mol Pharm 9 (2012) 2111–2120.
[83] R.L. Cleek, A.L. Bunge, A new method for estimating dermal absorption from chemical exposure. 1. General approach, Pharm. Res. 10 (1993) 497–506.
[84] A.L. Bunge, R.L. Cleek, A new method for estimating dermal absorption from chemical exposure: 2. Effect of molecular weight and octanol-water partitioning, Pharmaceut. Res. 12 (1995) 88–95.
[85] X. Liu, Y.G. Anissimov, J.E. Grice, H.S. Cheruvu, P. Ghosh, S.G. Raney, H.I. Maibach, M.S. Roberts, Relating transdermal delivery plasma pharmacokinetics with in vitro permeation test (IVPT) findings using diffusion and compartment-in-series models, J. Control. Release 334 (2021) 37–51.
[86] X. Liu, S. Yousef, Y.G. Anissimov, J. van der Hoek, E. Tsakalozou, Z. Ni, J.E. Grice, M.S. Roberts, Diffusion modelling of percutaneous absorption kinetics. Predicting urinary excretion from in vitro skin permeation tests (IVPT) for an infinite dose, Eur. J. Pharm. Biopharm. 149 (2020) 30–44.
[87] M.S. Roberts, W.J. Pugh, J. Hadgraft, Epidermal permeability: penetrant structure relationships. 2. The effect of H-bonding groups in penetrants on their diffusion through the stratum corneum, Int. J. Pharm. 132 (1996) 23–32.
[88] J.M. Nitsche, T.F. Wang, G.B. Kasting, A two-phase analysis of solute partitioning into the stratum corneum, J. Pharm. Sci. 95 (2006) 649–666.
[89] P.V. Raykar, M.-C. Fung, B.D. Anderson, The role of protein and lipid domains in the uptake of solutes by human stratum corneum, Pharm. Res. 5 (1988) 140–150.
[90] B.D. Anderson, W.I. Higuchi, P.V. Raykar, Heterogeneity effects on permeability-partition coefficient relationships in human stratum corneum, Pharm Res 5 (1988) 566–573.
[91] L. Wang, L. Chen, G. Lian, L. Han, Determination of partition and binding properties of solutes to stratum corneum, Int. J. Pharm. 398 (2010) 114–122.
[92] M.H. Abraham, H.S. Chadha, R.C. Mitchell, The factors that influence skin penetration of solutes, J. Pharm. Pharmacol. 47 (1995) 8–16.
[93] M.H. Abraham, F. Martins, Human skin permeation and partition: General linear free-energy relationship analyses, J. Pharm. Sci. 93 (2004) 1508–1523.
[94] M.H. Abraham, F. Martins, R.C. Mitchell, Algorithms for skin permeability using hydrogen bond descriptors: the problem of steroids, J. Pharm. Pharmacol. 49 (1997) 858–865.
[95] W.J. Pugh, J. Hadgraft, Ab initio prediction of human skin permeability coefficients, Int. J. Pharm. 103 (1994) 163–178.
[96] M.S. Roberts, W.J. Pugh, J. Hadgraft, A.C. Watkinson, Epidermal permeability penetrant structure relationships.1. An analysis of methods of predicting penetration of monofunctional solutes from aqueous solutions, Int. J. Pharm. 126 (1995) 219–233.
[97] N. Jain, S.H. Yalkowsky, Estimation of the aqueous solubility I: application to organic nonelectrolytes, J. Pharm. Sci. 90 (2001) 234–252.
[98] S. Abbott, C.M. Hansen, H. Yamamoto, R.S. Valpey, Hansen Solubility Parameters in Practice. Skin deep (HSP and Skin Absorption), in: S. Abbott, C.M. Hansen, H. Yamamoto, R.S. Valpey. (Ed.), Hansen Solubility Parameters in Practice, Hansen-Solubility.com, 2013, Chapter 15. https://pirika.com/ENG/HSP/E-Book/Chap15.html.
[99] C. Ursin, C.M. Hansen, J.W. Van Dyk, P.O. Jensen, I.J. Christensen, J. Ebbehoej, Permeability of commercial solvents through living human skin, Am. Ind. Hyg. Assoc. J. 56 (1995) 651–660.
[100] S. Majumdar, J. Thomas, S. Wasdo, K.B. Sloan, The effect of water solubility of solutes on their flux through human skin in vitro, Int. J. Pharm. 329 (2007) 25–36.
[101] J. Juntunen, S. Majumdar, K.B. Sloan, The effect of water solubility of solutes on their flux through human skin in vitro: A prodrug database integrated into the extended Flynn database, Int. J. Pharm. 351 (2008) 92–103.
[102] Y.-B. Liou, H.-O. Ho, C.-J. Yang, Y.-K. Lin, M.-T. Sheu, Construction of a quantitative structure-permeability relationship (QSPR) for the transdermal delivery of NSAIDs, J. Control. Release 138 (2009) 260–267.
[103] P. Gramatica, E. Giani, E. Papa, Statistical external validation and consensus modeling: a QSPR case study for Koc prediction, J. Mol. Graph. Model. 25 (2007) 755–766.
[104] G.S. Collins, J.A. de Groot, S. Dutton, O. Omar, M. Shanyinde, A. Tajar, M. Voysey, R. Wharton, L.-M. Yu, K.G. Moons, External validation of multivariable prediction models: a systematic review of methodological conduct and reporting, BMC Med. Res. Method. 14 (2014) 1–11.
[105] M. Oja, U. Maran, pH-permeability profiles for drug substances: Experimental detection, comparison with human intestinal absorption and modelling, Eur. J. Pharm. Sci. 123 (2018) 429–440.
[106] S. Wold, L. Eriksson, S. Clementi, Statistical validation of QSAR results, in: H. Van De Waterbeemd (Ed.), Chemometric methods in molecular design, VCH, Weinheim, 1995, pp. 309–338.
[107] H.S. Cheruvu, X. Liu, J.E. Grice, M.S. Roberts, An updated dataset of human maximum skin fluxes, and epidermal permeability coefficients for drugs, xenobiotics and other solutes applied as aqueous solutions, Data in Brief (submitted), 2021.
[108] K.G. Moons, A.P. Kengne, D.E. Grobbee, P. Royston, Y. Vergouwe, D.G. Altman, M. Woodward, Risk prediction models: II. External validation, model updating, and impact assessment, Heart 98 (2012) 691–698.
[109] M. Barratt, Quantitative structure-activity relationships for skin permeability, Toxicol. In Vitro 9 (1995) 27–37.
[110] M.B. Brown, C.H. Lau, S.T. Lim, Y. Sun, N. Davey, G.P. Moss, S.H. Yoo, C. De Muynck, An evaluation of the potential of linear and nonlinear skin

permeation models for the prediction of experimentally measured percutaneous drug absorption, J. Pharm. Pharmacol. 64 (2012) 566–577.
[111] S. Mitragotri, A theoretical analysis of permeation of small hydrophobic solutes across the stratum corneum based on scaled particle theory, J. Pharm. Sci. 91 (2002) 744–752.
[112] G. Lian, L. Chen, L. Han, An evaluation of mathematical models for predicting skin permeability, J. Pharm. Sci. 97 (2008) 584–598.
[113] A. Wilschut, F. Wil, P.J. Robinson, T.E. McKone, Estimating skin permeation. The validation of five mathematical skin permeation models, Chemosphere 30 (1995) 1275–1296.
[114] B. Pecoraro, M. Tutone, E. Hoffman, V. Hutter, A.M. Almerico, M. Traynor, Predicting skin permeability by means of computational approaches: Reliability and caveats in pharmaceutical studies, J. Chem. Inf. Model. 59 (2019) 1759–1771.
[115] J. Thomas, S. Majumdar, S. Wasdo, A. Majumdar, K.B. Sloan, The effect of water solubility of solutes on their flux through human skin in vitro: an extended Flynn database fitted to the Roberts-Sloan equation, Int. J. Pharm. 339 (2007) 157–167.
[116] E.J. Lien, G.L. Tong, Physicochemical properties and percutaneous absorption of drugs, J. Soc. Cosmet. Chem. 24 (1973) 371–384.
[117] Q. Zhang, J.E. Grice, P. Li, O.G. Jepps, G.-J. Wang, M.S. Roberts, Skin solubility determines maximum transepidermal flux for similar size molecules, Pharm. Res. 26 (2009) 1974–1985.
[118] R. Scheuplein, I. Blank, G. Brauner, D.J. Macfarlane, Percutaneous absorption of steroids, J, Invest. Dermatol. 52 (1969) 63–70.
[119] M.E. Johnson, D. Blankschtein, R. Langer, Permeation of steroids through human skin, J. Pharm. Sci. 84 (1995) 1144–1146.
[120] P. Buchwald, N. Bodor, A simple, predictive, structure-based skin permeability model, J. Pharm. Pharmacol. 53 (2001) 1087–1098.
[121] Y. Sun, M.B. Brown, M. Prapopoulou, N. Davey, R. Adams, G.P. Moss, The application of stochastic machine learning methods in the prediction of skin penetration, Appl. Soft Comput. 11 (2011) 2367–2375.
[122] D.G. Petlin, M. Rybachuk, Y.G. Anissimov, Pathway distribution model for solute transport in stratum corneum, J. Pharm. Sci. 104 (2015) 4443–4447.
[123] M.T. Cronin, T.W. Schultz, Pitfalls in QSAR, J. Mol. Struct. (Thoechem) 622 (2003) 39–51.
[124] A. Naegel, M. Heisig, G. Wittum, Computational modeling of the skin barrier, in, Permeability Barrier (2011) 1–32.
[125] P. Singh, M.s. Roberts, Local deep tissue penetration of compounds after dermal application: structure-tissue penetration relationships, J. Pharmacol. Exp. Ther. 279 (1996) 908–917.
[126] P. Singh, M.S. Roberts, Dermal and underlying tissue pharmacokinetics of salicylic acid after topical application, J. Pharmacokinet. Biopharm. 21 (1993) 337–373.
[127] S.K. Puttrevu, S. Arora, S. Polak, N.K. Patel, Physiologically based pharmacokinetic modeling of transdermal selegiline and its metabolites for the evaluation of disposition differences between healthy and special populations, Pharmaceutics 12 (2020) 942.
[128] E. Tsakalozou, A. Babiskin, L. Zhao, Physiologically-based pharmacokinetic modeling to support bioequivalence and approval of generic products: a case for diclofenac sodium topical gel, 1%, CPT: Pharmacometrics Syst. Pharmacol. 10 (2021) 399–411.
[129] A.S. Krishnatry, V. Damian, Understanding dermal drug disposition using TCAT™ – a novel PBPK model (webinar link-https://www.simulations-plus.com/resource/understanding-dermal-drug-disposition-using-tcat-novel-pbpk-model/). Accessed 28 July, 2021), (2017).
[130] A.M. Barbero, H.F. Frasch, Effect of stratum corneum heterogeneity, anisotropy, asymmetry and follicular pathway on transdermal penetration, J. Control. Release 260 (2017) 234–246.
[131] L. Chen, G. Lian, L. Han, Modeling transdermal permeation. Part I. Predicting skin permeability of both hydrophobic and hydrophilic solutes, AIChE J. 56 (2010) 1136–1146.
[132] T.F. Wang, G.B. Kasting, J.M. Nitsche, A multiphase microscopic diffusion model for stratum corneum permeability. I. Formulation, solution, and illustrative results for representative compounds, J. Pharm. Sci. 95 (2006) 620–648.
[133] J.M. Nitsche, G.B. Kasting, A microscopic multiphase diffusion model of viable epidermis permeability, Biophys. J . 104 (2013) 2307–2320.
[134] L.C. Nitsche, G.B. Kasting, J.M. Nitsche, Microscopic models of drug/chemical diffusion through the skin barrier: effects of diffusional anisotropy of the intercellular lipid, J. Pharm. Sci. 108 (2019) 1692–1712.
[135] J.J. Calcutt, Y.G. Anissimov, Physiologically based mathematical modelling of solute transport within the epidermis and dermis, Int. J. Pharm. 569 (2019) 118547.
[136] J. Wen, S.M. Koo, N. Lape, How sensitive are transdermal transport predictions by microscopic stratum corneum models to geometric and transport parameter input?, J Pharm. Sci. 107 (2018) 612–623.
[137] T. Yotsuyanagi, W. Higuchi, A two phase series model for the transport of steroids across the fully hydrated stratum corneum, J. Pharm. Pharmacol. 24 (1972) 934–941.
[138] W.J. Albery, J. Hadgraft, Percutaneous absorption: in vivo experiments, J. Pharm. Pharmacol. 31 (1979) 140–147.
[139] M.K. Nemanic, P.M. Elias, In situ precipitation: a novel cytochemical technique for visualization of permeability pathways in mammalian stratum corneum, J. Histochem. Cytochem. 28 (1980) 573–578.
[140] K. Kakemi, H. Kameda, M. Kakemi, M. Ueda, T. Koizumi, Model studies on percutaneous absorption and transport in the ointment. I. Theoretical aspects, Chem. Pharm. Bull. 23 (1975) 2109–2113.
[141] J. Hadgraft, Theoretical aspects of metabolism in the epidermis, Int. J. Pharm. 4 (1980) 229–239.
[142] R.H. Guy, J. Hadgraft, Percutaneous metabolism with saturable enzyme kinetics, Int. J. Pharm. 11 (1982) 187–197.
[143] K. Kubota, T. Ishizaki, A theoretical consideration of percutaneous drug absorption, J. Pharmacokinet. Biopharm. 13 (1985) 55–72.
[144] R.H. Guy, J. Hadgraft, H.I. Maibach, A pharmacokinetic model for percutaneous absorption, Int. J. Pharm. 11 (1982) 119–129.
[145] K.D. Mccarley, A.L. Bunge, Physiologically relevant one-compartment pharmacokinetic models for skin. 1. Development of models, J. Pharm. Sci. 87 (1998) 470–481.
[146] K.D. McCarley, A.L. Bunge, Physiologically relevant two-compartment pharmacokinetic models for skin, J. Pharm. Sci. 89 (2000) 1212–1235.
[147] K.D. Mccarley, A.L. Bunge, Pharmacokinetic models of dermal absorption, J. Pharm. Sci. 90 (2001) 1699–1719.
[148] A.A. Amarah, D.G. Petlin, J.E. Grice, J. Hadgraft, M.S. Roberts, Y.G. Anissimov, Compartmental modeling of skin transport, Eur. J. Pharm. Biopharm. 130 (2018) 336–344.
[149] Y.G. Anissimov, M.S. Roberts, A compartmental model of hepatic disposition kinetics: 1. Model development and application to linear kinetics, J. Pharmacokinet Pharmacodyn. 29 (2002) 131–156.
[150] M.E. Johnson, D. Blankschtein, R. Langer, Evaluation of solute permeation through the stratum corneum: lateral bilayer diffusion as the primary transport mechanism, J. Pharm. Sci. 86 (1997) 1162–1172.
[151] P.S. Talreja, G.B. Kasting, N.K. Kleene, W.L. Pickens, T.-F. Wang, Visualization of the lipid barrier and measurement of lipid pathlength in human stratum corneum, Aaps Pharmsci 3 (2001) 48–56.
[152] J. Crank, The mathematics of diffusion, Second ed., Oxford university press, 1979.
[153] G. Kasting, J. Nitsche, Mathematical models of skin permeability: microscopic transport models and their predictions, Computat. Biophys. Skin (2014) 187–215.
[154] A. Rougier, C. Lotte, P. Corcuff, H.I. Maibach, Relationship between skin permeability and corneocyte size according to anatomic site, age, and sex in man, J. Soc. Cosmet. Chem 39 (1988) 15–26.
[155] I. Iwai, H. Han, L. Den Hollander, S. Svensson, L.-G. Öfverstedt, J. Anwar, J. Brewer, M. Bloksgaard, A. Laloeuf, D. Nosek, The human skin barrier is organized as stacked bilayers of fully extended ceramides with cholesterol molecules associated with the ceramide sphingoid moiety, J. Invest. Dermatol. 132 (2012) 2215–2225.
[156] A. Narangifard, C.L. Wennberg, L. den Hollander, I. Iwai, H. Han, M. Lundborg, S. Masich, E. Lindahl, B. Daneholt, L. Norlén, Molecular Reorganization during the Formation of the Human Skin Barrier Studied In Situ, J. Invest. Dermatol. 141 (2021) 1243–1253, https://doi.org/10.1016/j.jid.2020.07.040.
[157] M. Haftek, 'Memory'of the stratum corneum: exploration of the epidermis' past, Br. J. Dermatol. 171 (2014) 6–9.
[158] A. Ishida-Yamamoto, S. Igawa, M. Kishibe, Molecular basis of the skin barrier structures revealed by electron microscopy, Exp. Dermatol. 27 (2018) 841–846.
[159] M. Fartasch, I. Bassukas, T. Diepgkn, Structural relationship between epidermal lipid lamellae, lamellar bodies and desmosomes in human epidermis: an ultrastructural study, Br. J. Dermatol. 128 (1993) 1–9.
[160] D. Bernard, A.M. Minondo, C. Camus, F. Fiat, P. Corcuff, R. Schmidt, M. Simon, G. Serre, Persistence of both peripheral and non-peripheral corneodesmosomes in the upper stratum corneum of winter xerosis skin versus only peripheral in normal skin, J Invest Dermatol. 116 (1) (2001) 23–30, https://doi.org/10.1046/j.1523-1747.2001.00208.x.
[161] A. Mundstock, R. Abdayem, F. Pirot, M. Haftek, Alteration of the structure of human stratum corneum facilitates transdermal delivery, Open Dermatol. J. 8 (2014).
[162] J.A. Bouwstra, Richard W.J. Helder, A. El Ghalbzouri, Human skin equivalents: Impaired barrier function in relation to the lipid and protein properties of the stratum corneum, Adv. Drug Deliv. Rev. 175 (2021) 113802.
[163] J. Hadgraft, M.E. Lane, Transepidermal water loss and skin site: a hypothesis, Int. J. Pharm. 373 (2009) 1–3.
[164] M. Machado, T.M. Salgado, J. Hadgraft, M.E. Lane, The relationship between transepidermal water loss and skin permeability, Int. J. Pharm. 384 (2010) 73–77.
[165] S. Hansen, A. Naegel, M. Heisig, G. Wittum, D. Neumann, K.-H. Kostka, P. Meiers, C.-M. Lehr, U.F. Schaefer, The role of corneocytes in skin transport revised—a combined computational and experimental approach, Pharm. Res. 26 (2009) 1379–1397.
[166] S. Hansen, A. Henning, A. Naegel, M. Heisig, G. Wittum, D. Neumann, K.-H. Kostka, J. Zbytovska, C.-M. Lehr, U.F. Schaefer, In-silico model of skin penetration based on experimentally determined input parameters Part I: experimental determination of partition and diffusion coefficients, Eur. J. Pharmaceut. Biopharm. 68 (2008) 352–367.
[167] A. Naegel, M. Heisig, D. Feuchter, M. Scherer, G. Wittum, Cellular Scale Modelling of the Skin Barrier, in: B. Querleux (Ed.), Computational Biophysics of the Skin, CRC Press, Boca Raton, FL, 2014, pp. 217–236.
[168] Apothem, https://en.wikipedia.org/wiki/Apothem in, Wikipedia, the free encyclopedia. Accessed 28 June 2021.

[169] T.F. Wang, G.B. Kasting, J.M. Nitsche, A multiphase microscopic diffusion model for stratum corneum permeability. II. Estimation of physicochemical parameters, and application to a large permeability database, J. Pharm. Sci. 96 (2007) 3024–3051.
[170] M.E. Johnson, D.A. Berk, D. Blankschtein, D.E. Golan, R.K. Jain, R.S. Langer, Lateral diffusion of small compounds in human stratum corneum and model lipid bilayer systems, Biophys. J . 71 (1996) 2656–2668.
[171] L. Coleman, G. Lian, S. Glavin, I. Sorrell, T. Chen, In silico simulation of simultaneous percutaneous absorption and xenobiotic metabolism: model development and a case study on aromatic amines, Pharm. Res. 37 (2020) 1–10.
[172] P. Kattou, G. Lian, S. Glavin, I. Sorrell, T. Chen, Development of a two-dimensional model for predicting transdermal permeation with the follicular pathway: demonstration with a caffeine study, Pharm. Res. 34 (2017) 2036–2048.
[173] R.J. Scheuplein, Mechanism of percutaneous absorption: II. Transient diffusion and the relative importance of various routes of skin penetration, J. Invest. Dermatol. 48 (1967) 79–88.
[174] X. Liu, J.E. Grice, J. Lademann, N. Otberg, S. Trauer, A. Patzelt, M.S. Roberts, Hair follicles contribute significantly to penetration through human skin only at times soon after application as a solvent deposited solid in man, Br. J. Clin. Pharmacol. 72 (2011) 768–774.
[175] K.D. Peck, A.-H. Ghanem, W.I. Higuchi, Hindered diffusion of polar molecules through and effective pore radii estimates of intact and ethanol treated human epidermal membrane, Pharm. Res. 11 (1994) 1306–1314.
[176] M.S. Roberts, P.M. Lai, Y.G. Anissimov, Epidermal iontophoresis: I. Development of the ionic mobility-pore model, Pharmaceut. Res. 15 (1998) 1569–1578.
[177] H. Tang, S. Mitragotri, D. Blankschtein, R. Langer, Theoretical description of transdermal transport of hydrophilic permeants: Application to low-frequency sonophoresis, J. Pharm. Sci. 90 (2001) 545–568.
[178] G.B. Kasting, M.A. Miller, T.D. LaCount, J. Jaworska, A composite model for the transport of hydrophilic and lipophilic compounds across the skin: steady-state behavior, J. Pharm. Sci. 108 (2019) 337–349.
[179] S. Seif, S. Hansen, Measuring the stratum corneum reservoir: desorption kinetics from keratin, J. Pharm. Sci. 101 (2012) 3718–3728.
[180] H. Boddé, M. Kruithof, J. Brussee, H. Koerten, Visualisation of normal and enhanced HgCl2 transport through human skin in vitro, Int. J. Pharm. 53 (1989) 13–24.
[181] J.A. Neelissen, C. Arth, M. Wolff, A.H. Schrijvers, H.E. Junginger, H.E. Bodde, Visualization of percutaneous 3H-estradiol and 3H-norethindrone acetate transport across human epidermis as a function of time, Acta Dermato Venereologica-Supplement (2000) 36–43.
[182] B. Mueller, Y.G. Anissimov, M.S. Roberts, Unexpected clobetasol propionate profile in human stratum corneum after topical application in vitro, Pharm. Res. 20 (2003) 1835–1837.
[183] O. Simonetti, J. Kempenaar, M. Ponec, A. Hoogstraate, W. Bialik, A. Schrijvers, H. Boddé, Visualization of diffusion pathways across the stratum corneum of native and in-vitro-reconstructed epidermis by confocal laser scanning microscopy, Arch. Dermatol. Res. 287 (1995) 465–473.
[184] I. Iachina, I. Antonescu, J. Dreier, J. Sørensen, J. Brewer, The nanoscopic molecular pathway through human skin, Biochimica et Biophysica Acta (BBA)-General Subjects 1863 (2019) 1226–1233.
[185] Y.G. Anissimov, M.S. Roberts, Diffusion modeling of percutaneous absorption kinetics: 3. Variable diffusion and partition coefficients, consequences for stratum corneum depth profiles and desorption kinetics, J. Pharm. Sci. 93 (2004) 470–487.
[186] G. Box, Science and Statistics, J. Am. Stat. Assoc. 71 (1976).
[187] G.E. Box, A. Luceño, M. del Carmen Paniagua-Quinones, Statistical control by monitoring and adjustment, John Wiley & Sons, 2009, https://onlinelibrary.wiley.com/doi/book/10.1002/9781118164532.
[188] A. Einstein, On the method of theoretical physics, Philos. Sci. 1 (1934) 163–169.
[189] M. Lundborg, C.L. Wennberg, A. Narangifard, E. Lindahl, L. Norlén, Predicting drug permeability through skin using molecular dynamics simulation, J. Control. Release 283 (2018) 269–279.
[190] N.I. Papadimitriou, M.E. Kainourgiakis, S.N. Karozis, G.C. Charalambopoulou, Studying the structure of single-component ceramide bilayers with molecular dynamics simulations using different force fields, Mol. Simul. 41 (2015) 1122–1136.
[191] S.A. Pandit, H.L. Scott, Molecular-dynamics simulation of a ceramide bilayer, J. Chem. Phys. 124 (2006).
[192] C. Das, M.G. Noro, P.D. Olmsted, Simulation studies of stratum corneum lipid mixtures, Biophys. J . 97 (2009) 1941–1951.
[193] Y. Imai, X.L. Liu, J. Yamagishi, K. Mori, S. Neya, T. Hoshino, Computational analysis of water residence on ceramide and sphingomyelin bilayer membranes, J. Mol. Graph. Model. 29 (2010) 461–469.
[194] M. Lundborg, A. Narangifard, C.L. Wennberg, E. Lindahl, B. Daneholt, L. Norlén, Human skin barrier structure and function analyzed by cryo-EM and molecular dynamics simulation, J. Struct. Biol. 203 (2018) 149–161.
[195] E. Antunes, A. Cavaco-Paulo, Stratum corneum lipid matrix with unusual packing: a molecular dynamics study, Colloids Surf. B-Biointerfaces 190 (2020).
[196] R. Gupta, D. Sridhar, B. Rai, Molecular dynamics simulation study of permeation of molecules through skin lipid bilayer, J. Phys. Chem. B 120 (2016) 8987–8996.
[197] R. Notman, W.K. den Otter, M.G. Noro, W.J. Briels, J. Anwar, The permeability enhancing mechanism of DMSO in ceramide Bilayers simulated by molecular dynamics, Biophys. J . 93 (2007) 2056–2068.
[198] M.W. de Jager, G.S. Gooris, I.P. Dolbnya, W. Bras, M. Ponec, J.A. Bouwstra, The phase behaviour of skin lipid mixtures based on synthetic ceramides, Chem Phys Lipids 124 (2003) 123–134.
[199] R. Notman, J. Anwar, W.J. Briels, M.G. Noro, W.K. den Otter, Simulations of skin barrier function: free energies of hydrophobic and hydrophilic transmembrane pores in ceramide bilayers, Biophys. J . 95 (2008) 4763–4771.
[200] R. Gupta, B. Rai, Electroporation of skin stratum corneum lipid bilayer and molecular mechanism of drug transport: a molecular dynamics study, Langmuir 34 (2018) 5860–5870.
[201] M.I. Hoopes, M.G. Noro, M.L. Longo, R. Faller, Bilayer structure and lipid dynamics in a model stratum corneum with oleic acid, J. Phys. Chem. B 115 (2011) 3164–3171.
[202] G. Wan, X.X. Dai, Q.Q. Yin, X.Y. Shi, Y.J. Qiao, Interaction of menthol with mixed-lipid bilayer of stratum corneum: a coarse-grained simulation study, J. Mol. Graph. Model. 60 (2015) 98–107.
[203] C.J. Huang, H.J. Wang, L.D. Tang, F.C. Meng, Penetration enhancement of menthol on quercetin through skin: insights from atomistic simulation, J. Mol. Model. 25 (2019).
[204] R. Gupta, Y. Badhe, B. Rai, S. Mitragotri, Molecular mechanism of the skin permeation enhancing effect of ethanol: a molecular dynamics study, RSC Adv. 10 (2020) 12234–12248.
[205] R. Gupta, B.S. Dwadasi, B. Rai, S. Mitragotri, Effect of Chemical permeation enhancers on skin permeability: in silico screening using molecular dynamics simulations, Sci. Rep. 9 (2019).
[206] R.J. Scheuplein, L.J. Morgan, "Bound water" in keratin membranes measured by a microbalance technique, Nature 214 (1967) 456–458.
[207] S. Yousef, X. Liu, A. Mostafa, Y. Mohammed, J.E. Grice, Y.G. Anissimov, W. Sakran, M.S. Roberts, Estimating maximal in vitro skin permeation flux from studies using non-sink receptor phase conditions, Pharm. Res. 33 (2016) 2180–2194.
[208] R. Gupta, B. Rai, Penetration of gold nanoparticles through human skin: unraveling its mechanisms at the molecular scale, J. Phys. Chem. B 120 (2016) 7133–7142.
[209] R. Gupta, N. Kashyap, B. Rai, Transdermal cellular membrane penetration of proteins with gold nanoparticles: a molecular dynamics study, PCCP 19 (2017) 7537–7545.
[210] R. Gupta, B. Rai, In-silico design of nanoparticles for transdermal drug delivery application, Nanoscale 10 (2018) 4940–4951.
[211] R. Gupta, N. Kashyap, B. Rai, Molecular mechanism of transdermal co-delivery of interferon-alpha protein with gold nanoparticle – a molecular dynamics study, Mol. Simul. 44 (2018) 274–284.
[212] K.M. Gupta, S. Das, P.S. Chow, Molecular dynamics simulations to elucidate translocation and permeation of active from lipid nanoparticle to skin: complemented with experiments, Nanoscale 13 (2021) 12916–12928.
[213] J.E. Rim, P.M. Pinsky, W.W. van Osdol, Multiscale modeling framework of transdermal drug delivery, Ann. Biomed. Eng. 37 (2009) 1217–1229.
[214] K. Gajula, R. Gupta, D.B. Sridhar, B. Rai, In-silico skin model: a multiscale simulation study of drug transport, J. Chem. Inf. Model. 57 (2017) 2027–2034.
[215] M.E. Bozdaganyan, P.S. Orekhov, Synergistic effect of chemical penetration enhancers on lidocaine permeability revealed by coarse-grained molecular dynamics simulations, Membranes 11 (2021) 410.
[216] E. Wang, J.B. Klauda, Structure and permeability of ceramide bilayers and multilayers, J. Phys. Chem. B 123 (2019) 2525–2535.
[217] ReportLinker, Global Topical Drug Delivery Market to Reach $129.9 Billion by 2027, https://www.reportlinker.com/p06033143/?utm_source=GNW, in: Global Topical Drug Delivery Industry, GLOBE NEWSWIRE, New York, 2021, Accessed 25 June 2021.
[218] D. Lalonde, N. Joukhadar, J. Janis, Simple effective ways to care for skin wounds and incisions, Plast. Reconstruct. Surg. Global Open 7 (2019).
[219] E. Proksch, E. Berardesca, L. Misery, J. Engblom, J. Bouwstra, Dry skin management: practical approach in light of latest research on skin structure and function, J. Dermatol. Treat. 31 (2020) 716–722.
[220] M.D. Bhatt, B.D. Bhatt, J.T. Dorrian, B.N. McLellan, Increased topical generic prices by manufacturers, J. Am. Acad. Dermatol. 80 (2019) 1353–1357.
[221] M. Miranda, J.J. Sousa, F. Veiga, C. Cardoso, C. Vitorino, Bioequivalence of topical generic products. Part 2. Paving the way to a tailored regulatory system, Eur. J. Pharm. Sci. 122 (2018) 264–272.
[222] C.M. Schoellhammer, D. Blankschtein, R. Langer, Skin permeabilization for transdermal drug delivery: recent advances and future prospects, Expert Opin. Drug Del. 11 (2014) 393–407.
[223] M.S. Roberts, Y. Mohammed, M.N. Pastore, S. Namjoshi, S. Yousef, A. Alinaghi, I.N. Haridass, E. Abd, V.R. Leite-Silva, H.A.E. Benson, J.E. Grice, Topical and cutaneous delivery using nanosystems, J. Control. Release 247 (2017) 86–105.
[224] C.M. Nastiti, T. Ponto, E. Abd, J.E. Grice, H.A. Benson, M.S. Roberts, Topical nano and microemulsions for skin delivery, Pharmaceutics 9 (2017) 37.
[225] M.A. Ngo, H.I. Maibach, 15 Factors of Percutaneous Penetration of Pesticides, in: Parameters for Pesticide QSAR and PBPK/PD Models for Human Risk Assessment, American Chemical Society, 2012, pp. 67-86. https://doi.org/10.1021/bk-2012-1099.ch006.
[226] J.E. Grice, S. Ciotti, N. Weiner, P. Lockwood, S.E. Cross, M.S. Roberts, Relative uptake of minoxidil into appendages and stratum corneum and permeation through human skin in vitro, J. Pharm. Sci. 99 (2010) 712–718.

[227] S.E. Cross, M.S. Roberts, R. Jiang, H.A. Benson, Can increasing the viscosity of formulations be used to reduce the human skin penetration of the sunscreen oxybenzone?, J Invest. Dermatol. 117 (2001) 147–150.
[228] E.G. Samaras, J.E. Riviere, T. Ghafourian, The effect of formulations and experimental conditions on in vitro human skin permeation-Data from updated EDETOX database, Int. J. Pharm. 434 (2012) 280–291.
[229] N.J. Hewitt, S. Gregoire, R. Cubberley, H. Duplan, J. Eilstein, C. Ellison, C. Lester, E. Fabian, J. Fernandez, C. Genies, C. Jacques-Jamin, M. Klaric, H. Rothe, I. Sorrell, D. Lange, A. Schepky, Measurement of the penetration of 56 cosmetic relevant chemicals into and through human skin using a standardized protocol, J. Appl. Toxicol. 40 (2020) 403–415.
[230] S. Tata, N. Weiner, G. Flynn, Relative influence of ethanol and propylene glycol cosolvents on deposition of minoxidil into the skin, J. Pharm. Sci. 83 (1994) 1508–1510.
[231] C.M. Heard, D. Kung, C.P. Thomas, Skin penetration enhancement of mefenamic acid by ethanol and 1,8-cineole can be explained by the 'pull' effect, Int. J. Pharm. 321 (2006) 167–170.
[232] Y.G. Anissimov, M.S. Roberts, Diffusion modeling of percutaneous absorption kinetics: 2. Finite vehicle volume and solvent deposited solids, J. Pharm. Sci. 90 (2001) 504–520.
[233] R.J. Scheuplein, L.W. Ross, Mechanism of percutaneous absorption. V. Percutaneous absorption of solvent deposited solids, J. Invest. Dermatol. 62 (1974) 353–360.
[234] P.A. Lehman, A simplified approach for estimating skin permeation parameters from in vitro finite dose absorption studies, J. Pharm. Sci. 103 (2014) 4048–4057.
[235] A.C. Williams, B.W. Barry, Penetration enhancers, Adv. Drug. Deliv. Rev. 56 (2004) 603–618.
[236] S.A.V. Morris, R.T. Thompson, R.W. Glenn, K.P. Ananthapadmanabhan, G.B. Kasting, Mechanisms of anionic surfactant penetration into human skin: investigating monomer, micelle and submicellar aggregate penetration theories, Int. J. Cosmet. Sci. 41 (2019) 55–66.
[237] E. Abd, H.A.E. Benson, Y.H. Mohammed, M.S. Roberts, J.E. Grice, Permeation mechanism of caffeine and naproxen through in vitro human epidermis: effect of vehicles and penetration enhancers, Skin Pharmacol. Physiol. 32 (2019) 132–141.
[238] E. Abd, H.A.E. Benson, M.S. Roberts, J.E. Grice, Minoxidil skin delivery from nanoemulsion formulations containing eucalyptol or oleic acid: enhanced diffusivity and follicular targeting, Pharmaceutics 10 (2018).
[239] E. Abd, M.S. Roberts, J.E. Grice, A comparison of the penetration and permeation of caffeine into and through human epidermis after application in various vesicle formulations, Skin Pharmacol. Physiol. 29 (2016) 24–30.
[240] S. Gungor, E. Kahraman, Nanocarriers mediated cutaneous drug delivery, Eur. J. Pharm. Sci. 158 (2021) 105638.
[241] M.N. Pereira, S. Tolentino, F.Q. Pires, J.L.V. Anjos, A. Alonso, T. Gratieri, M. Cunha-Filho, G.M. Gelfuso, Nanostructured lipid carriers for hair follicle-targeted delivery of clindamycin and rifampicin to hidradenitis suppurativa treatment, Colloids Surf B Biointerfaces 197 (2021) 111448.
[242] S. Saleem, M.K. Iqubal, S. Garg, J. Ali, S. Baboota, Trends in nanotechnology-based delivery systems for dermal targeting of drugs: an enticing approach to offset psoriasis, Expert. Opin. Drug. Deliv 17 (2020) 817–838.
[243] S. Raney, Bioequivalence of complex topical generics: in vitro and in vivo, in, 2020, pp. https://www.fda.gov/news-events/fda-meetings-conferences-and-workshops/bioequivalence-complex-topical-generics-vitro-and-vivo-10082020-10082020.
[244] E. Abd, S.A. Yousef, M.N. Pastore, K. Telaprolu, Y.H. Mohammed, S. Namjoshi, J.E. Grice, M.S. Roberts, Skin models for the testing of transdermal drugs, Clin. Pharmacol.: Adv. Appl. 8 (2016) 163–176.
[245] J. Lademann, U. Jacobi, C. Surber, H.J. Weigmann, J.W. Fluhr, The tape stripping procedure - evaluation of some critical parameters, Eur. J. Pharm. Biopharm. 72 (2009) 317–323.
[246] S. Yousef, Y. Mohammed, S. Namjoshi, J. Grice, W. Sakran, M. Roberts, Mechanistic evaluation of hydration effects on the human epidermal permeation of salicylate esters, AAPS J. 19 (2017) 180–190.
[247] U.S. FDA, Draft guidance on Acyclovir, Guidance for industry ANDA submissions. Recommended December 2014; Revised December 2016. https://www.accessdata.fda.gov/drugsatfda_docs/psg/Acyclovir_topical%20cream_RLD%2021478_RV12-16.pdf. Accessed 30 June 2021 in.
[248] U.S. FDA, Draft guidance on Metronidazole, Guidance for industry ANDA submissions. Metronidazole Gel draft product specific guidance, 2019. https://www.accessdata.fda.gov/drugsatfda_docs/psg/PSG_019737.pdf. Accessed 30 June 2021 in.
[249] U.S. FDA, Metronidazole Cream draft product specific guidance, 2019. https://www.accessdata.fda.gov/drugsatfda_docs/psg/PSG_020743.pdf. Accessed 30 June 2021 in.
[250] U.S. FDA, Lidocaine-Prilocaine draft product-specific guidance, 2019. https://www.accessdata.fda.gov/drugsatfda_docs/psg/Lidocaine;%20Prilocaine_draft_Topical%20cream_RLD%20019941_RC12-14.pdf. Accessed 30 June 2021 in.
[251] M. Kelchen, P. Ghosh, T. Ramezanli, S.G. Raney, Strategic Analysis of the Roadmap for Implementing Characterization-Based Bioequivalence Approaches in Product-Specific Guidances for Generic Topical Dermatological Drug Products, in: AAPS PHARMSCI 360,, San Antonio, Texas, 2019, https://www.eventscribe.com/2019/PharmSci360/fsPopup.asp?efp=SUlFUEhHSFQ4MDkx&PosterID=240521&rnd=0.5859221&mode=posterinfo. Accessed 30 June 2021.
[252] S. Namjoshi, M. Dabbaghi, M.S. Roberts, J.E. Grice, Y. Mohammed, Quality by design: development of the quality target product profile (QTPP) for semisolid topical products, Pharmaceutics 12 (2020) 287.
[253] Y. Dancik, Y.G. Anissimov, O.G. Jepps, M.S. Roberts, Convective transport of highly plasma protein bound drugs facilitates direct penetration into deep tissues after topical application, Br. J. Clin. Pharmacol. 73 (2012) 564–578.
[254] P. Singh, M.S. Roberts, Dermal and underlying tissue pharmacokinetics of lidocaine after topical application, J. Pharm. Sci. 83 (1994) 774–782.
[255] Y. Dancik, C. Thompson, G. Krishnan, M.S. Roberts, Cutaneous metabolism and active transport in transdermal drug delivery, in: N.A. Monteiro-Riviere (Ed.), Toxicology of the Skin, Informa Healthcare, New York, 2010, pp. 69–82.
[256] J. Kao, J. Hall, Skin absorption and cutaneous first pass metabolism of topical steroids: in vitro studies with mouse skin in organ culture, J. Pharmacol. Exp. Ther. 241 (1987) 482–487.
[257] A.M. Ernesti, M. Swiderek, R. Gay, Absorption and metabolism of topically applied testosterone in an organotypic skin culture, Skin. Pharmacol. 5 (1992) 146–153.
[258] P.R. Imhof, T. Vuillemin, A. Gerardin, A. Racine, P. Muller, F. Follath, Studies of the bioavailability of nitroglycerin from a transdermal therapeutic system (Nitroderm TTS), Eur. J. Clin. Pharmacol. 27 (1984) 7–12.
[259] P. Singh, M.S. Roberts, Effects of Vasoconstriction on Dermal Pharmacokinetics and local tissue distribution of compounds, J. Pharm. Sci. 83 (1994) 783–791.
[260] K. Higaki, K. Nakayama, T. Suyama, C. Amnuaikit, K. Ogawara, T. Kimura, Enhancement of topical delivery of drugs via direct penetration by reducing blood flow rate in skin, Int. J. Pharm. 288 (2005) 227–233.
[261] S.G. Carter, Z. Zhu, G. Varadi, A. Veves, J.E. Riviere, Vasomodulation influences on the transdermal delivery of Ibuprofen, J. Pharm. Sci. 102 (2013) 4072–4078.
[262] J. Grayson, Cold and warmth vasoconstrictor responses in the skin of man, British Heart J. 13 (1951) 167–176.
[263] Y.G. Anissimov, M.S. Roberts, Modelling dermal drug distribution after topical application in human, Pharm. Res. 28 (2011) 2119–2129.
[264] M.A.M. Tabosa, M. Hoppel, A.L. Bunge, R.H. Guy, M.B. Delgado-Charro, Predicting topical drug clearance from the skin, Drug Delivery Translat. Res. 11 (2021) 729–740.
[265] Y. Yun, A. Edginton, Correlation-based prediction of tissue-to-plasma partition coefficients using readily available input parameters, Xenobiotica 43 (2013) 839–852.
[266] R.L. Bronaugh, R.F. Stewart, J.E. Storm, Extent of cutaneous metabolism during percutaneous absorption of xenobiotics, Toxicol. Appl. Pharmacol. 99 (1989) 534–543.
[267] R.L. Bronaugh, S.W. Collier, S.E. Macpherson, M. Kraeling, Influence of metabolism in skin on dosimetry after topical exposure, Environ. Health Perspect. 102 (1994) 71–74.
[268] N.J. Hewitt, R.J. Edwards, E. Fritsche, C. Goebel, P. Aeby, J. Scheel, K. Reisinger, G. Ouédraogo, D. Duche, J. Eilstein, A. Latil, J. Kenny, C. Moore, J. Kuehnl, J. Barroso, R. Fautz, S. Pfuhler, Use of human in vitro skin models for accurate and ethical risk assessment: metabolic considerations, Toxicol Sci 133 (2013) 209–217.
[269] T. Hu, Z.S. Khambatta, P.J. Hayden, J. Bolmarcich, R.L. Binder, M.K. Robinson, G.J. Carr, J.P. Tiesman, B.B. Jarrold, R. Osborne, T.D. Reichling, S.T. Nemeth, M.J. Aardema, Xenobiotic metabolism gene expression in the EpiDermin vitro 3D human epidermis model compared to human skin, Toxicol. In Vitro 24 (2010) 1450–1463.
[270] S.L. Hsia, Y.-L. Hao, Metabolic transformations of cortisol-4-[14C] in human Skin*, Biochemistry 5 (1966) 1469–1474.
[271] N.A. Mazer, W.E. Heiber, J.F. Moellmer, A.W. Meikle, J.D. Stringham, S.W. Sanders, K.G. Tolman, W.D. Odell, Enhanced transdermal delivery of testosterone: a new physiological approach for androgen replacement in hypogonadal men, J. Control. Release 19 (1992) 347–361.
[272] W. Herrmann, J. Habbig, Immunological demonstration of multiple esterases in human eccrine sweat, Brit. J. Dermatol. 95 (1976) 67–70.
[273] H.U. Schweikert, J.D. Wilson, Regulation of human hair growth by steroid hormones. I. Testosterone metabolism in isolated hairs, J. Clin. Endocrinol. Metabol. 38 (1974) 811–819.
[274] M.W. Coomes, A.H. Norling, R.J. Pohl, D. Müller, J.R. Fouts, Foreign compound metabolism by isolated skin cells from the hairless mouse, J. Pharmacol. Exp. Ther. 225 (1983) 770–777.
[275] R.J. Pohl, M.W. Coomes, R.W. Sparks, J.R. Fouts, 7-ethoxycoumarin O-deethylation activity in viable basal and differentiated keratinocytes isolated from the skin of the hairless mouse, Drug Metab. Dispos. 12 (1984) 25–34.
[276] D.R. Bickers, H. Mukhtar, T. Dutta-Choudhury, C.L. Marcelo, J.J. Voorhees, Aryl hydrocarbon hydroxylase, epoxide hydrolase, and benzo [a] pyrene metabolism in human epidermis: comparative studies in normal subjects and patients with psoriasis, J. Invest. Dermatol. 83 (1984).
[277] M.F. Cooper, J.B. Hay, D. Mcgibbon, S. Shuster, Correlations between Androgen Metabolism and Sebaceous-Gland Activity, Portland Press Ltd., 1978.
[278] G. Sansone, R.M. Reisner, Differential rates of conversion of testerone to dihydrotestosterone in acne and in normal human skin-A possible pathogenic factor in acne, J. Invest. Dermatol. 56 (1971) 366–372.
[279] S.P. Denyer, C. McNabb, Microbial metabolism of topically applied drugs, in: J. Hadgraft, R.H. Guy (Eds.), Transdermal Drug Delivery, Marcel Dekker, New York, 1989, pp. 113–134.

[280] F.L. Brookes, W.B. Hugo, S.P. Denyer, Transformation of betamethasone 17-valerate by skin microflora, J. Pharm. Pharmacol. 34 (1982), 61P-61P. https://doi.org/10.1111/j.2042-7158.1982.tb00892.x.
[281] H. Osman-Ponchet, A. Gaborit, J.M. Linget, C. Wilson, Expression of drug transporters in the human skin: comparison in different species and models and its implication for drug development, ADMET DMPK 5 (2017) 75.
[282] H. Osman-Ponchet, A. Boulai, M. Kouidhi, K. Sevin, M. Alriquet, A. Gaborit, B. Bertino, P. Comby, B. Ruty, Characterization of ABC transporters in human skin, Drug Metabol Drug Interact 29 (2014) 91–100.
[283] M. Alriquet, K. Sevin, A. Gaborit, P. Comby, B. Ruty, H. Osman-Ponchet, Characterization of SLC transporters in human skin, ADMET DMPK 3 (2015) 34–44.
[284] N. Hashimoto, N. Nakamichi, S. Uwafuji, K. Yoshida, T. Sugiura, A. Tsuji, Y. Kato, ATP binding cassette transporters in two distinct compartments of the skin contribute to transdermal absorption of a typical substrate, J. Control Release 165 (2013) 54–61.
[285] I.S. Haslam, C. El-Chami, H. Faruqi, A. Shahmalak, C.A. O'Neill, R. Paus, Differential expression and functionality of ATP-binding cassette transporters in the human hair follicle, Br. J. Dermatol. 172 (2015) 1562–1572.
[286] D.C. Blaydon, D.P. Kelsell, Defective channels lead to an impaired skin barrier, J. Cell Sci. 127 (2014) 4343–4350.
[287] M. Boury-Jamot, R. Sougrat, M. Tailhardat, B.L. Varlet, F. Bonté, M. Dumas, J.M. Verbavatz, Expression and function of aquaporins in human skin: Is aquaporin-3 just a glycerol transporter?, Biochimica et Biophysica Acta (BBA) - Biomembranes 1758 (2006) 1034–1042
[288] R. Inoue, E. Sohara, T. Rai, T. Satoh, H. Yokozeki, S. Sasaki, S. Uchida, Immunolocalization and translocation of aquaporin-5 water channel in sweat glands, J. Dermatol. Sci. 70 (2013) 26–33.
[289] K. Krause, K. Foitzik, Biology of the hair follicle: the basics, Semin Cutan Med Surg 25 (2006) 2–10.
[290] A. Vogt, S. Hadam, M. Heiderhoff, H. Audring, J. Lademann, W. Sterry, U. Blume-Peytavi, Morphometry of human terminal and vellus hair follicles, Exp. Dermatol. 16 (2007) 946–950.
[291] N. Otberg, H. Richter, A. Knuttel, H. Schaefer, W. Sterry, J. Lademann, Laser spectroscopic methods for the characterization of open and closed follicles, Laser Phys. Lett. 1 (2004) 46–49.
[292] A. Pagnoni, A.M. Kligman, S.E. Gammal, T. Stoudemayer, Determination of density of follicles on various regions of the face by cyanoacrylate biopsy: correlation with sebum output, Br. J. Dermatol. 131 (1994) 862–865.
[293] R.J. Feldmann, H.I. Maibach, Regional variation in percutaneous penetration of 14C cortisol in man, J Invest Dermatol 48 (1967) 181–183.
[294] N. Otberg, H. Richter, H. Schaefer, U. Blume-Peytavi, W. Sterry, J. Lademann, Variations of hair follicle size and distribution in different body sites, J. Invest. Dermatol. 122 (2004) 14–19.
[295] A. Patzelt, J. Lademann, Drug delivery to hair follicles, Expert Opin. Drug Del. 10 (2013) 787–797.
[296] M. Ossadnik, H. Richter, A. Teichmann, S. Koch, U. Schäfer, R. Wepf, W. Sterry, J. Lademann, Investigation of differences in follicular penetration of particle- and nonparticle-containing emulsions by laser scanning microscopy, Laser Phys. 16 (2006) 747–750.
[297] A. Vogt, N. Mandt, J. Lademann, H. Schaefer, U. Blume-Peytavi, Follicular Targeting – A promising tool in selective dermatotherapy, J. Investigat. Dermatol. Sympos. Proc. 10 (2005) 252–255, https://doi.org/10.1111/j.1087 0024.2005.10124.x.
[298] C. Mathes, J.M. Brandner, M. Laue, S.S. Raesch, S. Hansen, A.V. Failla, S. Vidal, I. Moll, U.F. Schaefer, C.-M. Lehr, Tight junctions form a barrier in porcine hair follicles, Eur. J. Cell Biol. 95 (2016) 89–99.
[299] H.J. Weigmann, J. Lademann, S. Schanzer, U. Lindemann, R. von Pelchrzim, H. Schaefer, W. Sterry, V. Shah, Correlation of the local distribution of topically applied substances inside the stratum corneum determined by tape-stripping to differences in bioavailability, Skin Pharmacol. Appl. Skin Physiol. 14 (Suppl 1) (2001) 98–102.
[300] J. Lademann, N. Otberg, H. Richter, H.J. Weigmann, U. Lindemann, H. Schaefer, W. Sterry, Investigation of follicular penetration of topically applied substances, Skin Pharmacol Appl Skin Physiol 14 (Suppl 1) (2001) 17–22.
[301] J. Allec, A. Chatelus, N. Wagner, Skin distribution and pharmaceutical aspects of adapalene gel, J. Am. Acad. Dermatol. 36 (1997) S119–S125.
[302] T. Tschan, H. Steffen, A. Supersaxo, Sebaceous-gland deposition of isotretinoin after topical application: an in vitro study using human facial skin, Skin. Pharmacol. 10 (1997) 126–134.
[303] J. du Plessis, C. Ramachandran, N. Weiner, D.G. Müller, The influence of particle size of liposomes on the deposition of drug into skin, Int. J. Pharm. 103 (1994) 277–282.
[304] S. Valiveti, J. Wesley, G.W. Lu, Investigation of drug partition property in artificial sebum, Int J Pharm 346 (2008) 10–16.
[305] Y.Y. Grams, J.A. Bouwstra, Penetration and distribution of three lipophilic probes in vitro in human skin focusing on the hair follicle, J. Control. Release 83 (2002) 253–262.
[306] A. Lauterbach, C.C. Muller-Goymann, Applications and limitations of lipid nanoparticles in dermal and transdermal drug delivery via the follicular route, Eur. J. Pharm. Biopharm. 97 (2015) 152–163.
[307] A. Lauterbach, C.C. Mueller-Goymann, Development, formulation, and characterization of an adapalene-loaded solid lipid microparticle dispersion for follicular penetration, Int. J. Pharm. 466 (2014) 122–132.
[308] V. Iannuccelli, D. Bertelli, M. Romagnoli, S. Scalia, E. Maretti, F. Sacchetti, E. Leo, In vivo penetration of bare and lipid-coated silica nanoparticles across the human stratum corneum, Colloids Surf B Biointerfaces 122 (2014) 653–661.
[309] B. Illel, Formulation for transfollicular drug administration: some recent advances, Crit. Rev. Ther. Drug Carrier Syst. 14 (1997) 207–219.
[310] E.A. Essa, M.C. Bonner, B.W. Barry, Human skin sandwich for assessing shunt route penetration during passive and iontophoretic drug and liposome delivery, J. Pharm. Pharmacol. 54 (2002) 1481–1490.
[311] Y. Frum, M.C. Bonner, G.M. Eccleston, V.M. Meidan, The influence of drug partition coefficient on follicular penetration: in vitro human skin studies, Eur. J. Pharm. Sci. 30 (2007) 280–287.
[312] V.M. Meidan, Methods for quantifying intrafollicular drug delivery: a critical appraisal, Expert Opin. Drug Del. 7 (2010) 1095–1108.
[313] F. Yu, K. Tonnis, G.B. Kasting, J. Jaworska, Computer simulation of skin permeability of hydrophobic and hydrophilic chemicals-influence of follicular pathway, J. Pharm. Sci. 110 (2021) 2149–2156.
[314] R. Toll, U. Jacobi, H. Richter, J. Lademann, H. Schaefer, U. Blume-Peytavi, Penetration profile of microspheres in follicular targeting of terminal hair follicles, J. Invest. Dermatol. 123 (2004) 168–176.
[315] H. Schaefer, F. Watts, J. Brod, B. Illel, Follicular penetration, in: R.C. Scott, R.H. Guy, J. Hadcraft (Eds.), Prediction of Percutaneous Penetration, Methods, Measurements, Modelling, IBC Technical Services, London, United Kingdom, 1990, pp. 163–173.
[316] A. Rolland, N. Wagner, A. Chatelus, B. Shroot, H. Schaefer, Site-specific drug delivery to pilosebaceous structures using polymeric microspheres, Pharm. Res. 10 (1993) 1738–1744.
[317] A. Patzelt, J. Lademann, Recent advances in follicular drug delivery of nanoparticles, Expert Opinion Drug Delivery 17 (2020) 49–60.
[318] R. Alvarez-Roman, A. Naik, Y.N. Kalia, R.H. Guy, H. Fessi, Skin penetration and distribution of polymeric nanoparticles, J. Control Release 99 (2004) 53–62.
[319] M. Ulmer, A. Patzelt, T. Vergou, H. Richter, G. Müller, A. Kramer, W. Sterry, V. Czaika, J. Lademann, In vivo investigation of the efficiency of a nanoparticle-emulsion containing polihexanide on the human skin, Eur. J. Pharm. Biopharm. 84 (2013) 325–329.
[320] A. Patzelt, H. Richter, F. Knorr, U. Schafer, C.M. Lehr, L. Dahne, W. Sterry, J. Lademann, Selective follicular targeting by modification of the particle sizes, J. Control Release 150 (2011) 45–48.
[321] A. Patzelt, H. Richter, F. Knorr, U. Schäfer, C.-M. Lehr, L. Dähne, W. Sterry, J. Lademann, Selective follicular targeting by modification of the particle sizes, J. Control. Release 150 (2011) 45–48.
[322] J. Lademann, A. Patzelt, H. Richter, C. Antoniou, W. Sterry, F. Knorr, Determination of the cuticula thickness of human and porcine hairs and their potential influence on the penetration of nanoparticles into the hair follicles, J. Biomed. Opt. 14 (2009) 021014.
[323] J. Lademann, H. Richter, A. Teichmann, N. Otberg, U. Blume-Peytavi, J. Luengo, B. Weiss, U.F. Schaefer, C.M. Lehr, R. Wepf, W. Sterry, Nanoparticles–an efficient carrier for drug delivery into the hair follicles, Eur. J. Pharm. Biopharm. 66 (2007) 159–164.
[324] M. Radtke, A. Patzelt, F. Knorr, J. Lademann, R.R. Netz, Ratchet effect for nanoparticle transport in hair follicles, Eur. J. Pharm. Biopharm. (2016).
[325] A. Patzelt, W.C. Mak, S. Jung, F. Knorr, M.C. Meinke, H. Richter, E. Ruhl, K.Y. Cheung, N.B. Tran, J. Lademann, Do nanoparticles have a future in dermal drug delivery?, J Control Release 246 (2017) 174–182.
[326] H.I. Labouta, M. Schneider, Interaction of inorganic nanoparticles with the skin barrier: current status and critical review, Nanomed.: Nanotechnol. Biol. Med. 9 (2013) 39–54.
[327] S. Jung, G. Nagel, M. Giulbudagian, M. Calderón, A. Patzelt, F. Knorr, J. Lademann, Temperature-enhanced follicular penetration of thermoresponsive nanogels, Z. Phys. Chem. 232 (2018) 805–817.
[328] P. Dong, F.F. Sahle, S.B. Lohan, S. Saeidpour, S. Albrecht, C. Teutloff, R. Bodmeier, M. Unbehauen, C. Wolff, R. Haag, J. Lademann, A. Patzelt, M. Schäfer-Korting, M.C. Meinke, pH-sensitive Eudragit® L 100 nanoparticles promote cutaneous penetration and drug release on the skin, J Control Release 295 (2019) 214–222.
[329] R. Goyal, L.K. Macri, H.M. Kaplan, J. Kohn, Nanoparticles and nanofibers for topical drug delivery, J. Control. Release 240 (2016) 77–92.
[330] A. Vogt, B. Combadiere, S. Hadam, K.M. Stieler, J. Lademann, H. Schaefer, B. Autran, W. Sterry, U. Blume-Peytavi, 40 nm, but not 750 or 1,500 nm, nanoparticles enter epidermal CD1a+ cells after transcutaneous application on human skin, J. Invest. Dermatol. 126 (2006) 1316–1322.
[331] A. Teichmann, U. Jacobi, M. Ossadnik, H. Richter, S. Koch, W. Sterry, J. Lademann, Differential stripping: determination of the amount of topically applied substances penetrated into the hair follicles, J. Invest Dermatol. 125 (2005) 264–269.
[332] V.R. Leite-Silva, D.C. Liu, W.Y. Sanchez, H. Studier, Y.H. Mohammed, A. Holmes, W. Becker, J.E. Grice, H.A. Benson, M.S. Roberts, Effect of flexing and massage on in vivo human skin penetration and toxicity of zinc oxide nanoparticles, Nanomed. (London, England) 11 (2016) 1193–1205.
[333] K. Sato, W.H. Kang, K. Saga, K.T. Sato, Biology of sweat glands and their disorders. I. Normal sweat gland function, J. Am. Acad. Dermatol. 20 (1989) 537–563.
[334] Y. Kuno, Variations in secretory activity of human sweat glands, The Lancet 231 (1938) 299–303.
[335] M. Shibasaki, C.G. Crandall, Mechanisms and controllers of eccrine sweating in humans, Front. Biosci. (Scholar edition) 2 (2010) 685.

[336] K. Semkova, M. Gergovska, J. Kazandjieva, N. Tsankov, Hyperhidrosis, bromhidrosis, and chromhidrosis: Fold (intertriginous) dermatoses, Clin. Dermatol. 33 (2015) 483–491.
[337] J.S. Beck, H.F. Coulson, N. Dove, T. Kealey, Evidence for sodium-coupled acid-base transport across the basolateral membrane of the reabsorptive duct of the human eccrine sweat gland, J, Invest. Dermatol. 117 (2001) 877–879.
[338] E. Holzle, K. AM, Factors influencing the anti-perspirant action of aluminium salts, (1979).
[339] H. Tronnier, Experimentelle Untersuchungen zur Wirkungsweise aluminiumhaltiger Antiperspiranzien, (1973).
[340] R. Brun, Studies on perspiration, J. Soc. Cosmetic Chem. 10 (1959) 70–77.
[341] F. Herrmann, M.B. Sulzberger, Control of axillary sweating and of body odor, J. Am. Med. Assoc. 167 (1958) 1115–1117.
[342] A.M. Holmes, I. Kempson, T. Turnbull, D. Paterson, M.S. Roberts, Imaging the penetration and distribution of zinc and zinc species after topical application of zinc pyrithione to human skin, Toxicol. Appl. Pharmacol. 343 (2018) 40–47.
[343] G.E. Folk, A. Semken, The evolution of sweat glands, Int. J. Biometeorol. 35 (1991) 180–186.
[344] K. Wilke, A. Martin, L. Terstegen, S.S. Biel, A short history of sweat gland biology, Int. J. Cosmet. Sci. 29 (2007) 169–179.
[345] S.R. Tripathi, E. Miyata, P.B. Ishai, K. Kawase, Morphology of human sweat ducts observed by optical coherence tomography and their frequency of resonance in the terahertz frequency region, Sci. Rep. 5 (2015) 9071.
[346] F. Sato, M. Owen, R. Matthes, K. Sato, C. Gisolfi, Functional and morphological changes in the eccrine sweat gland with heat acclimation, J. Appl. Physiol. 69 (1990) 232–236.
[347] J.G. Derraik, M. Rademaker, W.S. Cutfield, T.E. Pinto, S. Tregurtha, A. Faherty, J. M. Peart, P.L. Drury, P.L. Hofman, Effects of age, gender, BMI, and anatomical site on skin thickness in children and adults with diabetes, PLoS ONE 9 (2014) e86637.
[348] M.S. Roberts, S.E. Cross, Y.G. Anissimov, The skin reservoir for topically applied solutes, in: N. Dragicevic, H.I. Maibach (Eds.), Percutaneous Absorption: Drugs, Cosmetics, Mechanisms, Methods, 5th ed., CRC Press (in press), 2021, pp. 65–84, https://www.taylorfrancis.com/chapters/edit/10.1201/9780429202971-4/skin-reservoir-topically-applied-solutes-michael-roberts-sheree-cross-yuri-anissimov.
[349] M.S. Roberts, S. Cross, Y. Anissimov, Factors affecting the formation of a skin reservoir for topically applied solutes, Skin Pharmacol. Physiol. 17 (2004) 3–16.
[350] C.F. Vickers, Stratum corneum reservoir for drugs, Adv. Biol. Skin. 12 (1972) 177–189.
[351] M.S. Roberts, S.E. Cross, Y. Anissimov, The Skin Reservoir for Topically Applied Solutes, in: R. Bronaugh, H.I. Maibach (Eds.), Percutaneous Absorption, Taylor & Francis Group, Boca Raton, 2005, pp. 213–234.
[352] S. Yagi, K. Nakayama, Y. Kurosaki, K. Higaki, T. Kimura, Factors determining drug residence in skin during transdermal absorption: Studies on β-blocking agents, Biol. Pharm. Bull. 21 (1998) 1195–1201.
[353] K. Sauermann, S. Clemann, S. Jaspers, T. Gambichler, P. Altmeyer, K. Hoffmann, J. Ennen, Age related changes of human skin investigated with histometric measurements by confocal laser scanning microscopy in vivo, Skin Res. Technol. 8 (2002) 52–56.
[354] M.S. Roberts, S.E. Cross, A physiological pharmacokinetic model for solute disposition in tissues below a topical application site, Pharm. Res. 16 (1999) 1392–1398.
[355] R. Ibrahim, G.B. Kasting, Improved method for determining partition and diffusion coefficients in human dermis, J. Pharm. Sci. 99 (2010) 4928–4939.
[356] K. Kretsos, M.A. Miller, G. Zamora-Estrada, G.B. Kasting, Partitioning, diffusivity and clearance of skin permeants in mammalian dermis, Int. J. Pharm. 346 (2008) 64–79.
[357] J. Hadgraft, M.E. Lane, Drug crystallization–implications for topical and transdermal delivery, Expert Opinion on Drug Delivery 13 (2016) 817–830.
[358] A.M. Holmes, L. Mackenzie, M.S. Roberts, Disposition and measured toxicity of zinc oxide nanoparticles and zinc ions against keratinocytes in cell culture and viable human epidermis, Nanotoxicology 14 (2020) 263–274.
[359] A. Vieille-Petit, N. Blickenstaff, G. Coman, H.I. Maibach, Metrics and clinical relevance of percutaneous penetration and lateral spreading, Skin Pharmacol. Physiol. 28 (2015) 57–64.
[360] U. Jacobi, S. Schanzer, H.J. Weigmann, A. Patzelt, T. Vergou, W. Sterry, J. Lademann, Pathways of lateral spreading, Skin Pharmacol. Physiol. 24 (2011) 231–237.
[361] A.M. Holmes, Z. Song, H.R. Moghimi, M.S. Roberts, Relative penetration of zinc oxide and zinc ions into human skin after application of different zinc oxide formulations, ACS Nano 10 (2016) 1810–1819.
[362] L. Sandiford, A.M. Holmes, S.E. Mangion, Y.H. Mohammed, A.V. Zvyagin, M.S. Roberts, Optical characterisation of zinc pyrithione, Photochem. Photobiol. (2019).
[363] H.I. Maibach, R.J. Feldmann, T.H. Milby, W.F. Serat, Regional variation in percutaneous penetration in man, Arch. Environ. Health: Int. J. 23 (1971) 208–211.
[364] R.M. Law, M.A. Ngo, H.I. Maibach, Twenty clinically pertinent factors/observations for percutaneous absorption in humans, Am. J. Clin. Dermatol. 21 (2020) 85–95.
[365] M.A. Lampe, A.L. Burlingame, J. Whitney, M.L. Williams, B.E. Brown, E. Roitman, P.M. Elias, Human stratum corneum lipids: characterization and regional variations, J. Lipid Res. 24 (1983) 120–130.
[366] J. Nikolovski, G.N. Stamatas, N. Kollias, B.C. Wiegand, Barrier function and water-holding and transport properties of infant stratum corneum are different from adult and continue to develop through the first year of life, J. Invest. Dermatol. 128 (2008) 1728–1736.
[367] K.V. Roskos, H.I. Maibach, R.H. Guy, The effect of aging on percutaneous absorption in man, J. Pharmacokinet. Biopharm. 17 (1989) 617–630.
[368] E. Berardesca, M. Mariano, N. Cameli, Biophysical properties of ethnic skin, in: N.A. Vashi, H.I. Maibach (Eds.), Dermatoanthropology of Ethnic Skin and Hair, Springer, 2017, pp. 27–33.
[369] S. Gattu, H.I. Maibach, Modest but increased penetration through damaged skin: an overview of the in vivo human model, Skin. Pharmacol. Physiol. 24 (2011) 2–9.
[370] A.S. Halling-Overgaard, S. Kezic, I. Jakasa, K.A. Engebretsen, H.I. Maibach, J.P. Thyssen, Skin absorption through atopic dermatitis skin: a systematic review, Br. J. Dermatol. 177 (2017) 84–106.
[371] P. Depeille, P. Cuq, I. Passagne, A. Evrard, L. Vian, Combined effects of GSTP1 and MRP1 in melanoma drug resistance, Br. J. Can. 93 (2005) 216–223.
[372] U.S. FDA, Guidance for Industry- Extended release oral dosage forms: Development, evaluation, and application of in vitro/in vivo correlations, Food and Drug Administration, Center for Drug Evaluation and Research (CDER), https://www.fda.gov/media/70939/download (Accessed on July 14 2021) (1997) 1-27.
[373] Y.H. Mohammed, H.R. Moghimi, S.A. Yousef, N.C. Chandrasekaran, C.R. Bibi, S. C. Sukumar, J.E. Grice, W. Sakran, M.S. Roberts, Efficacy, safety and targets in topical and transdermal active and excipient delivery, in: N. Dragicevic, H.I. Maibach (Eds.), Percutaneous penetration enhancers drug penetration into/through the skin, Springer, Berlin, Heidelberg, 2017, pp. 369–391.
[374] P.J. Patel, A.-H. Ghanem, W.I. Higuchi, V. Srinivasan, E.R. Kern, Correlation of in vivo topical efficacies with in vitro predictions using acyclovir formulations in the treatment of cutaneous HSV-1 infections in hairless mice: an evaluation of the predictive value of the C∗ concept, Antiviral Res. 29 (1996) 279–286.
[375] A.A. Kyle, M.V. Dahl, Topical therapy for fungal infections, Am. J. Clin. Dermatol. 5 (2004) 443–451.
[376] B. Dréno, V. Bettoli, F. Ochsendorf, A.M. Layton, M. Perez, R. Dakovic, H. Gollnick, Efficacy and safety of clindamycin phosphate 1.2%/tretinoin 0.025% formulation for the treatment of acne vulgaris: pooled analysis of data from three randomised, double-blind, parallel-group, phase III studies, Eur. J. Dermatol. 24 (2014) 201–209.
[377] W.L. Chiou, Low intrinsic drug activity and dominant vehicle (placebo) effect in the topical treatment of acne vulgaris, Int. J. Clin. Pharmacol. Ther. 50 (2012) 434–437.
[378] F.S. Brandt, A. Cazzaniga, M. Hann, Cosmeceuticals: current trends and market analysis, Semin. Cutan. Med. Surg. 30 (2011) 141–143.
[379] J.A. Mennella, A.C. Spector, D.R. Reed, S.E. Coldwell, The bad taste of medicines: overview of basic research on bitter taste, Clin. Ther. 35 (2013) 1225–1246.
[380] D.R. Reed, A. Knaapila, Genetics of taste and smell: poisons and pleasures, Prog. Mol. Biol. Transl. Sci. 94 (2010) 213–240.
[381] H.L. Jacobs, K.N. Sharma, Taste versus calories: sensory and metabolic signals in the control of food intake, Ann. N Y Acad. Sci. 157 (1969) 1084–1125.
[382] R.-K. Chang, A. Raw, R. Lionberger, L. Yu, Generic development of topical dermatologic products: formulation development, process development, and testing of topical dermatologic products, The AAPS J. 15 (2013) 41–52.
[383] K. Andersson, C. Sonesson, M. Petzold, A. Carlsten, K. Lonnroth, What are the obstacles to generic substitution? An assessment of the behaviour of prescribers, patients and pharmacies during the first year of generic substitution in Sweden, Pharmacoepidemiol. Drug. Saf. 14 (2005) 341–348.
[384] W.H. Shrank, J.N. Liberman, M.A. Fischer, C. Girdish, T.A. Brennan, N.K. Choudhry, Physician perceptions about generic drugs, Ann Pharmacother 45 (2011) 31–38.
[385] K. Fent, P.Y. Kunz, E. Gomez, UV filters in the aquatic environment induce hormonal effects and affect fertility and reproduction in fish, Chimia 62 (2008) 368–375.
[386] V.R. Leite-Silva, M. Le Lamer, W.Y. Sanchez, D.C. Liu, W.H. Sanchez, I. Morrow, D. Martin, H.D.T. Silva, T.L.W. Prow, J.E. Grice, M.S. Roberts, The effect of formulation on the penetration of coated and uncoated zinc oxide nanoparticles into the viable epidermis of human skin in vivo, Eur. J. Pharm. Biopharm. 84 (2013) 297–308.
[387] S.E. Kemp, Sensory evaluation: a practical handbook, Wiley-Blackwell, Oxford, 2009.
[388] T.F. Cohen, The Power of Drug Color, October 14, 2014, https://www.theatlantic.com/health/archive/2014/10/the-power-of-drug-color/381156/. Accessed May 16, 2021.
[389] M. Darragh, J.W. Chang, R.J. Booth, N.S. Consedine, The placebo effect in inflammatory skin reactions: the influence of verbal suggestion on itch and weal size, J. Psychosom Res. 78 (2015) 489–494.
[390] A.M. Pensé-Lhéritier, Recent developments in the sensorial assessment of cosmetic products: a review, Int. J. Cosmet Sci. 37 (2015) 465–473.
[391] C.E. Dubin, G.W. Kimmel, P.W. Hashim, J.K. Nia, J.A. Zeichner, Objective evaluation of skin sensitivity across fitzpatrick skin types, J. Drugs Dermatol. 19 (2020) 699–701.
[392] I. Besné, C. Descombes, L. Breton, Effect of age and anatomical site on density of sensory innervation in human epidermis, Arch. Dermatol. 138 (2002) 1445–1450.

[393] G.V. Civille, K.N. Oftedal, Sensory evaluation techniques - make "good for you" taste "good", Physiol. Behav. 107 (2012) 598–605.
[394] G. Savary, L. Gilbert, M. Grisel, C. Picard, Instrumental and sensory methodologies to characterize the residual film of topical products applied to skin, Skin Res. Technol. 25 (2019) 415–423.
[395] G. Savary, M. Grisel, C. Picard, Impact of emollients on the spreading properties of cosmetic products: a combined sensory and instrumental characterization, Colloids Surf., B 102 (2013) 371–378.
[396] L.S. Calixto, V.H.P. Infante, P.M.B.G.M. Campos, Design and characterization of topical formulations: correlations between instrumental and sensorial measurements, Aaps Pharmscitech 19 (2018) 1512–1519.
[397] F. Langenbucher, B. Lange, Prediction of the application behaviour of cosmetics from rheological measurements, Pharm. Acta Helv. 45 (1970) 572–582.
[398] R. Marriott, Rheological measurements in the cosmetic industry, J. Soc. Cosm. Chem 12 (1961) 89.
[399] E.P. Vasyuchenko, P.S. Orekhov, G.A. Armeev, M.E. Bozdaganyan, CPE-DB: An open database of chemical penetration enhancers, Pharmaceutics 13 (2021) 66.
[400] S.K. Li, W.I. Higuchi, Mechanistic studies of permeation enhancers, in: N. Dragicevic, H.I. Maibach (Eds.), Percutaneous Penetration Enhancers Drug Penetration Into/Through the Skin, Springer, Berlin, Heidelberg, 2017, pp. 119–136.
[401] H. Lee, J.W. Kim, Diffusion behaviors of fluorescence probe molecules through the stratum corneum layer under physical stress, J. Membr. Biol. 246 (2013) 263–269.
[402] A. Al-Amoudi, J. Dubochet, L. Norlén, Nanostructure of the epidermal extracellular space as observed by cryo-electron microscopy of vitreous sections of human skin, J, Invest. Dermatol. 124 (2005) 764–777.
[403] O.G. Jepps, Y. Dancik, Y.G. Anissimov, M.S. Roberts, Modeling the human skin barrier—Towards a better understanding of dermal absorption, Adv. Drug Deliv. Rev. 65 (2013) 152–168.
[404] Z. Ya-Xian, T. Suetake, H. Tagami, Number of cell layers of the stratum corneum in normal skin–relationship to the anatomical location on the body, age, sex and physical parameters, Arch. Dermatol. Res. 291 (1999) 555–559.
[405] U.S. FDA, Orange book: approved drug products with therapeutic equivalence evaluations, in: USA: US Food & Drug Administration, 2013, https://www.accessdata.fda.gov/scripts/cder/ob/search_product.cfm. Accessed 25 June 2021.
[406] K. Harada, T. Murakami, E. Kawasaki, Y. Higashi, S. Yamamoto, N. Yata, In-vitro permeability to salicylic acid of human, rodent, and shed snake skin, J. Pharm. Pharmacol. 45 (1993) 414–418.
[407] A. Rougier, D. Dupuis, C. Lotte, R. Roguet, R. Wester, H.I. Maibach, Regional variation in percutaneous absorption in man: measurement by the stripping method, Arch. Dermatol. Res. 278 (1986) 465–469.
[408] C. Lotte, A. Rougier, D. Wilson, H.I. Maibach, In vivo relationship between transepidermal water loss and percutaneous penetration of some organic compounds in man: effect of anatomic site, Arch. Dermatol. Res. 279 (1987) 351–356.
[409] R.J. Feldmann, Regional variation in percutaneous penetration of 14C cortisol in man, J. Invest. Dermatol. 48 (1967) 181–183.
[410] A.K. Shah, G. Wei, R.C. Lanman, V.O. Bhargava, S.J. Weir, Percutaneous absorption of ketoprofen from different anatomical sites in man, Pharm. Res. 13 (1996) 168–172.
[411] S. Polak, C. Ghobadi, H. Mishra, M. Ahamadi, N. Patel, M. Jamei, A. Rostami-Hodjegan, Prediction of concentration–time profile and its inter-individual variability following the dermal drug absorption, J. Pharm. Sci. 101 (2012) 2584–2595.
[412] A. Böhling, S. Bielfeldt, A. Himmelmann, M. Keskin, K.P. Wilhelm, Comparison of the stratum corneum thickness measured in vivo with confocal Raman spectroscopy and confocal reflectance microscopy, Skin Res. Technol. 20 (2014) 50–57.
[413] W.B. Shelly, F.M. Melton, Factors accelerating the penetration of histamine through normal intact human skin, J Invest Dermatol. 13 (2) (1949) 61–71.
[414] S.E. Mangion, A.M. Holmes, M.S. Roberts, Targeted delivery of zinc pyrithione to skin epithelia, Int. J. Mol. Sci. 22 (2021) (accepted September 2021).
[415] M.S. Roberts, E.J. Triggs, R.A. Anderson, Permeability of solutes through biological membranes measured by a desorption technique, Nature 257 (1975) 225–227, https://www.nature.com/articles/257225a0.
[416] G.B. Kasting, M.A. Miller, P.S. Talreja, Evaluation of stratum corneum heterogeneity in percutaneous absorption: drugs, cosmetics, mechanisms, methods, in: Nina Dragićević, Howard I. Maibach (Eds.), fifth ed., CRC Press, Boca Raton, 2022, pp. 143–164, https://www.taylorfrancis.com/books/edit/10.1201/9780429202971/percutaneous-absorption-nina-dragi%C4%87evi%C4%87-howard-maibach?refId=2bbdd3ef-8870-4e8d-b44b-42a70dd373b0.
[417] Q. Zhang, J.E. Grice, G.J. Wang, M.S. Roberts, Cutaneous metabolism in transdermal drug delivery, Curr. Drug Metab. 10 (2009) 227–235, https://doi.org/10.2174/138920009787846350.
[418] H.I. Maibach, Cutaneous metabolism of xenobiotics, in: Nina Dragićević, Howard I. Maibach (Eds.), Percutaneous Absorption: Drugs, Cosmetics, Mechanisms, Methods, fifth ed., CRC Press, Boca Raton, 2022, pp. 447–457, https://www.taylorfrancis.com/chapters/edit/10.1201/9780429202971-33/cutaneous-metabolism-xenobiotics-howard-maibach.
[419] B.W. Barry, Dermatological formulations: percutaneous absorption, Marcel Dekker, New York, 1983, pp. 1–485.
[420] Y. Dancik, O.G. Jepps, M.S. Roberts, Beyond stratum corneum, in: M.S. Roberts, K.A. Walters (Eds.), Dermal absorption and toxicity assessment, second ed., Marcel Dekker, New York, 2008, pp. 209–250, https://doi.org/10.3109/9780849375927-16.
[421] M.S. Roberts, K.A. Walters, The relationship between structure and barrier function of skin, in: M.S. Roberts, K.A. Walters (Eds.), Dermal absorption and toxicity assessment, Marcel Dekker, New York, 1998, pp. 1–42.
[422] K.A. Walters, A.C. Watkinson, K.R. Brain, In vitro skin permeation evaluation: the only realistic option, Int. J. Cosmet. Sci. 20 (1998) 307–316, PMID: 18505515. https://doi.org/10.1046/j.1467-2494.1998.181622.x.
[423] K.A. Walters, Preface, in: K.A. Walters (Ed.), Dermatological and Transdermal Formulations, New York, Marcel Dekker, 2002, pp. 1–42, https://www.taylorfrancis.com/books/edit/10.1201/9780824743239/dermatological-transdermal-formulations-kenneth-walters.